COASTAL RESEARCH AND TRANSPORTATION EDUCATION
TIER 1 UNIVERSITY TRANSPORTATION CENTER
U.S. DEPARTMENT OF TRANSPORTATION

Bio-waste Materials as Supplementary Cementitious Materials for Coastal Concrete Applications

August 31, 2025

Chong, Beng Wei, Ph.D. Student at Texas State University, Ingram School of Engineering, 601 University Drive, San Marcos, TX 78666; ORCID https://orcid.org/0000-0002-2185-0894; Email: bengwei.chong@txstate.edu

Majumder, Amlan, Ph.D. Student at Texas State University, Ingram School of Engineering, 601 University Drive, San Marcos, TX 78666; ORCID https://orcid.org/0000-0001-5135-1810; Email: amlan.majumder@txstate.edu

Shi, Xijun, Ph.D., P.E., Assistant Professor at Texas State University, Ingram School of Engineering, 601 University Drive, San Marcos, TX 78666; ORCID https://orcid.org/ 0000-0003-2858-8603; Email: xijun.shi@txstate.edu

Final Research Report
Prepared for:
Coastal Research and Transportation Education

CREATE

Technical Report Documentation Form

1. Report No.	2. Government Accession No.	3. Recipient's Catalog No.
2301-7	01895205	n/a

4. Title and Subtitle

Bio-Waste Materials as Supplementary Cementitious Materials for Coastal Concrete Applications

5. Report Date

8/31/2025

6. Performing Organization Code

n/a

7. Author(s): Beng Wei Chong, PhD. Student Texas State ISOE 0000-0002-218500894 email: benwei.chong@txstate.edu; Amlan Majumder, Ph.D. Student, Texas State University ISOE 0000-0001-5135-1810 email: amlan.majunder@txstate.edu; Xijun Shi, Ph.D. PE, Assistant Professor Texas State University ISOE, 0000-0003-2858-8603 email: xijun.shi@txstate.edu

8. Performing Organization Report No.

n/a

9. Performing Organization Name and Address

Ingram School of Engineering, Texas State University 601 University Dr. San Marcos, TX 78666

10. Work Unit No. (TRAIS)

n/a

12. Sponsoring Agency Name and Address

Office of the Assistant Secretary for Research and Technology
University Transportation Centers Program
Department of Transportation
Washington, DC United States 20590

11. Contract or Grant No.

69A3552348330

13. Type of Report and Period Covered

Final Project Report
9/01/2023-5/31/2025

14. Sponsoring Agency Code

OST-R

15. Supplementary Notes

https://create.engineering.txst.edu/

16. Abstract

This study explores the use of agricultural bio-waste such as eggshell powder and sugarcane bagasse ash (SCBA) as sustainable alternatives to cement production. Eggshell powder was evaluated as partial substitutes for limestone filler with and without heat treatment. SCBA, a silica-rich byproduct of sugar production, was investigated for its potential as a supplementary cementitious material (SCM) akin to Class F fly ash. Experimental methods included material characterization using SEM, XRD, XRF, TGA, and LOI testing, as well as evaluations of fresh and hardened concrete properties. Results demonstrated that treated eggshell and SCBA samples exhibited favorable morphological and chemical properties for use in blended cement systems. Eggshell powder can be used as an alternative to limestone at lower proportions of inclusion, However, heat treatment is recommended to denature the organic content from eggshell membrane at high proportion of inclusion. Meanwhile, SCBA is a pozzolanic material that can be blended with cement for optimal strength and durability. The findings support the feasibility of incorporating bio-waste into concrete formulations, contributing to sustainability efforts in construction and transportation infrastructure.

17. Key Words

Supplementary cementitious materials, eggshell, sugarcane bagasse ash, fresh properties, hardened properties

18. Distribution Statement

No Restrictions

19. Security Classification (of this report)	20. Security Classification (of this page)	21. No. of Pages	22. Price
Unclassified	Unclassified	85	n/a

ACKNOWLEDGMENT

This study was funded, partially or entirely, by the U.S. Department of Transportation through the Coastal Research and Transportation Education University Transportation Center under Grant Award Number 69A3552348330. The work was conducted at the Texas State University. The authors would like to thank Nest Fresh Eggs for supplying waste eggshell samples. The authors also thank Micah Stark from Texas A&M University for assisting with the processing and analysis of the waste materials. A heartfelt gratitude towards the Rio Grande Valley, Sugarcane Growers, Inc. for letting the authors visit their plant and collect necessary ashes for the testing.

DISCLAIMER

Table of Contents

List of Figures

List of Table

ABSTRACT

This study explores the use of agricultural bio-waste such as eggshell powder and sugarcane bagasse ash (SCBA) as sustainable alternatives to cement production. Eggshell powder was evaluated as partial substitutes for limestone filler with and without heat treatment. SCBA, a silica-rich byproduct of sugar production, was investigated for its potential as a supplementary cementitious material (SCM) akin to Class F fly ash. Experimental methods included material characterization using SEM, XRD, XRF, TGA, and LOI testing, as well as evaluations of fresh and hardened concrete properties. Results demonstrated that treated eggshell and SCBA samples exhibited favorable morphological and chemical properties for use in blended cement systems. Eggshell powder can be used as an alternative to limestone at lower proportions of inclusion, However, heat treatment is recommended to denature the organic content from eggshell membrane at high proportion of inclusion. Meanwhile, SCBA is a pozzolanic material that can be blended with cement for optimal strength and durability. The findings support the feasibility of incorporating bio-waste into concrete formulations, contributing to sustainability efforts in construction and transportation infrastructure.

Keywords: Supplementary cementitious materials, eggshell, sugarcane bagasse ash, fresh properties, hardened properties.

1. INTRODUCTION

1.1 Background

Cement, and by extension concrete, is the most used construction material in the world. Fundamentally, concrete has superior strength, moldability, great durability when exposed to the elements and is relatively cost-effective. Hence, the consumption and production of cement had been growing exponentially. In between 2018 and 2020, approximately 4,000 metric tons of cement were produced, which amounted to 30 times the amount of cement production from the year 1950 (Andrew, 2019). The increased production and consumption of cement will only continue to increase with urbanization and the construction of more infrastructure. The utilization of cement and concrete is not restricted to construction on the land. In coastal applications, concrete is widely used in the construction of seawalls, quays, ports, and more. For instance, approximately 14,000 miles of U.S. shoreline is reinforced by concrete structures, (Keegan, 2020), highlighting the compatibility of the material in marine applications despite durability concerns.

However, massive use of concrete, and by extension cement, has its downsides. Chief among them is the greenhouse gas emissions caused by the production of clinkers. Emission is directly tied to the chemical process of cement production itself, in which calcium carbonate is transformed into calcium oxide (lime) by the release of carbon dioxide (CO_2). Moreover, cement production is an energy intensive process achieved by the combustion of fossil fuels that also requires an additional amount of electrical energy to operate massive machines (Afkhami et al., 2015). As a result, the cement industry is responsible for about 8% of global anthropogenic CO_2 emissions (Cheng et al., 2023). Due to growing environmental awareness and concern, the cement industry is actively pursuing decarbonization. In the United States, such demand is being echoed by various professional groups. For example, the Portland Cement Association (PCA) is committed to carbon neutrality by 2050 (Henley & Ruiz, 2021), and similar efforts are being undertaken by multiple states across the nation (Pisciotta et al., 2023).

The major approach to decarbonize the cement industry is the direct reduction of clinker content within concrete mixtures. This is often accomplished by the replacement of clinker by a material with lower embodied carbon, like fine limestone powder. Originally, limestone powder was mainly explored as a filler material to improve the particle packing of concrete. The idea

quickly took off when it was discovered that the calcium carbonate within limestone was able to enhance the reaction of clinker (Lothenbach et al., 2008). Today, portland cement with up to 15% limestone is replacing OPC in the U.S. and other nations as outlined in ASTM C595 ("ASTM C595/C595M-24 Standard Specification for Blended Hydraulic Cements," 2024), AASHTO M 240 ("AASHTO M 240 Standard Specification for Blended Cement," 2023), CSA-A3000 ("CSA A3000-18 Cementitious materials compendium," 2018) and more. Moreover, in Europe, the EN 197-1 ("EN 197-1:2011 Cement - Part 1: Composition, specifications and conformity criteria for common cements,") has permitted up to 35% substitution of clinker with limestone powder in certain applications.

While the usage of limestone powder is more environmentally friendly than cement clinker, the mining and processing of limestone is still detrimental to the environment, causing dust pollution, groundwater contamination, land use pattern change, etc. (Parthiban et al., 2023). Every metric ton of limestone mined generates approximately 3.13kg of CO_2 (Kittipongvises, 2017). There are many alternative fillers with high calcium carbonate ($CaCO_3$) content and have sufficient fineness that could serve as limestone replacements in blended cement. $CaCO_3$ is an abundant mineral that can be found in various domestic/industrial wastes, including eggshells, oyster shells, sludge, quarry dust, and carbide lime waste, many of which are readily available waste materials that can be used as a cement constituent.

Apart from using $CaCO_3$ rich material, another popular method to reduce the clinker factor is to replace a portion of clinker with supplementary cementitious materials (SCMs). SCMs are defined as mineral admixtures that can react with calcium hydroxide to form calcium-silicate-hydrates (C-S-H), a favorable chemical reaction that improves the microstructure of the resulting cementitious composite. Like limestone, SCMs also have higher fineness compared to cement clinkers, allowing them to serve as nucleation sites for increased precipitation of cement hydration products. Common types of SCMs include silica fume, slag, metakaolin, fly ash, and more. In Texas, coal fly ash is the most used SCM (added to replace 15 to 35% of cement by mass) (Al-Shmaisani et al., 2018). Fly ash is a byproduct of coal-based plants; it is a powdery substance coming out of the combustion of ground or powdered coal.

Despite being a waste material, the supply of fly ash in the U.S. has lately become a matter of concern. Several factors have contributed to the fly ash shortage. One of the most important factors is the promotion of renewable and cheaper energy sources such as natural gas,

wind energy, and solar energy compared to coal-based power after the introduction of the Federal Sustainability Plan. As a result, numerous coal-based energy plants have shut down, limiting the availability of fly ash. Another factor is environmental regulation by the EPA to blend different types of coal which, in turn, reduces fly ash quality. This blended fly ash does not exhibit similar properties to Class F fly ash and thus affects concrete performance. Since these changes in the coal power energy sector are creating considerable uncertainty for the future supply and quality of fly ash, it is critical to identify and evaluate alternative supplementary cementitious materials that can offer concrete equivalent or better strength and durability characteristics to Class F fly ash.

This research explores the feasibility of using agricultural bio-waste in place of limestone and fly ash. Waste eggshell powder and sugar cane bagasse ash (SCBA), which behave similarly to fly ash, are explored as an alternative to limestone SCM in portland cement.

1.2 Research objectives

This project aims to investigate the feasibility of waste eggshell powder and SCBA as partial cement replacement. The hydration mechanism, fresh properties, hardened properties, volume change, and durability of cementitious composite prepared from the blended cements are explored. The specific objectives are to:

1) Investigate the performance of portland cement with waste eggshell powder compared to limestone powder.
2) Evaluate the performance of portland cement with waste eggshell powder based on different treatment methods.
3) Investigate the feasibility of using Texas produced sugarcane bagasse ash as an alternative SCM in portland cement concrete.

2. LITERATURE REVIEW

2.1 Waste eggshell generation and disposal

Eggs are an inexpensive and efficient source of nutrients (Conrad et al., 2017), making them a common part of people's diet worldwide. The U.S. is the third largest egg producer in the world (Mench et al., 2011). Egg production in the U.S. exceeds one billion dozen per year. The annual per capita egg consumption of U.S. citizens was reported to be around 280 in a study in 2019, and the number has been continuously increasing for the past decade (Waheed et al.,

2020). As a result, eggshell waste is generated in abundance at egg-breaking plants, bakeries, and regular households. However, eggshell disposal is becoming a challenge, with the Environmental Protection Agency placing post-consumer eggshell on the list of major wastes that cause environmental degradation at the landfill (Ahmed et al., 2021). American companies have reported an annual cost of $100,000 for the disposal of eggshell waste (Owuamanam & Cree, 2020). An egg breaking plant that provided the eggshell for the study had reported the generation of about 1 ton of waste weekly. To make matters worse, eggshell waste is increasingly being rejected at the landfill due to its ability to attract vermin, posing a biohazard and challenges to solid waste management (Ummartyotin & Manuspiya, 2018). The European Union has classified eggshell as hazardous waste (Mignardi et al., 2020; Quina et al., 2017), further exacerbating concerns about the rising requirements for disposal in the future.

2.2 Eggshell powder as a limestone alternative

Eggshell powder has significant potential as a source of $CaCO_3$ to be used as a replacement for limestone powder in blended cement as the chemical compositions is similar to limestone (Cree & Rutter, 2015). Moreover, eggshell is 2.5-3.0 on the Mohs hardness scale, whereas limestone is 3.0-4.0, so eggshell is more easily broken down to a small particle size than limestone. The challenge of eggshell waste management persists despite multiple emerging innovations that use $CaCO_3$ derived eggshell for paper-making (Tutus et al., 2022), fertilizer, feed (Wijaya & Teo, 2019), etc. Utilization of un-calcined eggshell powder as an additive in portland cement concrete has been explored in various countries (Chong et al., 2020). Some literature reported that cementitious composites achieved a slight improvement in strength at up to 10% eggshell powder replacement (Chong et al., 2023). However, the replacement levels are generally lower than that of limestone powder. Another approach in reusing eggshells is to calcine the material at higher temperatures, which results in powders with compositions similar to quicklime (calcium oxide). This could allow for a higher proportion of incorporation and achieve better mechanical performance for the resulting concrete; other uses of quicklime also exist (Khan et al., 2023; Yang et al., 2022). While it is still more environmentally friendly than making OPC clinkers, the calcination process released a significant amount of carbon dioxide, which reduces the sustainability benefits and compromises the purpose of exploring a low carbon alternative to cement clinker.

Similar to limestone powder, eggshell powder can alter cement hydration favorably and provide nucleation sites for the precipitation of cement hydration products (Shiferaw et al., 2019). However, the interaction between limestone or eggshell powder with cement was notably different (He et al., 2022). The efficacy of eggshell powder as a limestone powder substitute was hindered by the presence of impurities, varying amounts of organic content, and heterogeneous surface properties (Grzeszczyk et al., 2022). In particular, the presence of eggshell membrane is a major challenge for the application of eggshell powder in cementitious composites. Eggshell membrane is made up of less than 5% of the material by mass. It acts as a semi-permeable layer that prevents the exudation of egg white and the invasion of pathogens into the egg (Vuong et al., 2018). The membrane is composed of 90% protein fiber, 3% lipid, 2% sugar, and traces of calcium and magnesium (Han et al., 2023). As a biomaterial, it has been extracted from eggshells through ultrasonication, chemical dissolution, enzymatic methods, and more. However, organic matter is generally unfavorable in cementitious materials as it impedes the hydration of clinker. Additionally, the decomposition of organic matter increases the porosity of the matrix (Clare & Sherwood, 2007). Hence, additional studies comparing the performance of limestone powder and eggshell powder are needed to facilitate a potential transition to the more sustainable construction materials.

2.3 Sugarcane Bagasse Ash (SCBA) as SCM

2.3.1 Processing of SCBA

Prevalent studies illustrated the significance of processing raw bagasse ash as they observed improvements in properties such as specific surface area, pozzolanic activity, particle size, etc. following processing measures (Barbosa and Cordeiro, 2021). Common ways to gain improved properties including sieving, burning, grinding and chemical processing are widely adopted. Several studies also have investigated the impact of combination of treatment measures. Raw SCBA demonstrates higher loss on ignition (LOI) and carbon contents. Raw ash, when burnt at temperatures between 500-1100 ˚C for a varied time period reduces LOI and carbon contents in addition to increasing pozzolanic reactivity. However, at high temperatures(>800˚C) crystallization and thermal decomposition of SCBA is observed (N. Amin, 2011; Bahurudeen and Santhanam, 2015; Chusilp et al., 2009a; Ganesan et al., 2007b; Joshaghani and Moeini, 2017; Rajasekar et al., 2018; Yadav et al., 2020; Zhang et al., 2020). Inadequate burning of raw SCBA often leaves fiber particles with high carbon contents that cause reduction in

pozzolanicity. Several investigations illustrated that sieves, ranging from 75-2000μm, are effective in processing SCBA (Almeida et al., 2015; Arenas-Piedrahita et al., 2016; Kazmi et al., 2017a; Sales and Lima, 2010). Influence of mechanical crushing of SCBA was investigated by several researchers who observed that the grinding period significantly influences the particle size, specific surface area and pozzolanic reactivity (Chusilp et al., 2009a, 2009b; Cordeiro et al., 2009; Joshaghani and Moeini, 2017). Chemicals such as acids, sulfates, chlorides, etc. are utilized in other treatment procedures, where the improvement in fineness and removal of impurities have been observed (Embong et al., 2016; Joshaghani and Moeini, 2017). Combinations of the aforementioned treatment measures reported the improvement in pozzolanic reactivity of SCBA (Almeida et al., 2015; Arenas-Piedrahita et al., 2016; Bahurudeen and Santhanam, 2015; Ganesan et al., 2007b; Joshaghani and Moeini, 2017; Kazmi et al., 2017a; Rajasekar et al., 2018; Sales and Lima, 2010). In a separate study, Lyra et al. compared original and washed ashes to assess the K_2O content from the SCBA. They demonstrated a significant reduction of potassium from 37.5% in raw SCBA to 2.65% in washed SCBA, and an improved pozzolanic reactivity due to increasing the SiO_2 contents (Lyra et al., 2021).

2.3.2 Properties of SCBA

Physical properties such as specific gravity, particle size, specific surface area, fineness modulus and chemical composition have a direct impact on the pozzolanic activities of agricultural by-products. Many researchers put an emphasis on characteristic profiling to assess the mechanical and durability properties of SCBA based concrete. Physical properties of SCBA, as reported by the earlier researchers, are listed in Table 1. Color, which is one of the physical properties of pozzolanic materials, depends on the burning time, temperature as well as the percentages of silica contents present in the SCBA samples (Ganesan et al., 2008; Jittin et al., 2021). Previous researchers reported black, greyish black, and reddish grey as the variations of SCBA samples they worked on. When SCBAs are burned fully at high temperatures above 800 ˚C, they appear grey and LOI becomes <10%. However, with the presence of volatile mass, SCBAs appear as black (Abdalla et al., 2022; Bahurudeen et al., 2014; Batool et al., 2020; Praveenkumar et al., 2020). Embong et al. reported white SCBA ash to be extracted after extended period of combustion (Embong et al., 2016).

Table 1 Physical properties of SCBA

Ref.	Color	Specific Gravity	Fineness (passing 45-micron m. in %)	Specific Surface Area (m^2/kg)	Soundness, expansion (mm)
(Murugesan et al., 2020)	-	1.96	-	142	3.8
(Murugesan et al., 2022)	-	2.16		296	1.36
(Batool et al., 2020)	Black	-	-	70.13	-
(Bahurudeen et al., 2014)	Black	1.91	-	145	-
(Abdalla et al., 2022)	Greyish Black	2.06	-	-	-
(Rukzon and Chindaprasirt, 2012)	-	-	98	1250	-
(Praveenkumar et al., 2020)	Reddish Grey	2.20	100	514	-
(Shah et al., 2022)	Grey	-	-	225	-
(Quedou et al., 2021)	Light Brown	2.05	-	-	-

Various researchers reported that the specific gravity of processed as well as unprocessed SCBA is between 1.78 to 2.88. Processing conditions have an impact on the specific gravity of SCBA, i.e., increased rate of grinding resulted in increased specific gravity. The specific gravity of SCBA remains lower than cement which varies between 2.9-3.15 in previous research works, ultimately indicating lower density of concrete when portland cement is replaced by SCBA compared to those of portland cement only. With the increase of portland cement replacement percentages, density will decrease further. The low specific gravity of SCBA can be attributed to porous, carbon-rich particles. Andrade Neto et al. characterized the materials and reported that not only is the surface area of portland cement significantly lower than SCBA, but also SCBA particles have considerable larger average diameter (D_{50}) (Andrade Neto et al., 2021). The performance of concrete is often influenced by the specific surface area which determines other physical parameters of the powder. Different researchers revealed the significance of SCBA treatment as it is found that treated SCBAs have higher specific surface area compared to that of raw SCBA (Bahurudeen et al., 2014; Chusilp et al., 2009a; Cordeiro et al., 2009; Ganesan et al., 2007a; Rukzon and Chindaprasirt, 2012; Shah et al., 2022; Somna et al., 2012). Also, several researchers found that specific surface area is lower than Blaine's surface area, which increases the need of superplasticizer and other admixtures to obtain similar workability as that of control

mixes. Jagadesh et al. recorded that the density of SCBA is 2454 kg/m^3, while another separate study by Kazmi et al. found the bulk density of SCBA to be 610.6 kg/m^3 (Jagadesh et al., 2020; Kazmi et al., 2017b). Previous research identified morphological variances among the bagasse ash particles that make SCBA particles that have a spherical, prismatic, fibrous and irregular shape (Abdalla et al., 2022; Bahurudeen and Santhanam, 2015; Jagadesh et al., 2018; M. Inbasekar* et al., 2016; Rukzon and Chindaprasirt, 2012; Teja et al., 2017; B. S. Thomas et al., 2021). Chemical compositions of the SCBA collected by researchers from different places are listed in Table 2. From Table 2, the sum of pozzolanic oxide contents (SiO_2+Al_2O_3+Fe_2O_3) of raw SCBA constituted between 61.72% and 92% of the total mass. One exception was a sample from the U.S., in which SiO_2, Al_2O_3 and Fe_2O_3 contents constituted only 27.2% of the total mass. Based on ASTM C618, almost all the samples meet the requirements, and most samples reported in Table 2 could be classified as class F pozzolan. Silica remains the major requirement of pozzolanic reactions, and preceding studies substantiate the ample presence of silica contents in the SCBA. Andrade Neto et al. attributed high pozzolanic activity of calcined SCBA to the silica and alumina substances present in the ash (Andrade Neto et al., 2021).

Table 2 Chemical compositions of raw SCBAs from different countries

Ref	Source	SiO_2	Al_2O_3	Fe_2O_3	CaO	MgO	SO_3	K_2O	Na_2O	LOI
(Subedi et al., 2019)	USA	22.95	2.65	1.60	1.55	0.45	-	1.50	0.30	12.28
(Wu et al., 2022)	China	62.44	12.1	9.44	2.52	1.97	0.02	-	-	26.04
(M. Singh et al., 2021)	India	61.13	0.07	0.52	0.27	0.02	0.32	1.02	0.15	24.58
(Cordeiro and Kurtis, 2017)	Brazil	80.8	5.1	1.6	3.1	-	1.5	6.3	-	0.4
(M. Amin et al., 2022)	Egypt	63.87	-	-	4.29	2.01	-	15.81	3.16	-
(Abdalla et al., 2022)	Kenya	80.00	8.923	3.19	1.482	2.372	-	2.705	-	15.08
(Alavéz-Ramírez et al., 2012)	Mexico	51.66	9.92	2.32	2.59	1.44	-	2.10	1.23	24.15
(Rerkpiboon et al., 2015)	Thailand	55.04	5.14	4.06	11.03	0.91	2.16	1.22	0.24	19.60
(Chusilp et al., 2009a)	Thailand	54.10	5.69	3.54	15.37	1.41	0.03	-	-	19.36
(Murugesan et al., 2022)	India	75.9	1.55	2.32	6.65	-	1.60	9.40	0.81	4
(Katare and Madurwar, 2021)	India	38.48	0.66	1.15	2.14	1.12	-	-	0.07	49.67

Table 3 Chemical properties of processed/treated SCBA from different countries

Ref	Source	SiO_2	Al_2O_3	Fe_2O_3	CaO	MgO	SO_3	K_2O	Na_2O	LOI
(Chusilp et al., 2009a)	Thailand	77.37	3.59	4.66	7.81	1.32	0.15	-	-	5.08
(de Siqueira and Cordeiro, 2022)	Brazil	53.8	18.1	10.8	3.40	-	2.70	4.30	-	3.90
(Sinyoung et al., 2022)	USA	76.16	8.38	2.71	2.32	1.47	0.24	3.97	0.19	2.46
(Sales and Lima, 2010)	Brazil	88.20	2.30	5.10	0.60	0.40	0.10	1.30	0.10	0.35
(Embong et al., 2016)	Malaysia	84.30	1.10	1.70	1.90	1.40	0.50	2.90	0.30	0.10
(Abdalla et al., 2022)	Kenya	76.18	3.62	8.71	2.88	-	-	5.495	-	5.82
(M. Singh et al., 2021)	India	70.09	0.19	0.93	2.91	10.75	0.83	4.26	0.84	6.27
(N. Amin, 2011)	Pakistan	87.40	3.60	4.90	2.56	0.69	0.11	0.15	0.11	8.25
(Ganesan et al., 2007a)	India	64.15	9.50	5.52	8.14	2.85	-	1.35	0.92	4.90
(Andreão et al., 2019a)	Brazil	73.5	8.50	2.90	4.5	-	2.4	3.5	-	3.00
(Katare and Madurwar, 2021)	India	80.39	1.17	1.23	2.91	2.39	-	-	0.16	2.53
(Shah et al., 2022)	Pakistan	66.70	9.24	1.53	10.07	4.60	-	2.51	1.30	2.21
(D.-H. Le et al., 2022)	Vietnam	74.9	6.48	2.14	1.41	1.13	-	2.752	0.78	9.07

Loss on ignition is the process of determining the volatility of contents by incinerating the desired content at high temperatures and observing the changes in weight. ASTM C618 requires the loss of ignition to remain lower than 10% for Class N pozzolans and 12% for Class F pozzolans ("ASTM C618-22 Standard Specification for Coal Fly Ash and Raw or Calcined Natural Pozzolan for Use in Concrete," 2022). Raw SCBAs reported in Table 2 demonstrated a higher amount of coarse and fine fibers in the raw SCBAs. This resulted in higher percentages of LOI except in Brazilian SCBAs that reported 0.4% of LOI. Higher percentages of LOI suggest that there might be unburned or partially burned carbon in the material. This can negatively affect the SCBA's ability to act as a pozzolan (Arif et al., 2016; Bahurudeen and Santhanam, 2015; Chusilp et al., 2009a; Cordeiro, Barroso, et al., 2018).

The LOI measurement might not accurately reflect the exact amount of unburned carbon (Batra et al., 2011; Zhang et al., 2020). However, after multi-step processing that includes sieving and/or burning, loss on ignition values remained within 0.10% to 9.07%. Cordeiro et al. reasoned that substandard LOI affects the initial and final setting time when compared among unchanged SCBA, re-burnt SCBA and a reference mix (Cordeiro, Barroso, et al., 2018). Murugesan et al. compared the performance of raw and sieved bagasse ash, ultimately revealing that raw bagasse ash fails to meet minimum requisites for pozzolanic reactivity, whereas sieved bagasse ash exceeds the raw bagasse ash (Murugesan et al., 2020). Previous studies attempted to find a relationship among three factors including the incineration duration, temperature and LOI values. Evidence suggested that heating duration and temperature have positive impacts on the LOI values. Several authors have also summarized that with an increase of combustion duration and temperature, the LOI value decreases.

The chemical constituents of ordinary portland cement (OPC) and other cementitious materials reported by previous researchers are listed below in Table 4. From Table 4, it is evident that ashes from other agricultural wastes, such as rice husk ash (RHA), coconut husk ash (CHA), wheat straw ash (WSA), bamboo leaf ash (BLA) and corn cob ash (CCA) can contain significant amounts of silica, alumina and ferric oxide compositions.

Table 4 Chemical composition of OPC and different SCMs

Oxides	OPC	FA	SF	GGBFS	RHA	CHA	WSA	BLA	CCA
SiO_2	19.10	52.00	92.26	34.62	88	42.5	47.5	70.50	66.38
Al_2O_3	4.80	30.19	0.792	11.82	-	17.7	1.5	0.632	7.48
Fe_2O_3	3.20	8.14	1.574	2.73	0.1	8.17	0.5	0.468	4.44
CaO	61.10	3.98	0.436	37.73	0.8	4.3	5.5	7.860	11.57
MgO	2.70	0.83	0.292	9.43	0.2	0.71	2.5	1.84	2.06
SO_3	3.40	0.36	0.335	1.42	-	0.55	-	2.87	1.07
Na_2O	0.24	0.48	0.383	0.35	0.7	0.93	0.1	-	0.41
K_2O	0.70	1.62	1.314	0.50	2.2	0.82	10.1	5.14	4.92
LOI	4.10	0.63	-	1.20	8.1	6.51	-	7.79	1.47
Ref.	(Andrade de Neto et al., 2021)	(Deng et al., 2020)	(Landa-Ruiz et al., 2021)	(Shen et al., 2020)	(Rodríguez de Sensale, 2006)	(Arel and Aydin, 2018)	(Jankovsky, 2017)	(Rodier et al., 2019)	(Adesanya and Raheem, 2009)

These agricultural waste ashes can be a significant source for pozzolanic content when compared to industrial by-products such as fly ash (FA), silica fume (SF) and ground granular blast furnace slag (GGBFS).

2.3.3 Properties of SCBA containing mortars and concrete

2.3.3.1 Initial and final setting time

Channa et al. reported that increasing the amount of SCBA led to changes in the setting times of the cement paste samples. At 0% SCBA, the initial setting time was 80 minutes, and the final setting time was 260 minutes. When the SCBA replacement was increased to 15%, the initial setting time extended to 110 minutes, and the final setting time reached 310 minutes (Channa et al., 2022). Le et al. reported improvements in the initial and final setting times with an increase of SCBA replacement percentages in self-compacting concretes (D.-H. Le et al., 2018). PraveenKumar et al. reported that when 30% bagasse ash was added, the initial setting time increased by 40 minutes and the final setting time by 70 minutes compared to the control paste sample, and reasoned that this increase in the final setting time of the paste samples happened because the addition of bagasse ash delayed the hydration process (Praveenkumar et

al., 2020). Similar increasing trends of setting time were also reported with SCBA and different agricultural wastes by other researchers (Arel and Aydin, 2018; Arif et al., 2016; Ganesan et al., 2007b; Jankovsky, 2017; Kazmi et al., 2017b; Rukzon and Chindaprasirt, 2012).

2.3.3.2 Heat of hydration

Cement hydration in concrete produces heat. Many studies reported a decline in this heat with an increase of SCBA replacement percentages (Chusilp et al., 2009b; Montakarntiwong et al., 2013). Bahurudeen et al. reported that using SBCA as a replacement resulted in nearly 10% reduction in the total heat when SCBA replacement level was 10% as well as a 20% reduction in the peak heat rate of concrete at 20% dosage rate when compared to the control specimen (Bahurudeen et al., 2015). Klathae et al. also reported that a high volume replacement (50 to 80%) of portland cement by ground bagasse ash could generate lower heat in concrete, which could lessen the thermal stress cracking of the concrete in early-ages (Klathae et al., 2020). Conclusively, the inclusion of SCBA in concrete seems promising due to reduction in heat of hydration.

2.3.3.3 Workability

The workability of fresh concrete is of paramount importance on the job site, and slump values are a common method of inferring this quality. Mangi et al. confirmed that an increase in slump values indicates better workability. They found that slump values fell within the low to medium range of workability. They tested this on two different concrete grades with SCBA replacement levels of 0, 5 and 10% and found that adding superplasticizers was not necessary (Mangi et al., 2017). Srinivasan and Sathiya reported the improvement in workability of SCBA concrete when replacing portland cement with SCBA at levels ranging from 5 to 25% and noted that the need for superplasticizers was nearly negligible (Srinivasan and Sathiya, 2010). Other studies also reported the improvement in workability when portland cement is replaced by SCBA (Rajasekar et al., 2018). However, with the increase of SCBA dosages, reduction in workability of fresh concrete was observed by Channa et al (2022). A similar trend was observed in previous studies (Praveenkumar et al., 2020). Andrade Neto et al. reported that the texture of SCBA particles could require more water and/or admixtures in concrete to maintain workability (Andrade Neto et al., 2021). Rerkpiboon et al. also suggested that an addition of ground bagasse ash necessitated an increased use of superplasticizers (Rerkpiboon et al., 2015).A similar pattern was observed by other researchers that attributed this to different characteristics such as texture,

shape and the high porosity of SCBA particles (Chusilp et al., 2009b; Montakarntiwong et al., 2013; Rukzon and Chindaprasirt, 2012).

2.3.3.4 Compressive strength

Compressive strength, a mechanical property of concrete, remains an important indicator of the general performance of cementitious materials for structural purposes. In Table 5, the results of data regarding the compressive strength of concrete made with SCBA are summarized. Previously, researchers found improvements in strength of SCBA blended concrete compared to concrete without SCBA (Srinivasan and Sathiya, 2010). When samples were prepared with an increase or decrease in replacement percentages from the optimum, significant reductions in compressive strength were observed. Previous studies also examined the effects of treatment and processing on the compressive strength of concrete and mortars made with SCBA. They found that strength development was slow at early stages. However, with longer curing periods, the pozzolanic nature of SCBA became evident, and the strength of the samples surpassed that of the control specimens (Cordeiro et al., 2019; Cordeiro, Paiva, et al., 2018; Rao and . Prabath, 2015). Singh et al. (2021) found that after processing, not only did the compressive strength increase at all ages, but the optimum replacement level also increased from 10% for ground bagasse ash to 20% for processed bagasse ash. This strength increase attributed to the presence of amorphous silica, prompted researchers to conclude that an increase in LOI and bagasse ash contents negatively impacts the compressive strength (M. Singh et al., 2021). A study by Quedou et al. revealed the importance of the curing period for concrete made with SCBA. The study found that, despite a decrease in compressive strength at an early stage due to porous SCBA and unburnt carbon content, strength increased with longer curing periods. For 5% and 10% SCBA replacements, compressive strength improved significantly after 120 days of curing (Quedou et al., 2021). Another study by Mangi et al. reported similar results (Mangi et al., 2017).

Table 5 Compressive strength development of SCBA blended concrete and mortars

Ref.	Design Strength / Mix Design	Cement Type	SCBA (%)	w/b ratio	7 days	14 days	28 days	90 days	Optimum dosage (%)
(Khan et al., 2021)	M40 (1:1.98:3.6)	OPC Grade 53	0	0.4	36.22	N.a.	50.16	N.a.	10%
(Khan et al., 2021)	M40 (1:1.98:3.6)	OPC Grade 53	10	0.4	37.46	N.a.	53.8	N.a.	10%
(Khan et al., 2021)	M40 (1:1.98:3.6)	OPC Grade 53	15	0.4	32.2	N.a.	48.04	N.a.	10%
(Khan et al., 2021)	M40 (1:1.98:3.6)	OPC Grade 53	20	0.4	31.62	N.a.	43.36	N.a.	10%
(Khan et al., 2021)	M40 (1:1.98:3.6)	OPC Grade 53	5	0.4	37.08	N.a.	51.1	N.a.	10%
(Loganayagan et al., 2021)	M20	OPC Grade 43	0	0.3825 to 0.395	19.18	N.a.	22.46	N.a.	10%
(Loganayagan et al., 2021)	M20	OPC Grade 43	10	0.3825 to 0.395	13.44	N.a.	23.5	N.a.	10%
(Loganayagan et al., 2021)	M20	OPC Grade 43	15	0.3825 to 0.395	10.19	N.a.	21.05	N.a.	10%
(Loganayagan et al., 2021)	M20	OPC Grade 43	5	0.3825 to 0.395	17.01	N.a.	21.0	N.a.	10%
(Mangi et al., 2017)	M15 (1:2:4)	OPC (ASTM C150 Type-I)	0	-	17.3	18.5	24.11	N.a.	5%
(Mangi et al., 2017)	M15 (1:2:4)	OPC (ASTM C150 Type-I)	10	-	17.54	20.62	24.67	N.a.	5%
(Mangi et al., 2017)	M15 (1:2:4)	OPC (ASTM C150 Type-I)	5	-	18.89	21.95	27.2	N.a.	5%
(Mangi et al., 2017)	M20 (1:1.5:3)	OPC (ASTM C150 Type-I)	0	-	18.07	20.68	26.6	N.a.	5%
(Mangi et al., 2017)	M20 (1:1.5:3)	OPC (ASTM C150 Type-I)	10	-	19.52	22.84	5.81	N.a.	5%
(Mangi et al., 2017)	M20 (1:1.5:3)	OPC (ASTM C150 Type-I)	5	-	21.39	26.78	29.92	N.a.	5%
(Rao and Prabath, 2015)	M25	OPC Grade 53	0	0.42	29.13	N.a.	36.18	37.93	10%
(Rao and Prabath, 2015)	M25	OPC Grade 53	10	0.42	27.26	N.a.	37.52	39.85	10%
(Rao and Prabath, 2015)	M25	OPC Grade 53	15	0.42	24.44	N.a.	33.93	35.41	10%
(Rao and Prabath, 2015)	M25	OPC Grade 53	20	0.42	21.93	N.a.	30.07	31.56	10%
(Rao and Prabath, 2015)	M25	OPC Grade 53	25	0.42	19.26	N.a	24.85	26.52	10%
(Rao and Prabath, 2015)	M25	OPC Grade 53	5	0.42	28.15	Na.	36.89	38.67	10%

Other researchers also investigated blending SCBA with different industrial and agricultural wastes, such as silica fumes, GGBS, RHA, coal bottom ash, and others in OPC (Bheel et al., 2022). Landa-Ruiz et al. found that 30% replacement of portland cement by the combination of SCBA and silica fume is the optimum mixture for increased compressive strength after 180 days of curing (Landa-Ruiz et al., 2021). A study by Klathae et al. showed that the incorporation of limestone powder at 60-80 wt.% of binder in high strength concrete made with SCBA increases compressive strength significantly at 28 days, even after a minimal presence of cement in the mixture (Klathae et al., 2021). In a separate study, Khan et al. tested the durability of different concrete specimens by immersing them in two distinct acid solutions (H_2SO_4 and HCl) after curing them for 28 days under normal conditions. They reported a compressive strength reduction in all the concrete samples. Concrete made with a mix of 10% SCBA and 10% micro silica proved to be optimum replacement (Khan et al., 2021). Other studies replaced OPC with 25% SCBA and reported strength development equal to or higher than reference mixtures even during early ages (Akram et al., 2009; Bahurudeen et al., 2016; de Siqueira and Cordeiro, 2022; Shafiq et al., 2018). Findings from existing studies suggest that 5% to 20% replacements of OPC by SCBA are optimum (Bahurudeen et al., 2015; Mangi et al., 2017; Quedou et al., 2021; Rajasekar et al., 2018; M. Singh et al., 2021).

2.3.3.5 Tensile and flexural strength

Using SCBA, a very similar pattern was observed in the growth of the concrete's splitting tensile strength and compressive strength (Minnu et al., 2021). Zareei et al. reported a reduction in tensile strength with the increase of replacement percentages of SCBA (Zareei et al., 2018). Klathae et al. reported an influence of curing period and observed an increase in tensile strength at the later ages compared to an early age (Klathae et al., 2020). Reduction of tensile strength with an addition of SCBA beyond 20% was observed in several studies (N. Amin, 2011; Ganesan et al., 2007b; Praveenkumar and Sankarasubramanian, 2019; S. Singh et al., 2018). The optimum range was found to be in between 5 and 20 % (Ganesan et al., 2007b; Sanchana sri and Ramesh, 2017; Srinivasan and Sathiya, 2010).

In existing literature, flexural strength analysis showed similar trends of compressive strength with increasing dosage rates of SCBA (Minnu et al., 2021). Researchers studied the effects of incorporating various contents of SCBA in pavement concrete and found that at 28 days, flexural strength decreases with the increase of SCBA replacement levels (Chindaprasirt et

al., 2019). Joshaghani et al. observed a maximum flexural strength at 10% SCBA replacement (Joshaghani and Moeini, 2017). Others found that adding bagasse ash usually lowered the flexural strength of concrete, except in mixtures with 5% and 10% bagasse ash. The mixture with 10% bagasse ash showed the highest strength, suggesting that substituting 10% of the material with bagasse ash optimizes flexural strength (Batool et al., 2020). From other reviewed studies, at 28 days, 5%-20% replacement levels have proved to be the optimum (Dhengare et al., 2015; Srinivasan and Sathiya, 2010).

2.3.3.6 Durability

Durability analysis conducted by Andrade Neto et al. revealed a reduction in concrete porosity as well as sorptivity when portland cement is replaced by SCBA up to 15%. They also extended that SCBA replacement leads to a prolonged lifespan against chlorine ion penetration due to reduced chloride diffusivities. Longevity rose up to 95.7% for concrete containing 15% SCBA. Authors also observed that adding 5% SCBA reduced alkali-silica reactivity (ASR) due to the pozzolanic reaction, which enhances C-S-H formation and refines pores. However, higher amounts of SCBA (10% and 15%) gradually increased ASR because of the rising alkali content in the SCBA (Andrade Neto et al., 2021). Khan et al. revealed through durability testing that SCBA concrete is more susceptible to sulfate attacks than chlorine attacks (Khan et al., 2021). Bahurudeen et al. suggested that the increase in chloride resistance of concrete with SCBA is related to presence of higher pozzolanic constituents and improved pore structure of SCBA (Bahurudeen et al., 2015). A similar trend in chloride resistance of concrete made with varying percentages of bagasse ash was noted in past studies (Rerkpiboon et al., 2015). Rukzon and Chindaprasirt reported a reduction in chloride ion penetration when SCBA replacement percentages increased (Rukzon and Chindaprasirt, 2012).

Katare et al. revealed an optimum mixture of treated bagasse ash and ground granular blast furnace slag that has substantial water permeability reduction as well as an improvement in the chloride ion permeability resistance (Katare and Madurwar, 2021). A similar trend in the reduction of water penetration with increasing SCBA replacement percentages was observed by Bahurudeen et al (Bahurudeen et al., 2015). Mahima et al. reported that as the amount of SCBA used to replace cement in concrete increased, the permeability of the concrete significantly decreased. They attributed this improvement to the greater pozzolanic reactivity of the SCBA. (Mahima et al., 2017). Arenas-Piedrahita et al. observed a significant decrease in permeability of

mortar made with 20% untreated SCBA (Arenas-Piedrahita et al., 2016). An increase in resistance to Na_2SO_4 with addition of ground bagasse ash in concrete when compared to control mix was observed by Rerkpiboon et al (Rerkpiboon et al., 2015).

3. EXPERIMENTAL METHODOLOGIES

3.1 Material characterization

3.1.1 Processing of waste eggshell

The eggshell powder was sourced from an egg breaking plant from Pennsylvania, United States. The as-received eggshell powder is shown in Figure 1. Hubercarb® M300 limestone powder was used as a comparison. A series of procedures were conducted to process the eggshell into a finer powder form for use in the experiment, and the material was characterized. Table 6 summarizes the processes and experiments undertaken in this section. As-received raw eggshell contained a significant amount of water and had an average particle size of 300µm. The raw material was first placed in an oven and heated at 105˚C for 1 day. From the test, a mass loss of 20% was measured, which indicated the moisture content of the material. Additional lab processing of eggshell powder was conducted by grinding the eggshell with a ball mill, followed by sieving through 150µm and 45µm sieves. Powder passing through 45µm sieve was collected and used as the cement replacement.

Table 6 Summary of eggshell characterization and processing with key findings

Process	Description	Findings
Drying	As-received eggshell was oven dried at 105ºC for 1 day	Based on mass loss, as-received eggshell contained 20% water content.
Milling and sieving	Eggshells were milled using a ball mill and sieved through 150µm and 45µm sieve.	Eggshell samples retained above 150µm sieve and passing 45µm sieve were collected for the subsequent test.
Loss of ignition	Eggshell powder samples were incinerated at 300˚C, 500˚C, and 700˚C for 2 hours.	The loss of ignition curve is shown in Figure 2. Eggshell samples above 150µm lost more mass, indicating higher organic content.
Imaging	Eggshell powder passing 45µm to be used in the experiment was imaged with SEM.	SEM images of both materials are presented in Figure 3. Eggshell powder and limestone powder had similar morphology.

Figure 1 As-received waste eggshell from egg breaking plant.

It is critical to understand the influence of eggshell membrane on particle size distribution and material processing. Hence, as-received powder, retained powder above 150µm, and ground powder passing 45µm were incinerated at 300˚C, 500˚C, and 700˚C for 2 hours. The mass loss of each sample is plotted in Figure 2. The mass loss at 300˚C corresponded to the loss of some organic material, and the mass loss at 700˚C corresponded to the removal of all organic matter as well as the beginning of $CaCO_3$ decomposition. As presented in Figure 2, the raw and ground powder had a similar mass loss across all temperature ranges. However, the retained powder (>150µm) lost a greater portion of its mass when incinerated, indicating a higher organic content. This showed that during the milling process, larger portions of the eggshell membrane could not be broken down to smaller sizes, presumably due to the flexibility of protein fiber present in the membrane. Hence, mechanical milling was partially effective in reducing the organic content in eggshell powders. However, even eggshell powder passing through the 45µm sieve lost about 9% of its dry mass at 700˚C. In another test, the percentage of eggshell passing 150µm and that after 300˚C incineration was compared. The test showed that there was no significant difference between the yield, and for that reason, the data was not presented in the report. It was concluded that incineration did not aid the separation and filtration of the membrane in the eggshell powder.

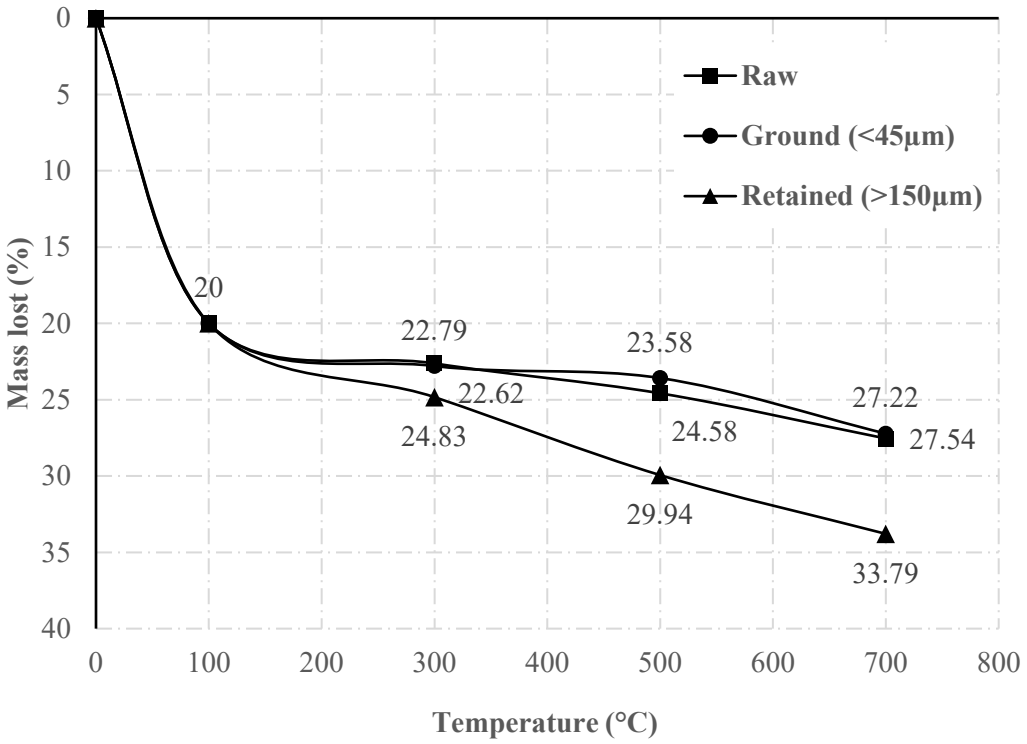

Figure 2 Mass loss for raw eggshell and eggshell powder after heat treatment.

Subsequently, scanning electron microscopy (SEM) of both limestone powder and eggshell powder were performed under a low vacuum as depicted in Figure 3. From the images at 3300× magnification, both limestone powder and eggshell powder have similar morphology which is angular and uneven. Using ImageJ, the information on the particles in another set of 1000× magnification SEM images were extracted, and the morphology of each particle was quantified using the "Circularity" function. The probability density was plotted in Figure 4 Probability density plot of eggshell and limestone sphericity., and it indicated that limestone particles had slightly higher sphericity compared to eggshell particles. The average sphericity of the powder was 0.54 for limestone and 0.47 for eggshell. Regardless, the morphology of both powders was similar, considering the difference in the milling and preparation process.

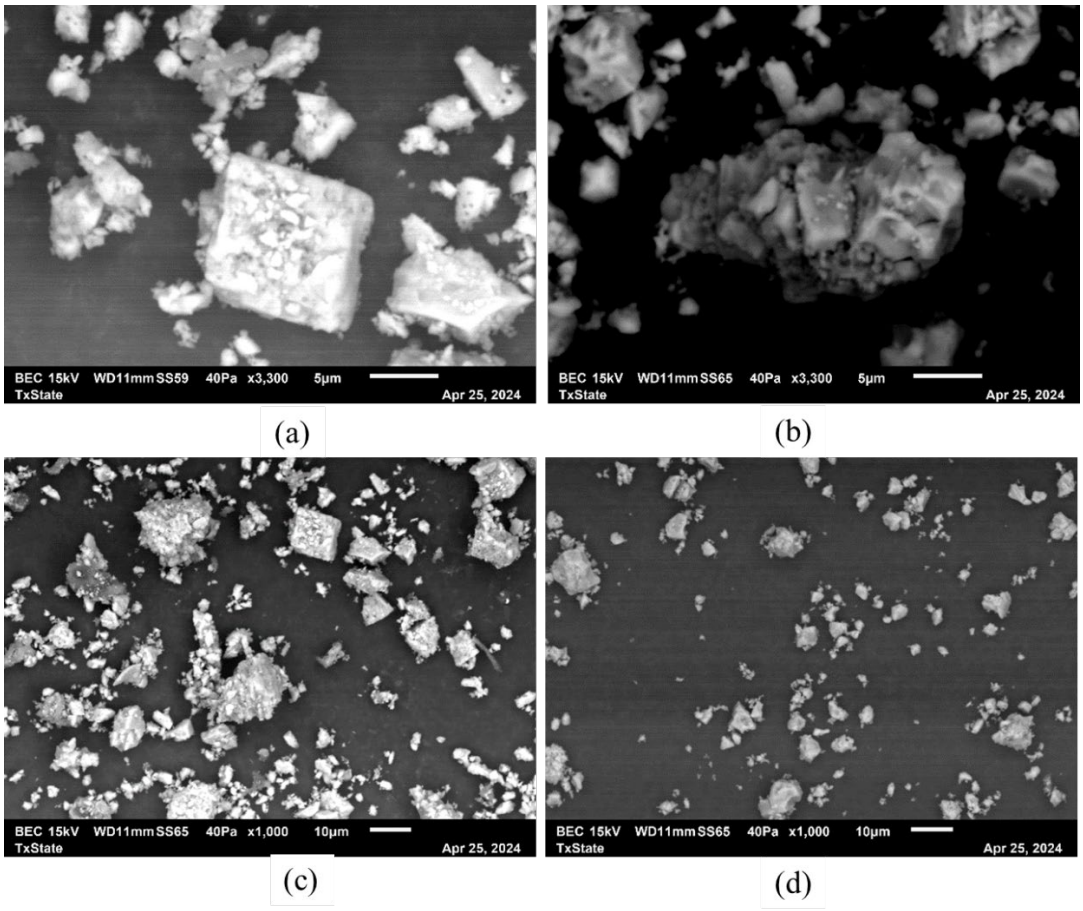

Figure 3 SEM image of (a) eggshell at 3300× (b) limestone at 3300× magnification (c) eggshell at 1000× (d) limestone at 1000×.

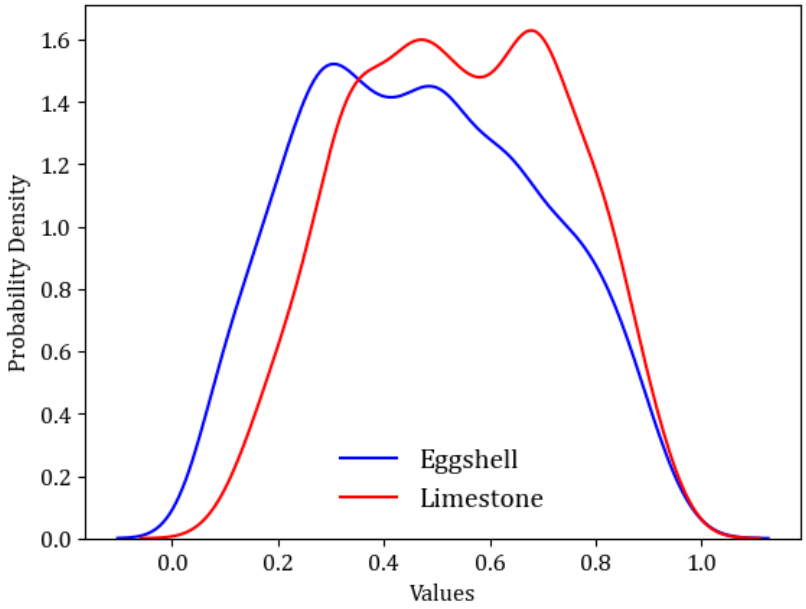

Figure 4 Probability density plot of eggshell and limestone sphericity.

3.1.2 Treatment of eggshell powder

Limestone powder and as-received eggshell powder served as the reference for comparing the efficacy of treatments. Eggshell powder was submerged into a large amount of water and stirred for 1 hour using a magnetic stirrer. Afterwards, the vessel was left in ambient condition for 24 hours to allow the mixture to stabilize. A part of the eggshell agglomerated into spherical lumps that gradually rose to the surface of the water. At the same time, sediments of a finer white substance remained at the bottom of the vessel. Due to the distribution of organic matter within the material, eggshell is not a homogenous material, and it contains particles of widely different densities which can be stratified by submerging eggshell particles in water, as shown in Figure 5. For further analysis, the floating and submerged material was separately collected to be dried at 105±5˚C for 24 hours. Additionally, the component on top (denoted as ES_T) and bottom (ES_B) were characterized and used for the preparation of blended cement paste. Upon drying, the yield of ES_B accounted for 90% of the mass of eggshell treated, and only 10% of eggshell by weight was collected from the water surface.

Figure 5: Stratification of eggshell powder in water, with sample collected from the water surface (left) and bottom of vessel (right).

Heat treatment of eggshell powder was conducted by incinerating as-received eggshell powder at 300±1˚C and 500±1˚C. The muffle furnace was set to reach the designated temperature after 15 minutes and maintain it for two hours. Two subsequent hours were necessary to cool the powder enough to be handled. Eggshell powder after burning is denoted as ES_{300} and ES_{500}. A summary of the cementitious powder to be tested is presented in Table 7.

Table 7 Nomenclature and description of powders tested.

Nomenclature	Description
LS	Commercialized limestone powder
ES	As-received eggshell powder ground and sieved to 45µm
ES_T	Eggshell powder ground and sieved to 45µm, submerged in water and collected from surface of water
ES_B	Eggshell powder ground and sieved to 45µm, submerged in water and collected from bottom of water
ES_{300}	Eggshell powder ground and sieved to 45µm, incinerated at 300˚C for 2 hours
ES_{500}	Eggshell powder ground and sieved to 45µm, incinerated at 500˚C for 2 hours

3.1.3 Characterization of eggshell powder

Thermogravimetric analysis (TGA) was performed on eggshell powder prior to any treatment to obtain a thorough thermal stability profile of organic impurities within the material, as shown in Figure 6. A comparison was made with commercial limestone. Slight differences were observed between the results of the two materials. Limestone powder was thermally stable and experienced negligible weight loss up to 600˚C, while eggshell powder steadily lost weight from 200˚C to 600˚C due to the decomposition of organic matter. From the derivative curve, a sharp steep in the curve was observed at around 300˚and the curve stabilized at around 400˚C, making suitable milestones for experimentation. Beyond 600˚C, both materials experienced a sudden, massive weight loss due to the calcination of $CaCO_3$ into CaO. The difference in the remaining weight of both materials was the 6% organic content of eggshell powder.

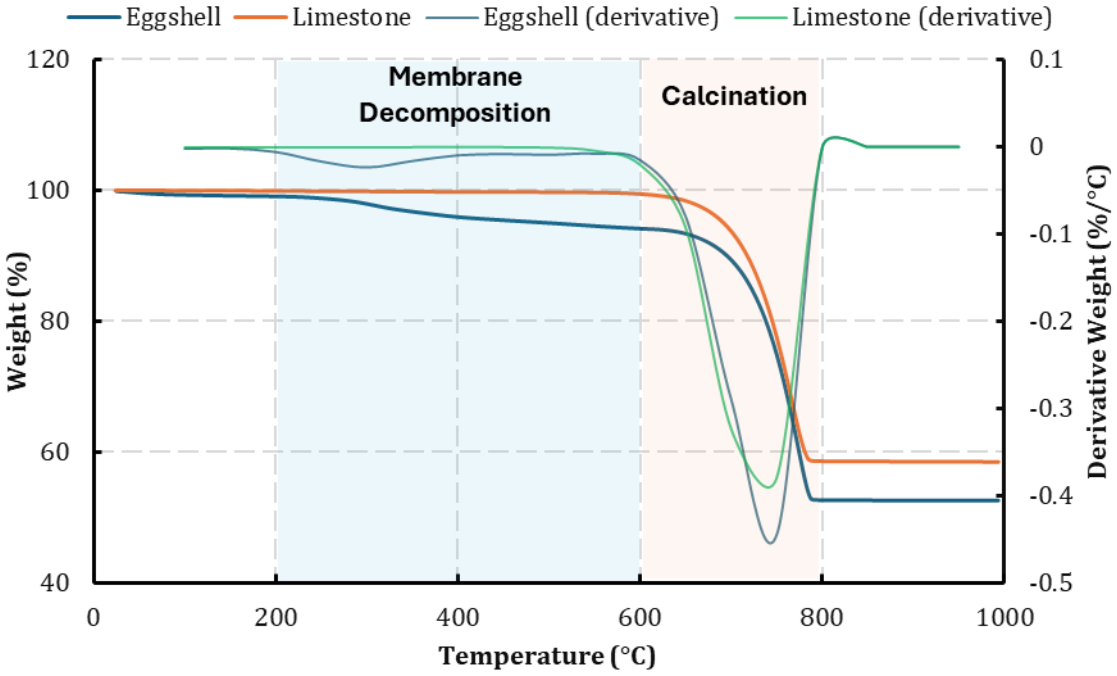

Figure 6 TGA analysis of eggshell and limestone.

Untreated ES, ES_{300}, and ES_{500} were characterized by X-Ray Diffraction (XRD) to investigate the phase composition of the materials. Figure 7 presents the diffractograms of the scanned powders. All scanned samples were comprised of calcite phase, as $CaCO_3$ is the major content of limestone and eggshell, and the presence of organic content could not be detected by XRD. Calcium oxide was not detected after the incineration of eggshell up to 500˚C, indicating that calcination did not occur from the process. The morphology of each powder was determined through Scanning Electron Microscope (SEM) imaging as presented in Figure 8(a), dendritic features were found on the surface of untreated eggshell particles, which suggested the presence of organic content adhering to calcium-rich particles. Such morphology may cause an increase in water demand due to increased total surface area which may hinder the bonding between the particles and cement matrix. After heat treatment, eggshell particles displayed an irregular and granular morphology due to the removal of organic matter, which may result in higher workability and the formation of a more cohesive cement matrix when included into cementitious binder.

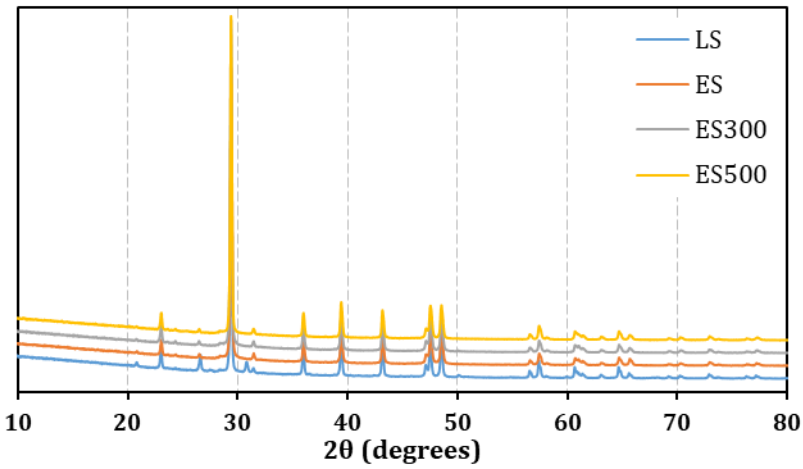

Figure 7 XRD diffractogram of limestone, as-received eggshell, and treated eggshell, with all powder comprised of only calcite phase.

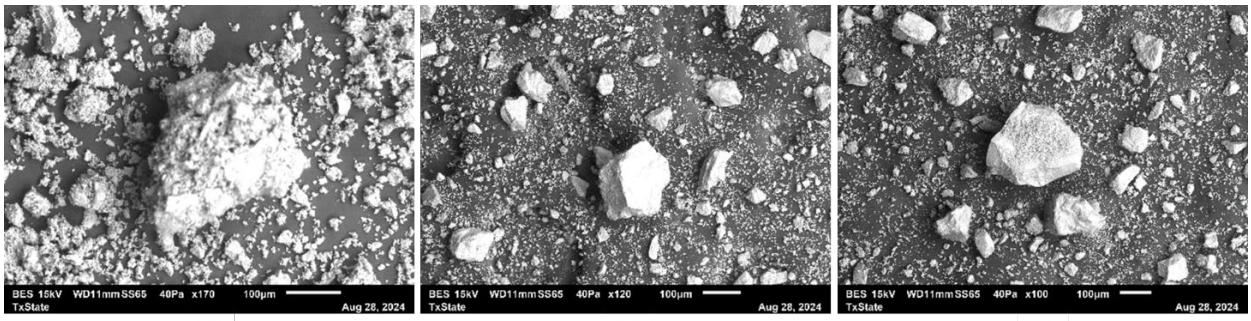

Figure 8 SEM image of a) untreated eggshell b) eggshell heated to 300˚C for 2 hours c) eggshell heated to 500˚C for 2 hours.

3.1.4 Characterization of SCBA

To evaluate the effects of thermal processing on the collected sugarcane bagasse ash samples, the ashes were recalcined through a bench top furnace, Keith model K-161220-B. Different temperature conditions from 500℃ to 900℃ were adopted, and the duration of processing was 2 hours for all specimens. The furnace was preheated at 15℃/min until it reached the desired temperature, after which 50 grams of ashes were recalcined for 2 hours at the target temperatures. Oxide compositions of sugarcane bagasse ashes were determined by X-ray Fluorescence (XRF). XRF testing was conducted using Rigaku Supermini200, which is shown in Figure 9.

Figure 9 Rigaku Supermini 200 XRF device.

Table 8 Oxide composition of differently processed SCBAs

Oxide Components (%)	**As-Received Sugarcane Bagasse ash**	**500 °C**	**600 °C**	**700 °C**	**900 °C**
SiO_2	65.74	67.74	68.21	67.79	66.40
Al_2O_3	5.12	5.73	5.79	5.88	5.87
Fe_2O_3	4.70	3.64	3.44	3.52	4.16
SiO_2+Al_2O_3+Fe_2O_3	75.56	78.10	78.44	77.19	76.43
K_2O	8.09	6.89	6.90	6.98	6.814
CaO	9.34	6.85	6.82	7.12	9.26
Na_2O	0.77	0.78	0.68	0.76	1.04
SO_3	1.82	1.76	1.81	2.76	1.87
MgO	0.98	1.52	1.42	1.42	1.40
P_2O_5	1.64	1.93	1.91	1.85	2.14
TiO_2	0.75	0.44	0.49	0.49	0.57
MnO	0.12	0.11	0.09	0.10	0.12

The collected sugarcane bagasse ash was oven-dried first. Some of the samples were then sieved through No. 200 sieves to discard the large, irregular-shaped and unburnt particles present in the raw ashes. Oven dried as-received SCBAs and sieved SCBAs were analyzed using Laser Diffraction Particle Size Distribution Analyzer. Table 9 summarizes the results from particle size analysis.

Table 9 Particle size analysis data[1]

Material	D_{10} µm	D_{50} µm	D_{90} µm	Mean Particle Diameter (µm)	Specific Surface Area (cm^2/cm^3)
Raw SCBA	15.21	45.24	118.66	58.37	1853.6
Sieved SCBA through 325 mesh	12.48	29.43	62.63	34.35	2530.2

Scanning Electron Microscopy (SEM) analysis was performed on the SCBA to determine if particle distribution was altered in the sieving processes. SEM was conducted using JSM-6010Plus/LA. Samples were loaded onto the SEM stub using copper conductive tape. The testing device is shown in the Figure 10.

XRD testing was also conducted in the Shared Research Operations (SRO) facility at Texas State University. The ash samples were tested for the range of 3° to 90° for 2θ at the step width of 0.002°, the radiation used at a voltage of 40kV and the monochromatic Cu-Kβ for the scanning. ICDD (PDF-2 Release 2020 RDB) was used during the analysis.

Figure 10 JEOL SEM device.

To determine moisture content of the collected SCBA samples, a representative sample that weighed two grams was collected. The sample was placed into a pre-weighed and pre-dried crucible, and then dried in an oven at 105 ± 5°C (221 ± 9°F) for 24 hours to remove evaporable moisture content (Bahurudeen et al., 2014). Once the sample was thoroughly dried, it was

[1] This test was conducted at Texas A&M University by Xincheng Ethan Wang

weighed once again after being cooled to room temperature in a desiccator. For loss on ignition (LOI) testing in this study, the test was conducted in the bench-top furnace at 950°C according to ASTM C114 ("ASTM C114-24 Standard Test Methods for Chemical Analysis of Hydraulic Cement," 2024). In the context of agricultural waste materials, a high LOI value might indicate the presence of unburnt carbon or other combustible impurities, which can affect the material's quality and performance. The loss on ignition test is essential for evaluating the purity and composition of materials such as portland cement, minerals, and various ashes, including SCBA.

The physical properties of SCM have an important impact on the fresh properties of concrete. The physical properties, including specific gravity, particle size and shape, color, stability, looseness and compacted bulk density of SCBA have already been studied thoroughly. Generally, the raw SCBA obtained from sugar mills is black, due to the relatively high amount of unburnt carbon. When the ash was burnt at higher temperatures in this study, a change in color was observed from black to reddish grey to white in color, as shown in Figure 11. The change of color is primarily affected by the recalcination temperature, duration and the structure of silica in ash.

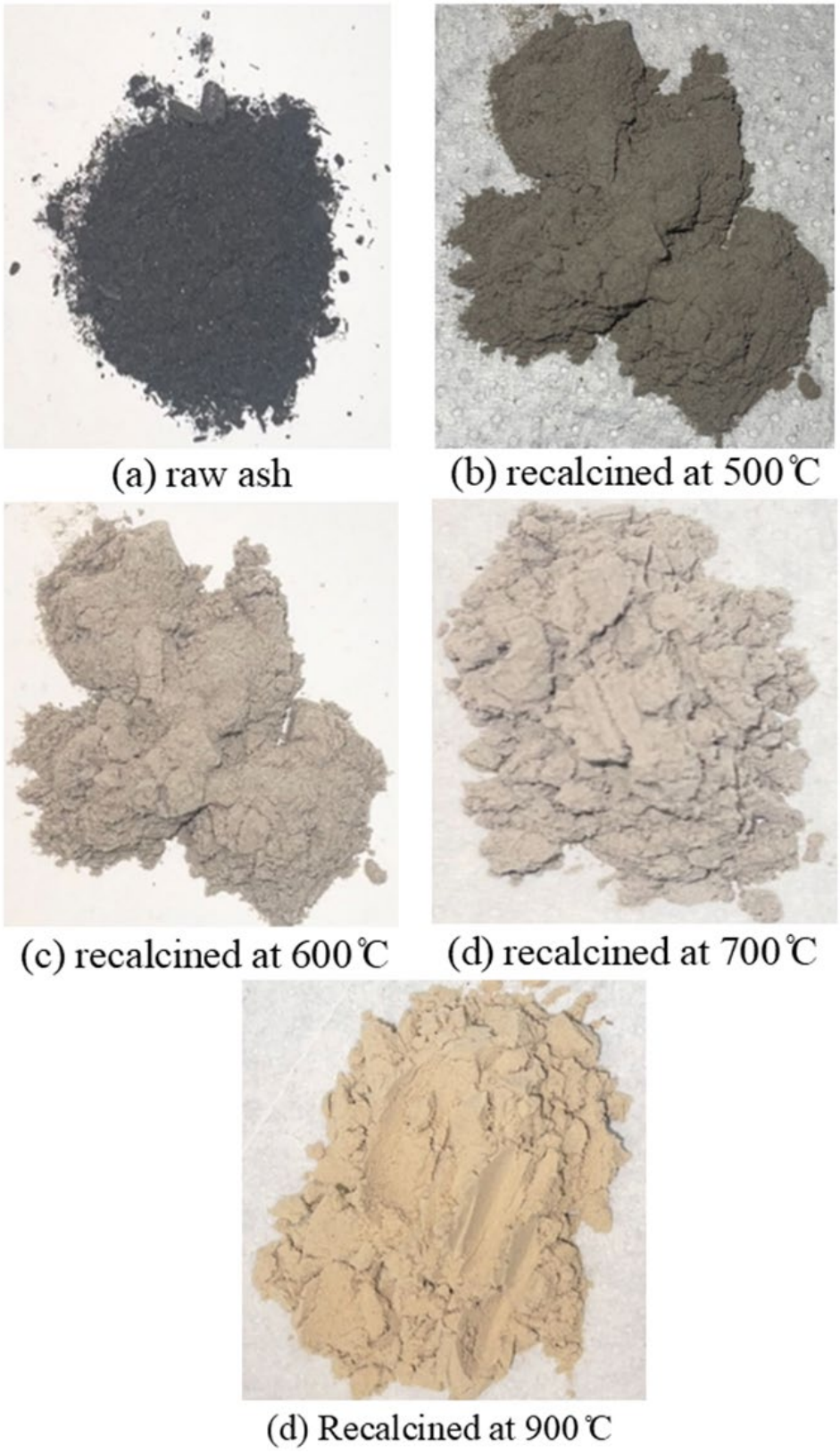

Figure 11 Change of color of SCBAs at different processing conditions.

Understanding the chemical characteristics of SCBA is crucial for its successful use as a substitute for cement in concrete. From Table 8, it can be concluded that all studied materials, irrespective of their thermal processing condition, fulfilled the standard requirements to be considered as Class F pozzolan. However, careful investigation of the dataset provides a detailed comparison of the chemical composition of as-received and thermally treated sugarcane bagasse ash (SCBA). The varying temperatures treated were specifically 500°C, 600°C, 700°C, and 900° for duration of 2 hours. This analysis follows the guidelines of ASTM C618, which sets the standards for the use of coal fly ash and raw or calcined natural pozzolan for use in concrete. ASTM C618 specifies that non-traditional Class F fly ashes must possess a minimum sum of 50% silica (SiO_2), alumina (Al_2O_3) and ferric oxide (Fe_2O_3) and a maximum of 18% calcium oxide contents. As-received SCBA contains 65.74% SiO_2, which increases moderately with temperature up to 600°C (68.21%) and then decreases again after burning to 900°C (66.40%). Higher SiO_2 content typically improves pozzolanic activity, enhancing the ash's ability to react with calcium hydroxide to form additional cementitious compounds. Al_2O_3 content increases consistently from 5.12% in as-received ash to 5.87% at 700°C, stabilizing slightly lower at 900°C (5.87%). Fe_2O_3 decreases with increasing temperature, from 4.70% in as-received ash to 3.44% at 600°C, with a partial rebound at 900°C (4.16%). The combined content of SiO_2, Al_2O_3, and Fe_2O_3 increases consistently, peaking at 600°C (78.44%), indicative of enhanced pozzolanic potential according to ASTM C618, which requires a minimum of 70%. CaO decreases initially from 9.34% in as-received ash to 6.82% at 600°C, then fluctuates slightly at higher temperatures. Lower CaO might reduce the self-cementing properties of the ash, favoring its use as a pozzolan rather than as a cementitious material. K_2O decreases from 8.09% in as-received ash to about 6.90% by 600°C and remains stable thereafter. Na_2O shows slight variability but generally remains within the 0.68% to 0.78% range. These alkalis can affect the reaction rate and durability of the concrete, potentially leading to alkali-silica reactions if not properly managed. MgO, P_2O_5, and TiO_2 generally increase with temperature, which could contribute to various properties such as the modification of setting time and color in concrete. SO_3 peaks significantly at 900°C (2.76%), which could impact the sulfate resistance of concrete. MnO remains relatively stable across all temperatures. In conclusion, the thermal treatment of SCBA generally increases the content of silicon dioxide and aluminum oxide, essential for pozzolanic activity, while reducing components like calcium oxide, which could influence the material's hydraulic

properties. The chemical components of SCBA at 600°C show a promising balance, optimizing the pozzolanic potential while maintaining lower levels of less desirable oxides like Fe_2O_3. This research found that heating the ashes didn't greatly change their chemical makeup, which is important for their pozzolanic reactivity. Additionally, producing ashes with a bench-top furnace is more expensive due to higher energy costs and slower production rates. Because of these findings, the study focused only on using ash in two forms: as-received and after it was sieved through a no. 200 sieve and oven-dried.

From the moisture content test, the collected raw samples contained moisture of 35%, which can be due to collection of samples from the ash pond where it was kept for primary removal of harmful chemicals through aeration and floatation. From the Loss on Ignition test, it is found that the LOI remains at 15.39% in as-received SCBA samples, which are higher than 10% for natural pozzolans and 6% for Class C pozzolans standard set by ASTM C618. Previous studies attributed the high LOI values as a result of the presence of unburnt carbons and organic impurities, which can lead to the reduction of pozzolanic reactivity and workability (Chusilp et al., 2009a). Similar results were observed for raw bagasse ashes in other prevalent research work as well (Bahurudeen and Santhanam, 2015). For the oven-dried SCBA samples, sieved through no. 200, LOI was found to be 2.29%. Thus, sieving reduces a portion of the burnt/unburnt coarse fibers, ultimately lowering the LOI of the ash sample and changing the color of the ash from blackish to grayish.

XRD testing was conducted on the SCBA and OPC to identify whether the structure of the material may be amorphous or crystalline. XRD patterns provided in the Figure 12 demonstrate distinct mineralogical characteristics of sieved SCBA, raw SCBA, and OPC. The green line, representing OPC, shows sharp peaks corresponding to well-known cement phases such as gypsum (1), C2S (2), C3S (3), C3A (4), and C3AF (5), indicative of OPC composition. These peaks are sharp and well-defined, suggesting a highly crystalline structure. The red line, for raw SCBA, displays broader and less intense peaks, signifying a less crystalline material with phases that are not as well-defined as in the OPC. Notable peaks correspond to quartz, cristobalite, and microcline, minerals commonly found in SCBA. These findings indicate the presence of amorphous or semi-crystalline silica in the raw SCBA, which could contribute to pozzolanic activity when used in concrete applications. The blue line, representing sieved SCBA, shows a similar pattern to raw SCBA but with slightly more pronounced peaks, particularly for

quartz and cristobalite, potentially altering its reactive properties. Microcline's presence in SCBA, as indicated by the XRD peaks, suggests that SCBA contains components derived from the clay minerals commonly found in sugarcane soils or ash residues. Microcline is a type of potassium feldspar characterized by its structure, which allows for the substitution of potassium by other cations, making it potentially reactive in certain chemical environments. The peaks corresponding to microcline in the XRD spectra are less sharp and intense compared to the quartz and cristobalite peaks, indicating a lower crystallinity or a less abundant presence. Broad scattering peaks (humps) between 15° and 30° on the 2θ axis indicate the formation of amorphous silica, which is the key component in pozzolans and is critical for pozzolanic reactions. Similar XRD patterns for bagasse ash, which highlight the presence of this amorphous silica, have been documented in prior studies as well (Ganesan et al., 2007b; Setayesh Gar et al., 2017).

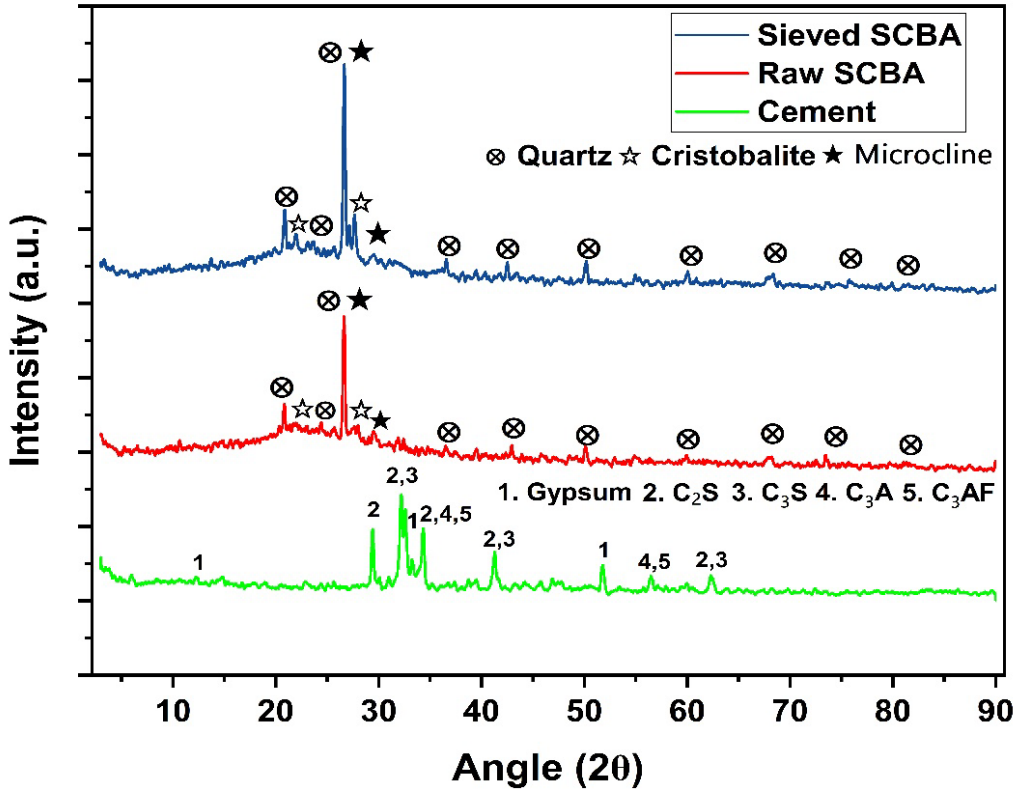

Figure 12 XRD Patterns of different specimens.

The comparison of these XRD patterns highlights the impact of processing on SCBA and underscores the inherently different properties of OPC. While OPC exhibits sharp, distinct peaks

from clinker phases, SCBA's broader peaks suggest the presence of amorphous silica, which contributes to pozzolanic activity that is beneficial for cementitious systems.

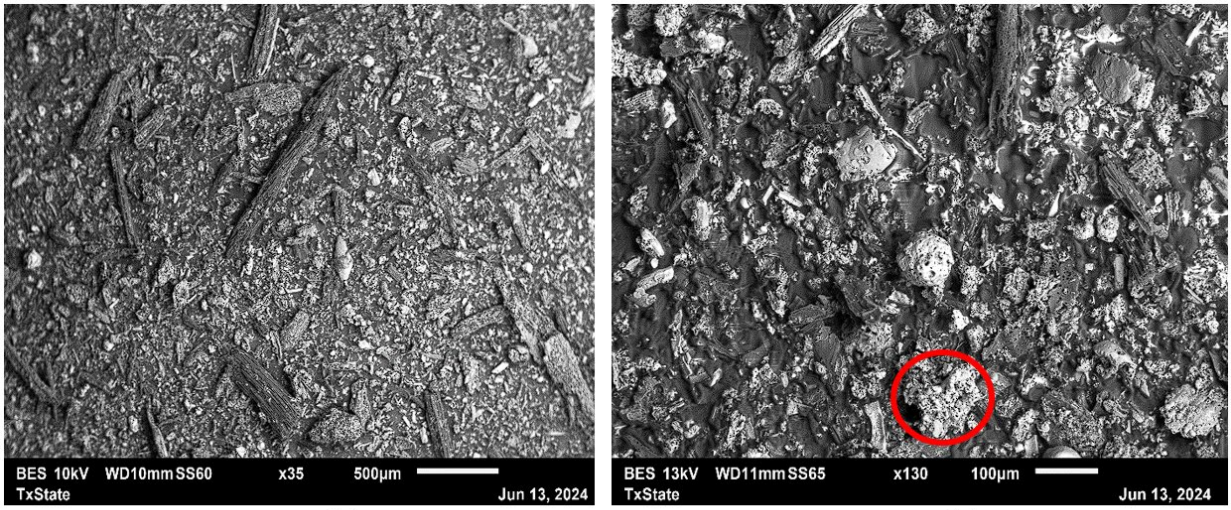

(a) (b)

Figure 13 (a, b) SEM images of SCBA with heterogenous particles.

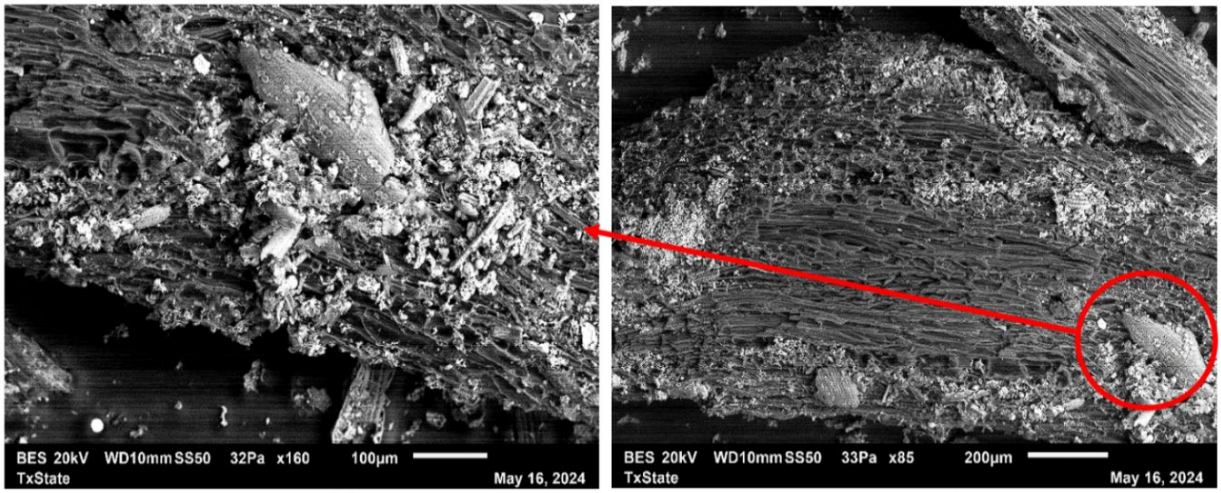

(c) (d)

Figure 14 (c, d) SEM images of porous, irregular shaped particles in SCBA.

Scanning electron microscopy analysis of the collected SCBA from Rio Grande Valley Sugar Growers Inc. is provided in figures below. shows a heterogeneous blend of cristobalite particles with a porous, sponge-like and smooth surface, which is quite common for organic and inorganic materials. Bagasse is primarily a fibrous particle. Even after combustion, it could produce particles of similar morphology of fibrous particles with rough and porous surfaces as observed in the Figure 13 & Figure 14. The presence of irregular shaped particles, which are observed in Figure 15 suggests that the burning temperature at the mill was not sufficient to

produce the melting of the inorganic contents. Thus, high combustion temperatures are required to remove the air bubbles and inorganic contents from the collected ashes.

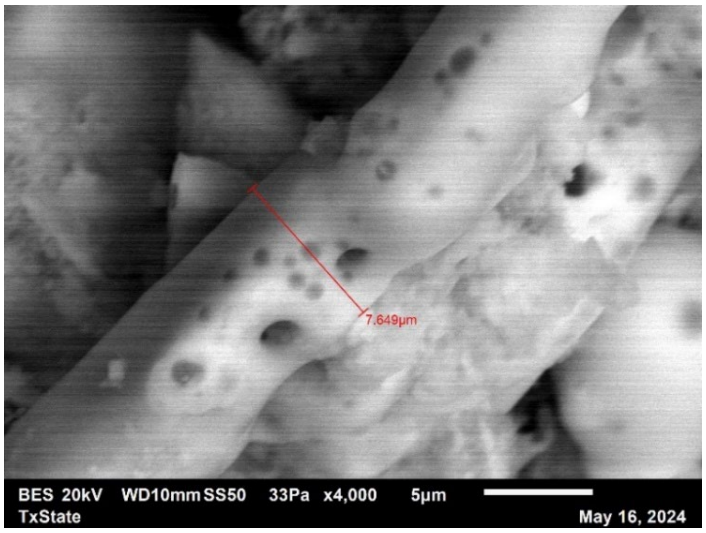

Figure 15 SEM images tubular, spongy particles in raw SCBA.

Sieving the collected ash through 200 mesh slightly improved the distribution of particles by reducing the irregular and large particles, which can be visible in Figure 16. However, fibrous and porous particles are still available, which could have caused the increased water demand due to the presence of unburnt carbons.

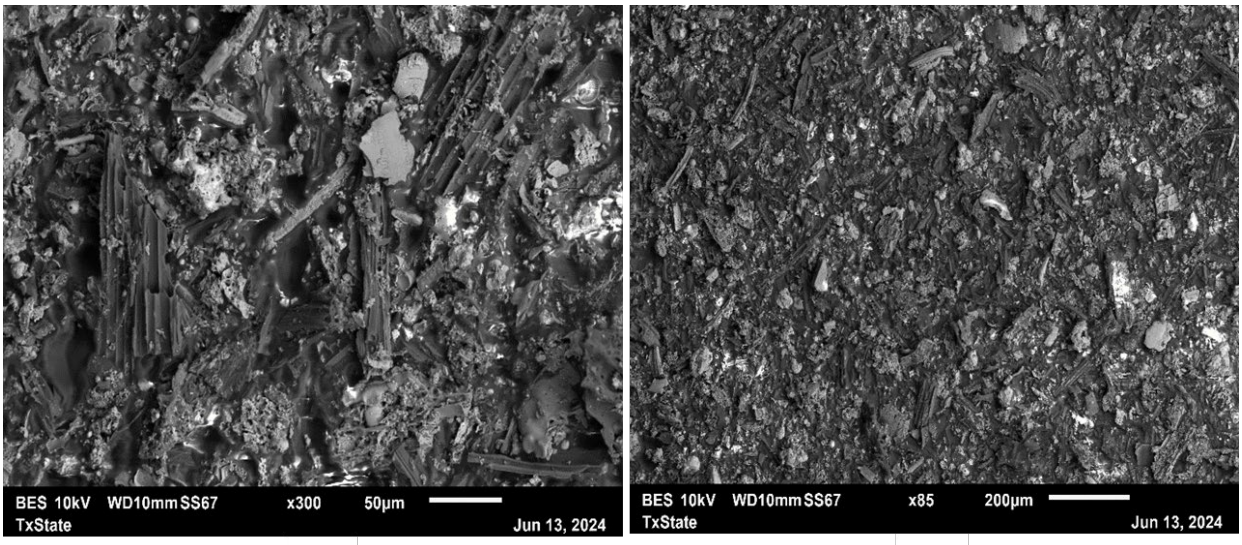

(a) (b)

Figure 16 SEM Images of (a, b) heterogenous particles in SCBA sieved through no. 200 mesh.

The specific surface area of a material is a critical determinant of its physical properties, notably its capacity to function as a filler and to facilitate additional nucleation sites. These characteristics significantly influence the performance of a cementitious matrix, including its

mechanical strength and durability. To determine the significance of material processing through sieving, the collected SCBAs were sieved through No. 325 sieves (45 µm) and particle size distribution tests of the raw and sieved ashes were conducted. It was found that sieving the ashes increases the surface area through processing. Raw SCBA samples have been reported to have a lower specific surface area compared with processed SCBA. In this study, from Table 9, the raw ashes had a surface area of 1853.6 (cm^2/cm^3), and after sieving through 45 µm, the surface area increased to 2530.2 (cm^2/cm^3). The particle size of raw SCBA is large, and the specific surface area is low. These characteristics are attributed to the presence of tubular particles and fibrous carbon particles in raw SCBA. Previous studies also corroborate the increase of bagasse ash surface area when sieved (Payá et al., 2002). 93% of OPC particles pass through a 45 µm sieve, while 50% of raw SCBA particles pass through a similar mesh. Therefore, most of the constituents of the raw SCBA are large particles that require further processing.

Figure 17 demonstrates the particle size distribution (PSD) of the ashes. It can be observed that raw SCBAs have a PSD from 5.67 to 300 µm, and the sieving process shifts the PSD to range from 5.67 to 200 µm. In the subsequent tests, the SCBAs are sieved only through No. 200 (75 µm) in place of No. 325 due to the low conversion rate (<15%). Limited amounts of ash were collected to complete all the necessary testing by using a single batch of materials to minimize the variability of material quality in different batches/collection ages.

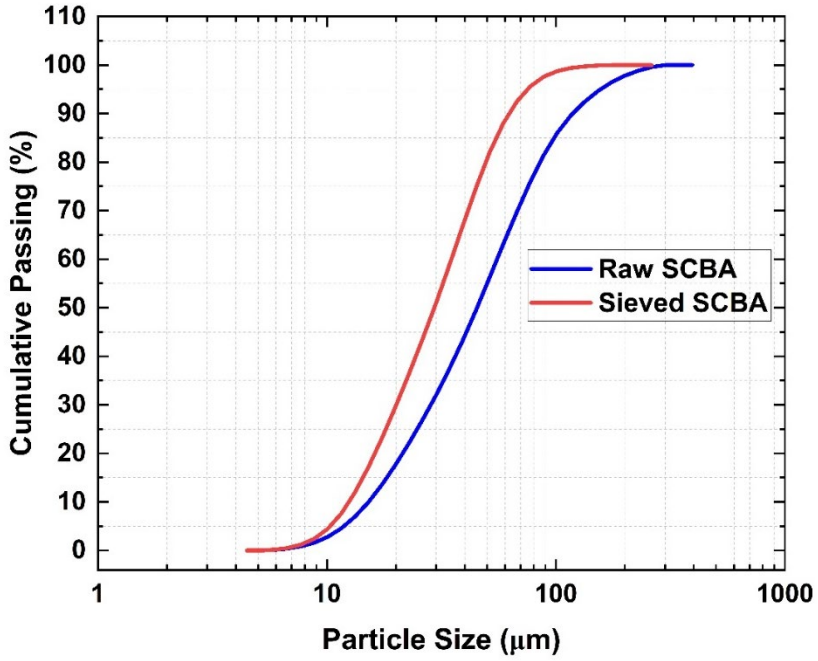

Figure 17 Particle size distribution of raw and sieved SCBA.

The particle size distribution of Raw SCBA and Sieved SCBA through a No. 325 mesh is demonstrated in Figure 18. Raw SCBA shows a broader particle size distribution with a peak of approximately 50 microns, suggesting a varied range of particle sizes. In contrast, sieved SCBA exhibits a narrower distribution and peaks at approximately 20 microns, indicating that the sieving process effectively reduces larger particles, resulting in a more uniform and finer material. This refinement likely enhances the material's reactivity and packing density when used in cementitious applications, potentially improving the mechanical properties of the resulting composite.

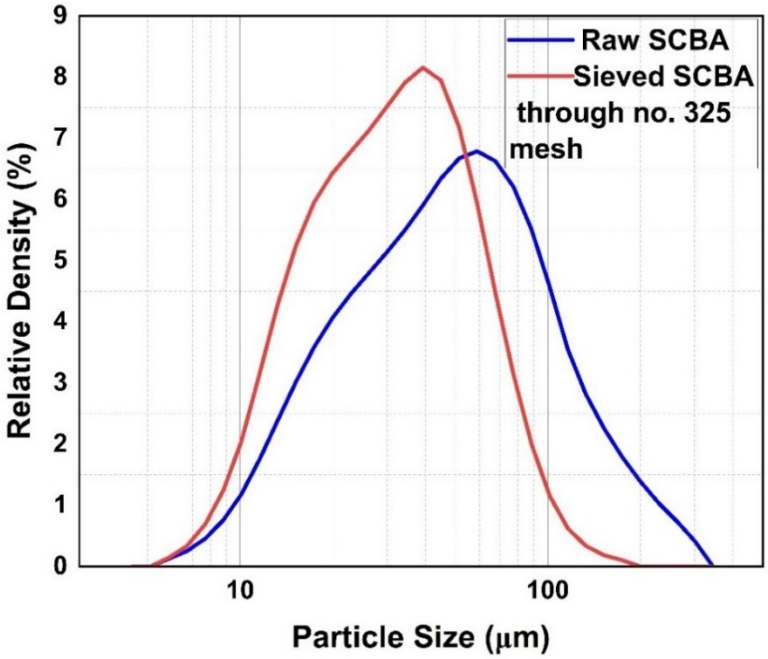

Figure 18 Frequency of particle distribution for raw and sieved ashes.

3.2 Mortar mixture proportion

3.2.1 Mixture proportion for eggshell cement

Mortar mixtures were designed based on the ASTM C270 standard ("ASTM C270-19 Standard Specification for Mortar for Unit Masonry," 2019). A binder to aggregate mass ratio of 1:2.25 was adopted for all mixtures. Oven-dried sand was used along with additional water considering the absorption capacity of sand to represent a saturated surface dry condition. Mortar with 15% and 35% portland cement replaced by limestone powder or eggshell powder by mass was prepared. The nomenclatures are based on the percentages of replacement, followed by the replacement material (LS for limestone and ES for eggshell). For example, 35LS represents a

mortar mixture with 35% limestone replacement. To compare the performance of the mixtures under identical application conditions, the water-cement ratio of mixtures was varied to produce a flow of 100% to 105% according to the flow table test outlined in ASTM C230 ("ASTM C230-20 Standard Specification for Flow Table for Use in Tests of Hydraulic Cement," 2020). A polycarboxylate-based superplasticizer (SP) was added at 0.50% by the mass of binder to improve the workability of mortar mixtures. It was noted that a limestone addition was favorable to the flow of mortar, while eggshell behaved in an opposite manner. This could be ascribed to surface wettability of the limestone powder and eggshell powder.

From Table 10, at a 15% binder replacement, the difference in replacement material did not constitute significant changes in water demand to achieve the desired flow. The difference between the water to cementitious material ratio became enormous at 35% replacement, where 35LS allowed for a slightly lower w/cm ratio (w/cm=0.38) while 35ES demanded much more water (w/cm=0.44). Since it was also in the interest of the author to study the efficacy of binder containing the two powders under identical conditions, an additional 35ES mixture was prepared with the same w/cm ratio as the 35LS mixture (w/cm=0.38), and the flow was attained by increasing the superplasticizer dosage to 1%. A suffix was added to the mixture, where “35ES I” implied the mixture was designed with additional water for constant flow, and “35ES II” was the mixture with the same w/cm ratio as 35LS.

Table 10 Mortar mixture proportion for studying unprocessed eggshell powder.

Mixture	Cement (%)	Limestone (%)	Eggshell (%)	w/cm ratio	SP (%)
OPC	100	–	–	0.40	0.5
15LS	85	15	–	0.40	0.5
35LS	65	35	–	0.38	0.5
15ES	85	–	15	0.42	0.5
35ES I	65	–	35	0.44	0.5
35ES II	65	–	35	0.38	1.0

To study the efficacy of heat treatment on eggshell, a second series of mixtures was conducted. 35% of portland cement was replaced by LS, ES, ES_{300} and ES_{500}, as the influence of each replacement material was higher at a greater proportion of incorporation. To examine the water demand of each powder, a constant w/cm ratio of 0.40 was adopted for all mixtures in the series. In addition, the workability of the mix was determined by the flow table test outlined in ASTM C230 ("ASTM C230/C230M-23 Standard Specification for Flow Table for Use in Tests

of Hydraulic Cement," 2023), recorded up to the nearest 5 mm value. The mixture proportion is shown in Table 11.

Table 11 Mortar mixture proportion for studying the performance of treated eggshell powder.

Mixture	Cement	Limestone	Eggshell	w/cm ratio
LS	65	35	–	0.40
ES	65	35	–	0.40
ES_{300}	65	–	35	0.40
ES_{500}	65	–	35	0.40

3.2.2 Mixture proportion for SCBA cement

Mortar mixtures contained 5% to 20% SCBA by mass, and the cementitious material to sand mass ratio is 1: 2.75. A fixed w/cm ratio of 0.485 was used for all mixtures. After mixing, for each mix ratio, mortars were cast into 15 50-mm cubic molds and stored in a 24℃±2℃ environment for 24 hours before the specimens were demolded and cured in lime-saturated water following ASTM C511 ("ASTM C511-21 Standard Specification for Mixing Rooms, Moist Cabinets, Moist Rooms, and Water Storage Tanks Used in the Testing of Hydraulic Cements and Concretes," 2021). Mortar cubes remained in the curing water until they reached the desired testing ages of 3, 7, 28, 56, or 90 days. To illustrate the mix properties of the mortar mixtures, Table 12 is presented below.

Table 12 Mix Proportions of reference, raw SCBA and sieved SCBA blended Mortars

Mixtures	Replacement Rate (%)	Cement (kg/m^3)	SCM (kg/m^3)	Sand (kg/m^3)	Water (kg/m^3)	Superplasticizer (kg/m^3)
Reference	0	679	0	1867	348	2.9
Oven Dried, Sieved SCBA	5	645	34	1867	348	4.1
	10	611	68	1867	348	5.9
	20	543	136	1867	348	10.1
Oven dried Raw SCBA	5	645	34	1867	348	4.4
	10	611	68	1867	348	6.5
	20	543	136	1867	348	10.9

To ascertain the ability of sugarcane bagasse ash to mitigate ASR in concrete, mortar bars with dimensions of 25 x 25 x 250mm (1x 1 x 11.25 in) were tested in accordance with ASTM C1567 (Accelerated Mortar Bar Test). A fresh property test (flow table test) was carried out for all mortar mixtures in accordance with ASTM1437. The amount of superplasticizer was

determined to obtain ± 7.5% of the flow of reference mixture without any supplementary cementitious material. Table 13 demonstrates the flow of the fresh mortar mixtures.

Table 13 Flow of mortar mixtures for ASR tests

Mixture	SCM Dosage (%)	Flow (%)
Reference	0	102.5
Oven Dried, Sieved SCBA	5	101.3
	10	103.3
	20	104.5
Oven Dried, Raw SCBA	5	100.0
	10	102.5
	20	103.3

A Type I OPC with an alkali content of 0.78 Na_2O_{eq} was used in this test. Mortar mixtures were prepared with a 5% to 20% replacement of OPC by mass for two different types of SCBA. The three sieved ashes and three as-received ash mortar samples were referred to as 5% S-SCBA, 10% S-SCBA, 20% S-SCBA, 5% R-SCBA, 10% R-SCBA, 20% R-SCBA respectively. A reactive siliceous river sand was used as fine aggregate in this test. This sand was sieved as prescribed in ASTM C1567. 10%, 25%, 25%, 25% and 15% of the sand retained on sieve number 8, 16, 30, 50 and 100 respectively was collected and used in the mortar. The water-to-cement ratio was fixed at 0.47. The physical properties of the reactive river sand were determined according to ASTM C128 are shown in Table 14.

Table 14 Physical properties of reactive sand for ASR

Aggregate	Bulk Specific Gravity (OD)	Bulk Specific Gravity (SSD)	Apparent Specific Gravity	Absorption (%)
Reactive Sand	2.57	2.61	2.64	1.0

The accelerated mortar bar test was carried out in accordance with ASTM C1567 ("ASTM C1567-23 Standard Test Method for Determining the Potential Alkali-Silica Reactivity of Combinations of Cementitious Materials and Aggregate (Accelerated Mortar-Bar Method)," 2023). The mixing process was completed in accordance with ASTM C305, and three mortar bars with dimensions of 25 x 25 x 250mm (1 x 1 x 11.25 in) were cast for each mix. The initial comparator readings were taken after demolding, and the zero readings were taken before the mortar bars were transferred from water to 1N sodium hydroxide solution. Subsequent readings

were taken on days 3, 5, 7, 10, and 14. An oven, capable of maintaining a temperature of 80°C ± 2°C, ensures that the storage environment meets the requirements specified in ASTM C1567.

Sodium hydroxide in the form of micro pellets was used to produce the 1N sodium hydroxide solution required for this test. The reference mixture was produced in accordance with the ASTM C1567 standard with Type I OPC, but the remainder of the mixes involved the addition of SCBA to partially replace cement. A total of 7 mixtures were produced for this test. The mixture proportion for this test is shown Table 15.

Table 15 Mix proportion of ASR

Mixtures	**Replacement Rate (%)**	**Cement (kg/m^3)**	**SCM (kg/m^3)**	**Sand (kg/m^3)**	**Water (kg/m^3)**	**Superplasticizer (kg/m^3)**
Reference	0	619	0	1391	305	0
Oven Dried, Sieved SCBA	5	587	32	1391	305	1.5
	10	556	63	1391	305	3.9
	20	494	125	1391	305	5.6
Oven dried Raw SCBA	5	587	32	1391	305	1.8
	10	556	63	1391	305	4.2
	20	496	125	1391	305	6.0

3.3 Experimental test methods

3.3.1 Surface wettability test

Contact angle measurements of limestone, untreated eggshell powder, and eggshell powder after each treatment method were assessed to understand the interactions of each filler with water. A customized sessile drop method adopted from (Nowak et al., 2013) was developed by our research team using a novel sample preparation method. About 30g of powder specimens were spread into a dish of 55mm Ø ×15mm, then tampered and compressed. This formed a flat surface of the powder which emulated a solid sample typically used for wettability analysis. A 2µl deionized water droplet was formed using a pipette and was dispensed onto the powder surface. The images of the water droplet were captured using a tabletop microscope at 40× magnification. ImageJ software was used to obtain the angle between the baseline of the drop and the tangent drawn at the boundary of the drop. Measurements were made in triplicate for each sample.

3.3.2 Isothermal calorimetry and paste minerology tests

The heat evolution and hydration mechanism of cement paste were studied using a TAM Air isothermal calorimeter. The mixture proportion was based on those outlined in Table 10. 5g of the blended cements were mixed with water and then placed into the calorimeter, maintained at 23˚C to simulate the hydration of cement in ambient conditions. The heat evolution of the system was captured for up to 7 days. The hydration mechanism was observed through the heat flow over time, while the total amount of heat released provided insight into the extent of exothermic chemical reactions that occurred within the system. To thoroughly investigate the mechanism of hydration as well as the variations caused by limestone and eggshell powders, a derivative of the heat flow was plotted to pinpoint the time at which notable stages of hydration occur. Referring to the method postulated by (Hu et al., 2014), the initial setting time, alite peak, sulfate depletion point, and belite peak of cement hydration may be inferred from the intercept of the derivative plot, allowing for the quantification and comparison of these parameters across mixtures with different binders. The cited study took the intercept of the derivative plot as the initial and final setting time. In this study, the data extraction was altered to a slight degree to consider the hydration peak and instead assumed the minima of the derivative as the final setting time. The minima translated to the inflection point in the heat flow curve where it 'flatlined' after the completion of the main hydration sequence. An illustration of the data collection points using the hydration curve of an OPC in which the sulfate depletion point was visible is presented in Figure 19.

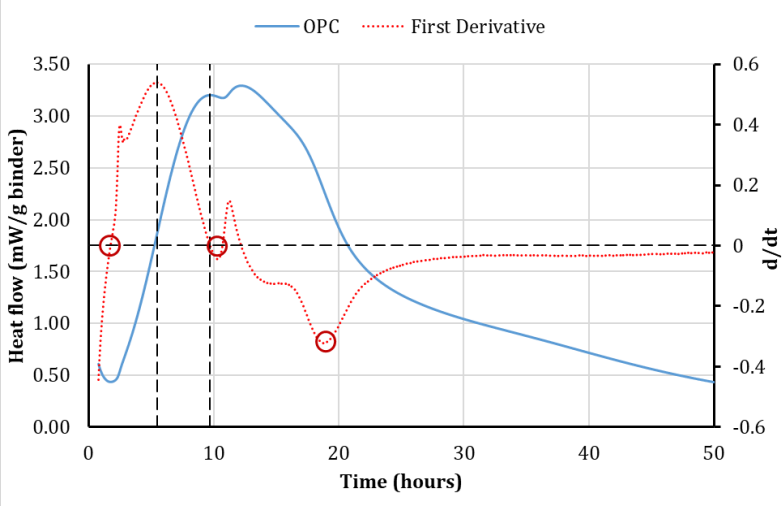

Figure 19 Derivative plot of heat flow curve for OPC.

Moreover, the extent and mechanism by which eggshell powder retards hydration could be illustrated. For obtaining the phase assemblage of the cement mixtures, a second set of pastes was prepared and hydrated for 3, 7 and 28 days. At the designated period, the pastes were crushed using a pestle and mortar and then soaked in isopropyl alcohol to stop the hydration, followed by washing with diethyl ether. The procedure was in accordance with the recommendation outlined in (Snellings et al., 2018). XRD analysis of fine paste was conducted. To account for the amorphous content of hydrated paste, the internal standard method was employed using 20% Rutile. Rietveld refinement was subsequently employed to quantify the composition of hydrated phases. The evolution of phase composition of the pastes over time was presented and analyzed.

3.3.3 Degree of hydration test

An additional set of 5±0.1g paste specimens were prepared and allowed to cure at 90% relative humidity following the condition prescribed to the curing of mortar. After 3, 7, and 28 days, specimens were dried at 105±5˚C for 24 hours to remove all evaporable water. Then, they were crushed into powder and ignited at 950±1˚C for 3 hours for the removal of bound water. The mass of paste specimens was measured on a scale with 0.001g sensitivity. Bound water content (W_b) was taken as the percentage mass loss between dried (W_d) and ignited (W_i) sample, considering the LOI of OPC and limestone/eggshell incurred during the process, as shown in Eq. (1):

$$W_b = \left[\frac{W_d - W_i}{W_d} - LOI\right] \times 100\% \quad (1)$$

Cement chemistry theory has determined that 1g of portland cement will bound up to 0.23g of water at complete reaction (Friedemann et al., 2006; Lura et al., 2017; Narmluk & Nawa, 2011). The degree of hydration (α) for binder can hence be inferred by taking the ratio between W_b and 0.23, as presented in Eq. (2):

$$\alpha = \frac{w_b}{0.23} \times 100\% \quad (2)$$

3.3.4 Chemical shrinkage test

Chemical shrinkage of cement mixes with 35% replacement of each powder specimen was conducted in accordance with ASTM C1608 ("ASTM C1608-17 Standard Test Method for Chemical Shrinkage of Hydraulic Cement Paste," 2017). 5±0.1g of cement paste was first cast into

a glass bottle. After the paste hardened, the vessel was filled with deionized water and sealed. The setup was placed in a water bath maintained at 23±0.5˚C. Chemical shrinkage was obtained from the reading of a graduated pipette protruding from the bottle cap, and measurement was performed until 28 days. The magnitude of chemical shrinkage was associated with the hydration powder of cement and was used to complement the data obtained from calorimetry and degree of hydration.

3.3.5 Mortar tests

The list of experiments conducted on mortar specimens in this project is outlined in Table 16. The mechanical properties of mortar were evaluated through compressive strength tests alone, as compressive strength is a key parameter in design of structures with cementitious composites. To corroborate the hydration mechanism study from the previous section, an electrical resistivity test of mortar prism specimens was conducted using an instrument conforming to ASTM C1876 ("ASTM C1876-19 Standard Test Method for Bulk Electrical Resistivity or Bulk Conductivity of Concrete," 2019). The surface resistivity of concrete can be correlated with its packing density, which provides insight into the packing effect of blended cement as well as the efficacy of hydration through results at early and later ages. Meanwhile, autogenous and drying shrinkage tests were performed using a mortar bar test according to ASTM C157 ("ASTM C157/C157M-24 Standard Test Method for Length Change of Hardened Hydraulic-Cement Mortar and Concrete," 2024). After demolding, samples for the autogenous shrinkage test were wrapped with aluminum foil to isolate the sample from the dry environment, and samples for the drying shrinkage test were placed in a controlled chamber of 20˚C, 50RH. At regular intervals, the samples were measured using a length change compactor, and the shrinkage value was computed.

Table 16 Testing regime on mortar specimens

Experiment	Standard	Specimen Size (mm)	Testing Age (day)
Compressive strength	ASTM C109	50 × 50 × 50	3, 7, 28, 90
Electrical resistivity	ASTM C1879	40 × 40 × 160	7, 14, 21, 28
Autogenous shrinkage	ASTM C157	25 × 25 × 280	Up to 90 days
Drying shrinkage	ASTM C157	25 × 25 × 280	Up to 90 days

4. HYDRATION MECHANISM

4.1 Hydration mechanism of eggshell cement

4.1.1 Surface wettability test

Figure 20 presents the contact angle values of limestone, eggshell, and treated eggshell with water. The contact angle measurements revealed that the initial contact angles formed by water with limestone and eggshell powder were 62º and 168º, respectively. After heat treatment, the contact angle of ES_{300} was reduced to 128º and that of ES_{500} was reduced to 105º. It was observed that the water droplet permeated through the limestone powder and ES_{500} instantly. Meanwhile, the droplet remained on the surface of ES_{300} for about 15 to 20 seconds and ES_{500} for 90 to 120 seconds. The contact angle values indicated that limestone exhibits hydrophilic surface characteristics, whereas eggshell shows hydrophobic behavior. The hydrophobic nature of the eggshell powder can be attributed to the presence of protein membrane on its surface as can be observed from SEM images. On the contrary, the hydrophilic nature of the limestone powder represents its inherent characteristic of higher surface wettability, suggesting a higher potential for interaction with water compared to eggshell powder. This could potentially lead to a higher rate of water uptake by LS compared to ES (Yang et al., 2018) and possibly influenced the hydration rate and kinetics of blended binders. In addition, contact angles of treated eggshell powders showed that the material was losing its hydrophobic nature as incineration was prescribed to denature the organic matter within the material. ES_{300} still displayed some hydrophobic nature but showed notable improvement to water affinity compared to ES. ES_{500} began to display clear hydrophilic properties like LS.

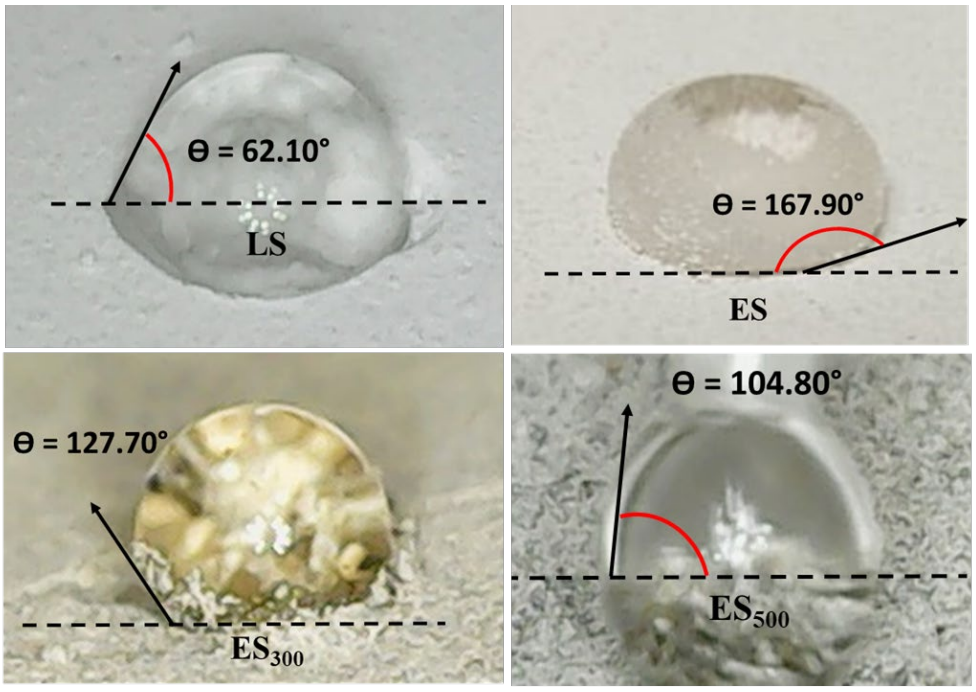

Figure 20 Contact angle values with water for limestone, untreated eggshell, and treated eggshell.

4.1.2 Isothermal calorimetry test

Figure 21 (a) presents the heat evolution for different pastes obtained from the isothermal calorimetry for up to 40 hours. The hydration of OPC reasonably had the highest peak heat flow compared to the remaining mixtures of blended cement. Since the heat evolution primarily originated from the hydration of clinker phases, the dilution of OPC with alternative replacement materials resulted in a weaker exothermic reaction. For 15LS and 15ES, the hydration peak occurred earlier than OPC. 15LS has a higher magnitude of heat flow compared to 15ES. At the same time, a slight shift in reaction rate between the two curves was observed. For the 35% mixtures, significant behavior changes between limestone and eggshell were observed. 35LS began and completed its main hydration reaction significantly earlier than other mixtures, while 35ES displayed the opposite behavior. At the same time, 35ES II, which had a lower water content (w/cm = 0.38), had greater heat release when compared to 35ES I (w/cm = 0.44). This implied that the water required to achieve the targeted flow did not always translate to the optimal ratio for hydration. Literature (Mantellato et al., 2019; Pang, 2015) had shown that dilution of mineral concentration in pore solutions affected the dissolution and precipitation rate of hydration phases when excessive w/cm ratio was used.

The cumulative heat release of all the mixtures up to 7 days is presented in Figure 21(b). OPC paste released the highest amount of heat at about 301J/g. 15LS mixture had slightly higher heat release at the early ages, which was surpassed by 15ES mixture at around the 80 hours mark. However, both mixtures had a comparable amount of heat evolution, where 15LS and 15ES mixtures released 280 J/g and 273J/g of heat. In contrast, the heat release of limestone powder and eggshell powder mixtures was notably different when 35% replacement was made. 35LS released 233J/g of heat in 7 days, while 35ES I and 35ES II only released 221J/g and 217J/g respectively. Hence, based on early age hydration performance it appears that substitution of limestone powder with eggshell powder was feasible at lower proportions but not optimal at higher proportions.

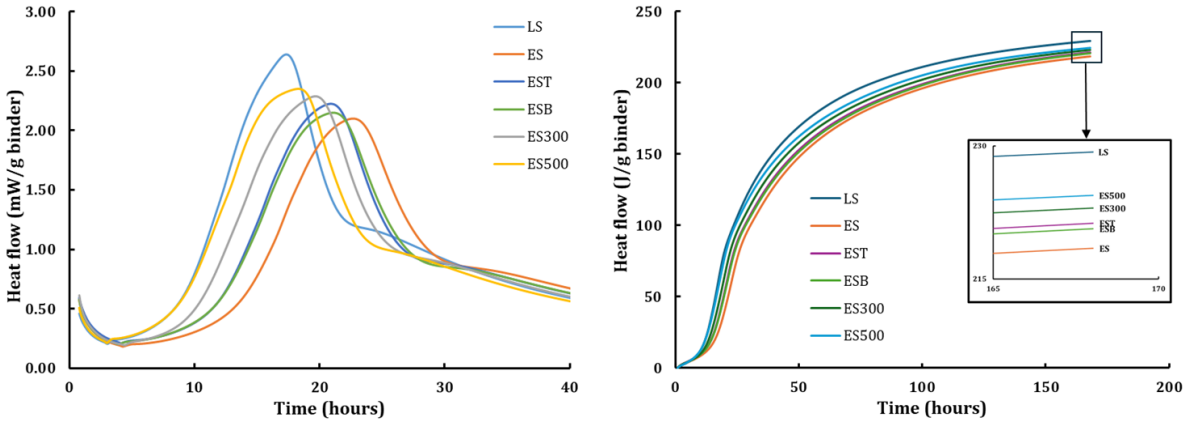

Figure 21 Calorimetry result for paste mixes with treated eggshell powder a) Heat flow curve b) Cumulative heat flow with final reading magnified for clarity.

Meanwhile, Figure 21 presented the calorimetry result for paste prepared with treated eggshell powder. For the 35LS sample, the evolution of heat began and peaked earlier compared to all ES mixes. This agreed with the established literature in which the replacement of clinker with limestone powder accelerated the hydration of cement. In contrast, eggshell powder significantly retarded the progress of hydration especially when included at a higher proportion. In addition, the peak heat evolved was lower for mixes with ES compared to LS, which may indicate a lessened efficacy of eggshell as a cement replacement. After washing, both ES_T and ES_B displayed a slightly faster hydration rate and a higher peak of hydration. This implied that the as-received ES contained impurities from the egg-breaking process in the industrial plant which was detrimental to its performance in portland cement. Meanwhile, ES_{300} and ES_{500} have

notably improved performance. The hydration mechanism of eggshell became closer to that of limestone after incineration, which was due to the degradation of organic content within ES. Similarly, from Figure 21(b), the cumulative heat evolved by ES samples became higher with both washing and incineration. Therefore, heat treatment of eggshell powder was successful at allowing a high proportion incorporation without compromising the hydration of cement.

4.1.3 Paste mineralogy test

The phase mineralogy of cement paste by mass is presented in Figure 22. To simplify the presentation and minimize deviation, the four clinker phases (C_2S, C_3S, C_3A, and C_4AF) were combined. The raw OPC contained approximately 3% to 5% calcite. Hydrated cement paste compositions shown are C-S-H, portlandite, ettringite, and the sum of minor phases such as hemicarboaluminate (Hc), monocarbonate (Mc), and monosulfate (Ms). Gypsum was not represented as it was expected to be consumed within the first day of hydration. Ettringite was precipitated between sulfate ions and calcium aluminate phases from the early hydration stage. It was present within 7 days, but the depletion of sulfate ions affected the sample. Due to progressing cement hydration, ettringite was gradually transformed to more stable forms such as monocarbonate in the presence of calcite. Consequently, only minor traces of ettringite were observed at a later age. Portlandite was formed from early hydration, and it occupied a consistent proportion of the solid in all mixtures.

The phase assemblage of all mixtures was similar, and the greatest difference stemmed from the dilution of clinker content based on limestone powder or eggshell replacement levels. For OPC, the composition of limestone powder remained constant. Minor traces of limestone in cement are known to enhance hydration and stabilize ettringite phases (Lothenbach et al., 2008). However, the limestone remained mostly in a stable phase and was not consumed or altered in the hydration reaction. At a higher proportion of replacement, limestone served primarily as a filler. In all mixtures, the rate of reaction, as indicated by the proportion of clinker phases consumed, was similar. At 28 days, 70% to 80% of the clinker was hydrated, forming primarily C-S-H.

Comparing mixtures with limestone powder and eggshell powder at the same level of replacement, no significant difference was observed for the rate of hydration and the formation of hydration products. For example, after 28 days, the percentages of C-S-H formation were 63% in 15LS and 66% in 15ES. Meanwhile, the C-S-H proportion of the three 35% mixtures at 28

days ranged from 52% to 57%. Phase quantification of hydrated cement paste was prone to deviation incurred by sample preparation, powder particle size, diffractogram condition, and Rietveld quantification. Accordingly, the difference observed in the study could not be attributed to a change in hydration kinetics between cement paste with the two calcite sources. Overall, substituting limestone with eggshell did not alter the hydration of cement significantly.

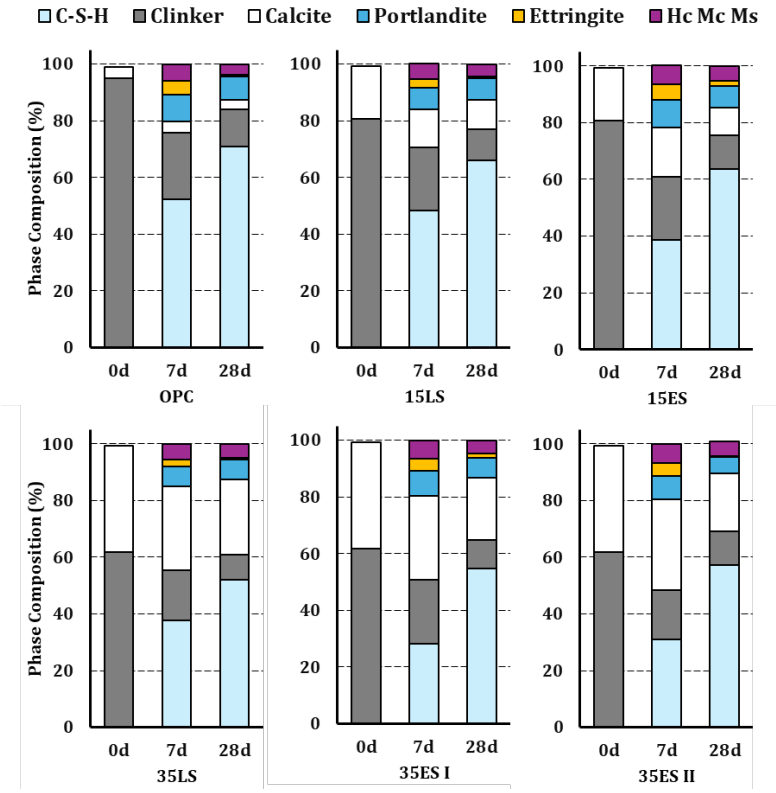

Figure 22 Phase quantification for OPC, LS and ES mixtures by mass.

4.1.4 Degree of hydration

The degree of hydration of the paste samples is shown in Figure 23. For comparison, OPC mix was also prepared for this test. The reading of blended mixes was normalized based on clinker content (65%). The degree of hydration hovered around 50% at 3 days and 70% at 28 days, which corresponded with the range and trend of cement hydration as presented in literature (Honorio et al., 2016). At all measured ages, LS mix showed a higher degree of hydration than OPC because of the nucleation effect contributing to increased hydration efficacy. On the other hand, ES mix significantly reduced the hydration of clinker because of the hydrophobic organic content within the powder. This was remedied by incineration, because ES_{300} and ES_{500} were

more hydrated despite still being drier than LS and OPC. These results demonstrate that heat treatment of ES was effective at improving the quality of the material.

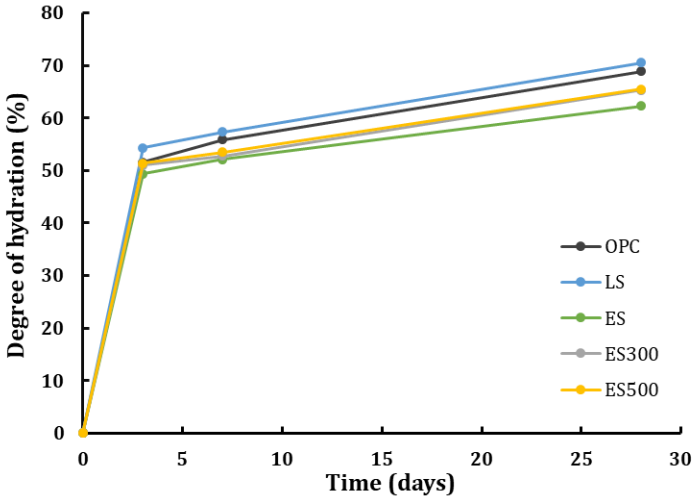

Figure 23 Degree of hydration of each paste at 3, 7 and 28 days.

4.1.5 Chemical shrinkage test

The chemical shrinkage of OPC and blended cement mixtures is shown in Figure 24. As expected, the OPC mixture has the highest chemical shrinkage. Chemical shrinkage is associated with the reduction in volume due to the density difference between raw clinker phases and the hydration product, which the replacement of cement with limestone and eggshell has been shown to reduce. From the figure, mixtures of the 35% replacement level have the lowest shrinkage, followed by those at 15% replacement. It is interesting to note that when comparing between blended binder of the same replacement percentages, binder containing eggshell powder measured more shrinkage than with limestone powder. For example, a significant offset of shrinkage was observed between 15ES and 15LS, and the chemical shrinkage of 15ES appeared to be higher than that of OPC. Moreover, 35ES observed a higher chemical shrinkage compared to 35LS. Chemical shrinkage is a reliable method to determine the hydration rate of cement and correlate it with the strength of the binder. However, the approach was not as reliable in evaluating eggshell powder due to the presence of eggshell membrane and other organic substances, which induce higher shrinkage value unrelated to the actual hydration reaction. The detailed causes and mechanism of the disruption warrant further study in the future.

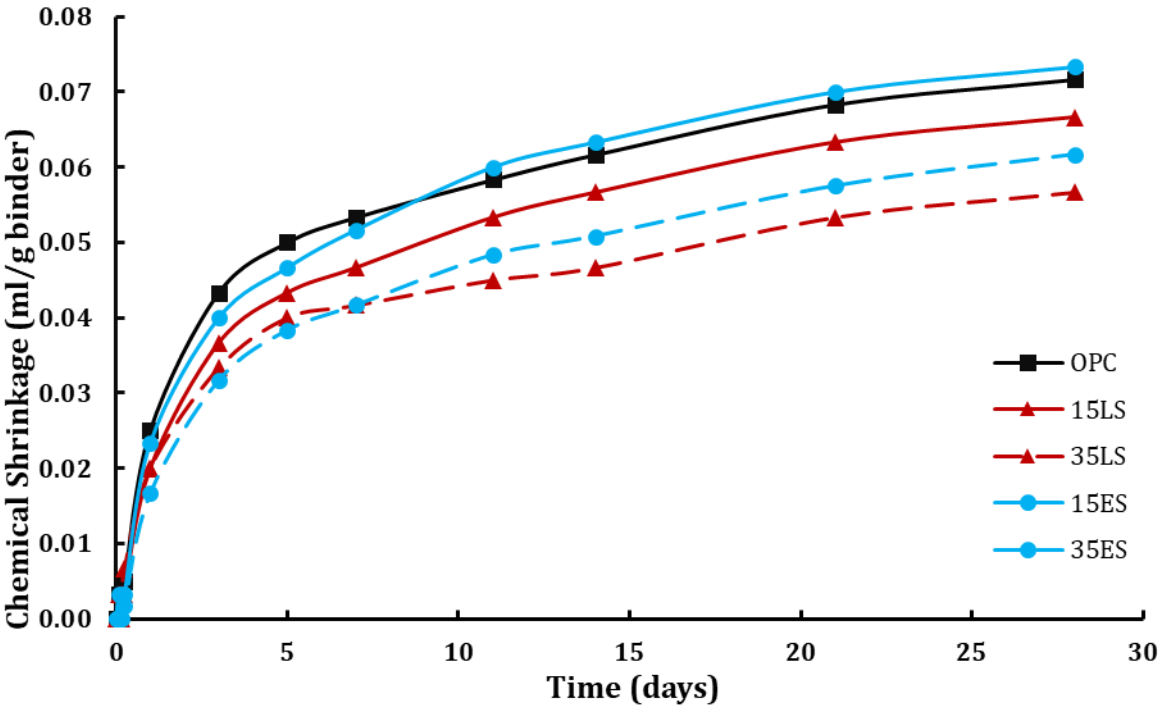

Figure 24 Chemical shrinkage of cement paste.

The chemical shrinkage of the paste mixtures with treated eggshell is shown on Figure 25. LS reasonably recorded the highest shrinkage value at 28 days of age. ES_{500} and ES_{300} experienced lower shrinkage, which agreed with all other tests that measured the efficacy of clinker hydration. Even though untreated ES mixture had the lowest degree of hydration, the chemical shrinkage value of ES was higher than ES_{300}. This is in contrast to the results of the heat released from calorimetry and the degree of hydration test. For the mixes with washed ES, ES_T also displayed a high shrinkage value, while ES_B had the lowest shrinkage value. This showed that the organic content within ES caused unusually higher shrinkage that is not associated with hydration. This may be attributed to the volume change of eggshell membrane within the environment. ES_T was collected floating from the water surface and contained large amounts of light organic content, hence its shrinkage value. Meanwhile, ES_B had less organic content and experienced the least shrinkage, correctly reflecting its weak ability at empowering clinker hydration. As-received ES mix was a combination of both components and hence experienced a moderate level of shrinkage. This indicates that the chemical shrinkage test was not suitable as a matrix for measuring clinker hydration when the replacement material contained significant organic content.

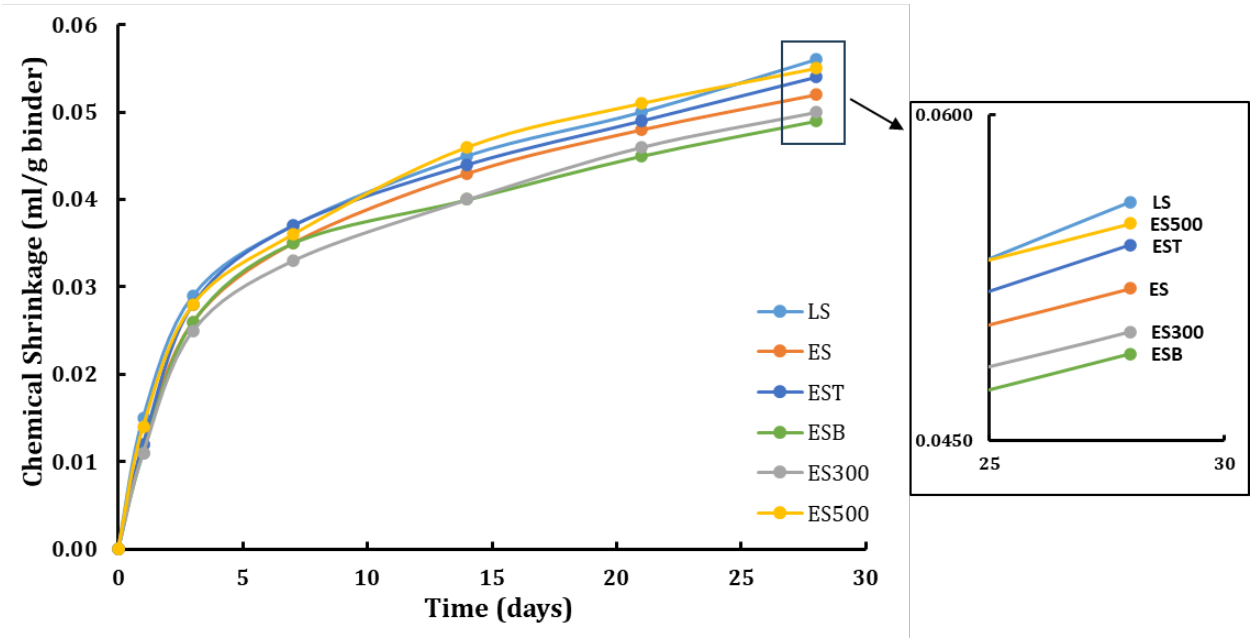

Figure 25 Chemical shrinkage of paste mixtures with treated eggshell powder, final reading magnified for clarity.

4.2 Hydration mechanism of SCBA cement

4.2.1 Isothermal calorimetry

The rate of heat flow per gram of cement for the pastes containing different dosages of raw sugarcane bagasse ashes along with the reference sample is shown in Figure 26.

Heat flow was normalized per gram of cementitious material to more easily compare SBCA's influence on the reaction. This was done to observe whether the inclusion of SCBA results in acceleration or retardation, as well as activation or suppression, of the reaction kinetics of the cement. As the mixes were produced outside of the calorimeter, the early reaction data, the first peak observed after a few minutes of testing, was not taken into account in this study. After 45 minutes, when the signal stabilized, data were collected. In the heat flow versus time curves, the result demonstrated a significant shift to the right in reference to when SCBA was used in place of cement. This showed that the presence of SCBA delayed hydration. This effect was more noticeable when there was a greater replacement of cement; the higher the SCBA level, the longer the induction duration. It is crucial to emphasize that, to achieve the same consistency as the reference mix, the pastes containing SCBA require noticeably larger superplasticizer dosages. The retarding effect was partly attributed to a high amount of superplasticizer, which was also observed by another researcher (Cordeiro et al., 2019).

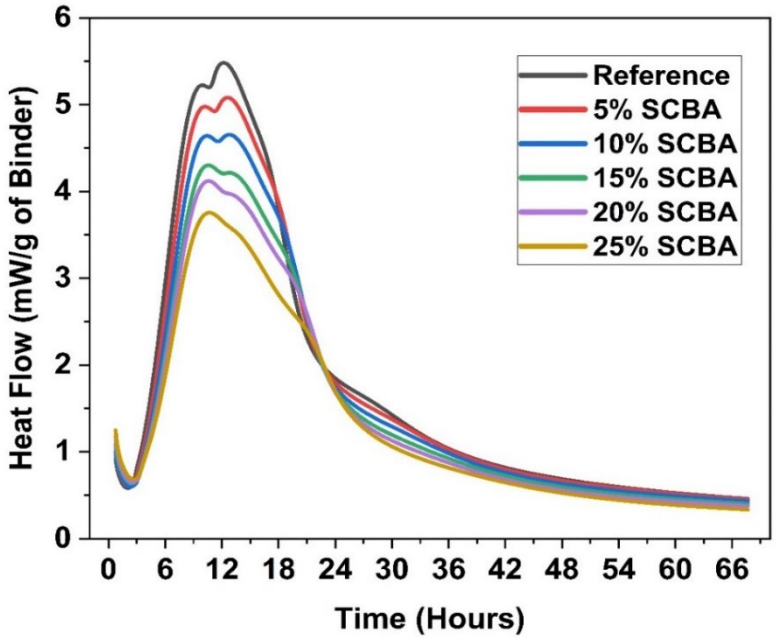

Figure 26 Hydration kinetics of reference and blended pastes at w/cm of 0.45

In this study, the average peak heat flow and the time it took to reach these peaks in different replacement rates of collected sugarcane bagasse ash were analyzed to assess the effect of replacement level on the hydration parameters. At approximately 12.17 hours, the reference mixture—which did not include any SCBA—showed the highest average peak heat flow, 5.48 mW/g of binder. The magnitude of peak heat flow was found to gradually decrease as the proportion of SCBA increased. The maximum average heat fluxes for mixes containing 5%, 10%, 15%, 20%, and 25% SCBA were 5.08, 4.65, 4.30, 4.12, and 3.75 mW/g of cementitious material, respectively. This trend highlights the influence of SCBA on the kinetics of cement hydration, suggesting a reduction in reactivity and a shift in the hydration timeline as SCBA content increases. Previous researchers attributed that the rate of heat evolution over time can be significantly influenced by the specific surface area of cement. Thus, the particle size and fineness of the SCBA play significant role in shifting the hydration performance (Ghiasvand et al., 2014; Graham et al., 2011).

The prolonged dormant period for pastes containing SCBA may have resulted from the presence of carbon, K_2O and SO_3 in SCBA (Andreão et al., 2019b; Cordeiro, Barroso, et al., 2018). Moreover, the dilution effect resulting from partially replacing cement with pozzolanic substances contributed to slowing down heat flow. The decrease in heat of hydration can be attributed to changes in the chemical composition of blended cement.

According to Graham et al. and Bahurudeen et al., cement's heat evolution is greatly influenced by its constituents, including C_3A, C_3S, and gypsum (Bahurudeen et al., 2015; Graham et al., 2011). By replacing portland cement with ashes, the binder contains fewer ingredients, resulting in a lower heat of hydration for cementitious pastes. High hydration temperatures can cause thermal cracking in large structures, including bridges. Thus, using agro-industrial residue such as SCBA as a partial replacement for portland cement can help mitigate these negative effects. Figure 27 demonstrates the cumulative heat flow measured by an isothermal calorimeter for different mixtures containing portland cement and sugarcane bagasse ashes at different replacement rates.

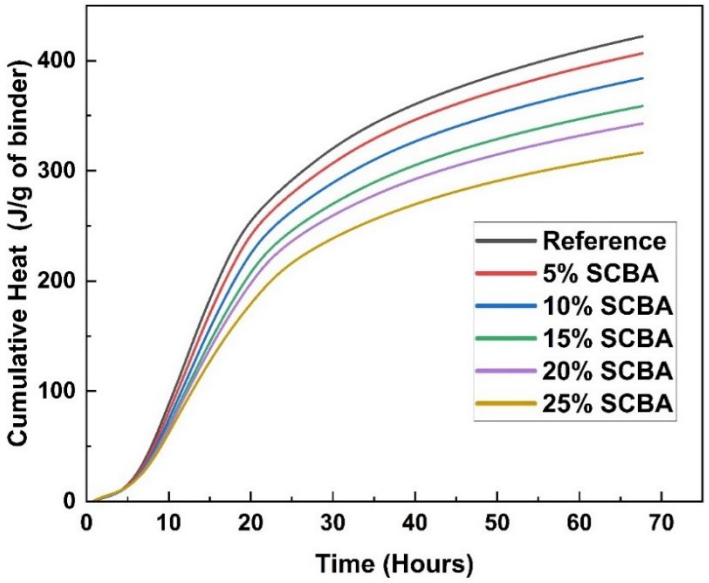

Figure 27 Cumulative heat of different paste mixtures at w/cm of 0.45

The reference mix shows the highest cumulative heat evolution throughout the 70-hour period, reaching approximately 422 J/g of binder. This high heat evolution suggests that the reference mix, which is OPC, exhibits rapid hydration, leading to a higher rate of heat release. All mixes containing SCBA show lower cumulative heat compared to the reference, which indicates that a dilution effect significantly impacted the hydration process and slowed down the reaction. The progression from 5% to 25% SCBA demonstrates a clear trend: as the percentage of SCBA increases, the cumulative heat at any given time decreases. A similar decreasing pattern was also observed in a previous study (Bahurudeen et al., 2015). At 70 hours, the mix with 5% SCBA reached around 406 J/g of binder, the closest to the reference. This suggests that a 5% replacement impacts the hydration process minimally. The mix containing 10% SCBA trended

slightly below the 5% R-SCBA, reaching around 384 J/g of binder by 70 hours. The additional ash seemed to moderately reduce the generation of heat. A 15% SCBA mix showed a more significant deviation from the reference which reached about 359 J/g of binder. This indicates a more pronounced impact on hydration kinetics. When 20% SCBA was added, cumulative heat further dropped, stabilizing around 343 J/g of binder. This level suggests a substantial alteration in the hydration process. A 25% SCBA replacement demonstrated the lowest heat development at approximately 316 J/g of cementitious material. The gradual decrease in cumulative heat with increasing R-SCBA content likely reflects the dilution and pozzolanic effects of the ash. R-SCBA replaces part of the cement, reducing the amount of clinker reacting per unit time and potentially contributing to pozzolanic reactions that occur later than the initial cement hydration reactions. While lower heat of hydration reduces the risk of thermal cracking in massive concrete structures, the impact on the early age mechanical properties, such as compressive strength, needs careful evaluation.

4.2.2 Chemical Shrinkage of Pastes

The analysis of trends in chemical shrinkage in pastes with varying percentages of sieved sugarcane bagasse ash (S-SCBA) and raw sugarcane bagasse ash (R-SCBA) reveals significant differences in performance. The test was conducted following the guidelines of ASTM C1608 ("ASTM C1608-23 Standard Test Method for Chemical Shrinkage of Hydraulic Cement Paste," 2023). From Figure 28, the reference sample shows a gradual increase in chemical shrinkage, reaching about 0.055 mL/g of binder by 240 hours. The 5% S-SCBA sample shows a shrinkage curve similar to the reference but slightly higher after 36 hours. The 10% S-SCBA has a higher initial shrinkage rate, surpassing the reference at around 30 hours and continuing to a higher final value, indicating increased reactivity. The 20% S-SCBA exhibits the highest shrinkage among the sieved samples, showing a significant increase in chemical reactivity and shrinkage.

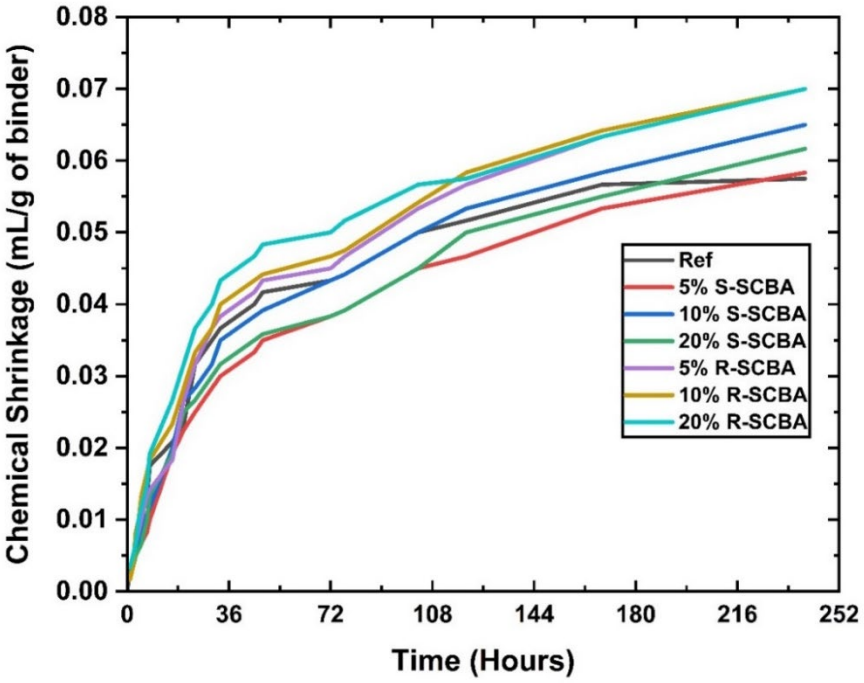

Figure 28 Chemical shrinkage of paste mixtures

For the raw SCBA samples, 5% R-SCBA shows higher initial shrinkage than both the reference and 5% S-SCBA, suggesting that raw SCBA contributes more to shrinkage. The 10% R-SCBA continues this trend, consistently showing higher shrinkage than the reference and 10% S-SCBA. The 20% R-SCBA shows the highest overall shrinkage, indicating significant reactivity and potential durability issues at high percentages. Sieved SCBA consistently shows lower shrinkage than raw SCBA at equivalent percentages, likely due to the removal of larger and coarser particles and impurities in the sieving process. Increasing SCBA content, whether sieved or raw, leads to higher chemical shrinkage, with the 20% samples showing the highest values, indicating a direct correlation between SCBA content and shrinkage. This behavior can be attributed to the low water-to-cement ratio in the paste mixture and porous nature of the SCBAs, which further increased water demand in the mixture containing SCBAs. Also, dilution plays a dominating role in pozzolanic reactivity of the SCBA blended pastes over the time. Thus, increasing the dosage of SCBA, both raw and sieved, eventually induces higher permeability and shrinkage in the paste mixtures.

4.2.3 Setting Time

Setting time is obtained by a method introduced by Hu et al., where an innovative approach based on the first derivative of the heat evolution curve is calculated to identify the

beginning and final set periods of mortar using calorimetry (Hu et al., 2014). This curve, which was created using test data on heat development, peaks at the first predetermined time. The quickest rate of increase in heat generation is shown by this peak. Once this peak is reached, the first derivative starts to fall. When the first derivative approaches zero, signifying that the peak rate of hydration has been attained, the final set time is determined. Figure 29.

Table 17 provides insight into the setting time of different mixtures containing SCBA bagasse ashes as well as the reference mixture without any substitution. The rate of hydration starts to decline after 11 hours. The first derivative of heat flow normalized to cementitious materials per gram for all the mixtures is demonstrated in Figure 29.

Table 17 Setting time of different mixtures from two distinct testing

Mix	Initial Setting Time (Hours)	Final Setting Time (Hours)
Reference	6.26	9.95
5% SCBA	6.60	10.22
10% SCBA	6.79	10.41
15% SCBA	6.88	10.57
20% SCBA	6.84	10.56
25% SCBA	6.89	10.67

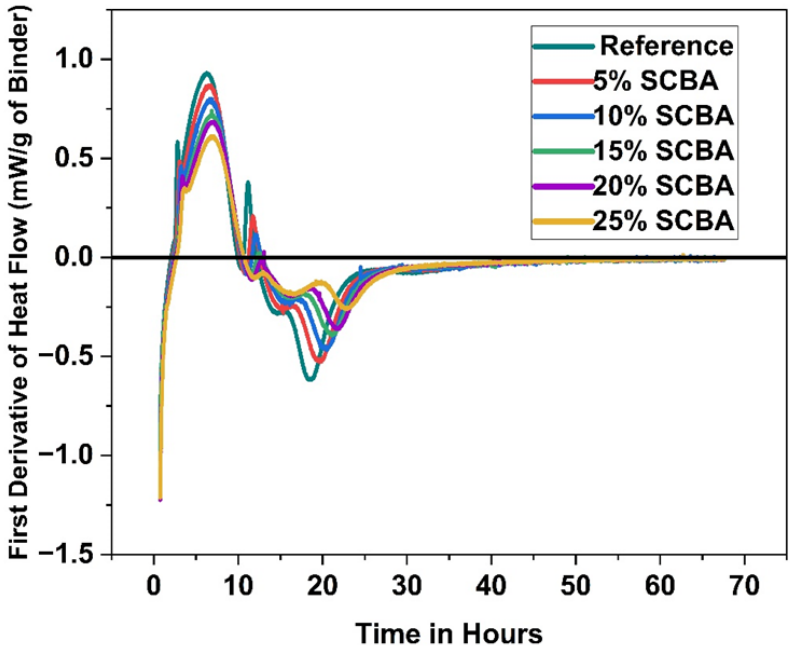

Figure 29 First derivative of heat flow.

When cement hydrates, the first setting period is a crucial stage when heat generation occurs at its quickest rate. This period includes the rapid reactions that take place when the cement begins to hydrate. From the first derivative of heat flow from isothermal calorimetry,

6.26 hours is the shortest initial setting time for the reference pastes among all the paste mixtures. This illustrates how typical cement hydrates without interference from pozzolanic materials. The first setting exhibits a discernible, albeit slow, delay as SCBA content rises from 5% to 20%. The main cause of this delay can be attributed to the pozzolanic reaction of SCBA, which creates more C-S-H by consuming calcium hydroxide. This reaction causes a slower initial rate of heat generation because it competes with the conventional hydration process, even though it increases long-term strength. When the percentage of SCBA is increased from 15% to 20%, the setting time lowers, indicating a complicated interplay between the chemical reactivity of SCBA and its physical characteristics, such as particle size and dispersion.

When the first derivative reaches zero, the final setting time is reached, indicating the peak of hydration activity prior to its dropping. This phase is critical because it signifies the change from a paste that is workable to one that has solidified. The reference samples exhibit the fastest final setting times, suggesting that the hydration reactions completed more rapidly. The final setting times consistently lengthen as the SCBA proportion rises from 5% to 25%. This prolongation is a sign of ongoing hydration product development over an extended period of time and prolonged pozzolanic action. This result implies that, even though SCBA delays the initial setting time, it may also improve strength by guaranteeing a longer and more thorough hydration process. Moreover, extended setting time allows for the use of SCBA as a concrete retarder.

5. MORTAR TEST

5.1 Mortar test of eggshell cement

5.1.1 Flowability and compressive strength

Figure 30 displays compressive strength test results. It was noted that the trend of compressive strength was well correlated with the heat release from calorimetry, indicating that the difference in strength was in large measure due to the strength of the binder. The OPC mixture performed the best at all ages as compared to the blended cement mixtures. 15LS mix achieved comparable strength with OPC, which was similar to the results of portland limestone cement studies. Meanwhile, 35LS has a lower compressive strength due to the higher level of portland cement replacement that leads to the dilution of clinker content. The 15ES mixture achieved a slightly lower strength compared to 15LS. One reason is the higher water demand of eggshell powder, so the 15ES mixture was prepared with a slightly higher w/cm ratio to achieve

the targeted flow. At the 35% replacement, the impact of water demand becomes more significant, shown by the significant difference in strength between 35LS and 35ES I. However, the strength reduction could be mitigated by maintaining the w/cm and the use of more superplasticizer. When the specimens were prepared with the same w/cm ratio as 35LS, the 35ES II mixture achieved comparable strength. However, eggshell powder is less efficient than limestone as a calcium-rich filler, which is evident by the lower strength of the eggshell mixtures compared to the limestone mixtures at the same replacement level.

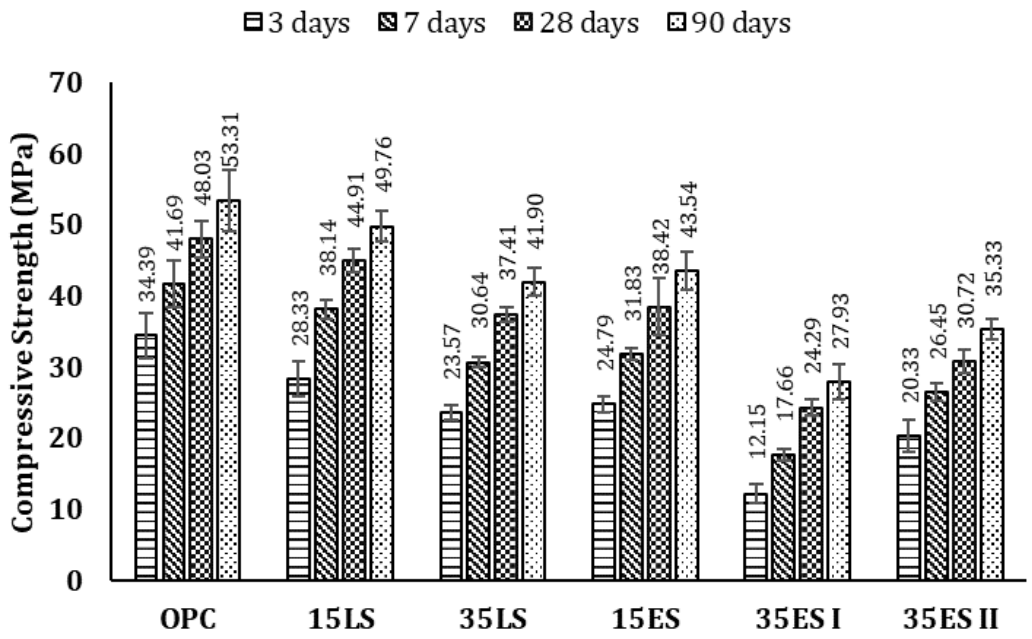

Figure 30 Compressive strength of mortar mixtures with untreated eggshell powder.

For treated eggshell mixtures, the flowability is presented on Figure 31. The control OPC achieved flowability of 205mm. The incorporation of limestone slightly increased the flowability of the LS mix because of its surface morphology and improved particle packing from having a predominantly finer particle size than portland cement (Wang et al., 2018). ES mix had significantly less flow due to its hydrophobicity interfering with the interaction between cementitious materials and water. The flowability of ES_{300} saw minor improvement as the incineration process denatured the organic content within eggshell powder. Further heat treatment fully overcame the disruption to flow as the flowability of ES_{500} became significantly higher, achieving the same flow as OPC.

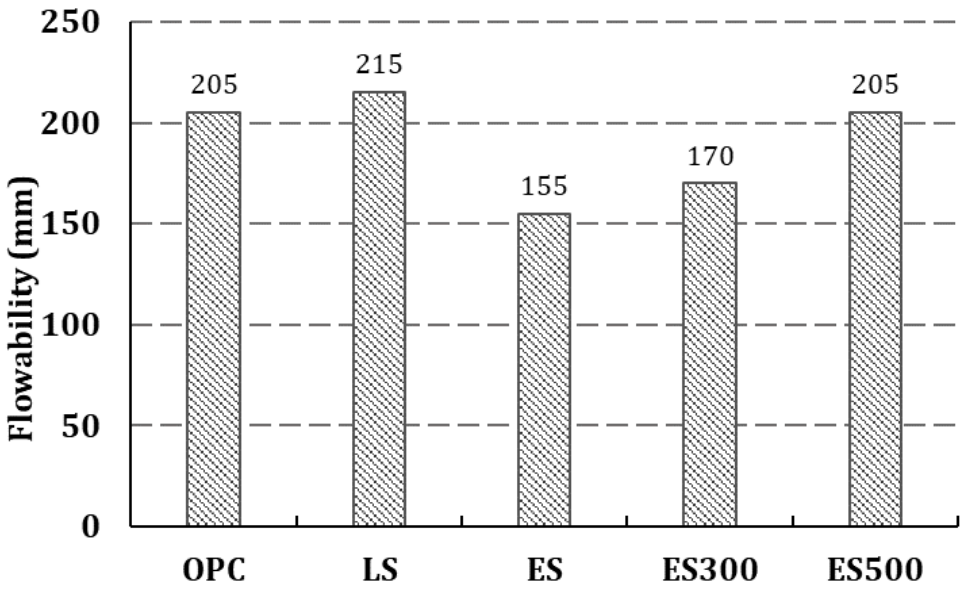

Figure 31 Flowability of mortar mixes from flow table test.

Figure 32 displays the compressive strength test results. OPC obviously measured the highest strength at all ages as compared to the blended cement mixes. At 35% replacement, the LS mix lost about 20% strength compared to OPC, as the dilution of clinker was compensated by increased efficacy of hydration induced by nucleation effect from fine limestone powders. However, ES lost about half its strength at the same proportion of replacement. This may be attributed to multiple factors, such as the detrimental effect of hydrophobicity, poor nucleation effect of organic matter as compared to calcite, and poor adhesion of eggshell particles to hydrated clinker due to the presence of organic matter. Denaturization of organic matter through incineration recovered significant strength, with ES_{300} and ES_{500} achieving similar strength levels as LS at 28 days and beyond. Evidence suggests that heat treatment at 300˚C was sufficient for a cementitious composite with eggshell to achieve the same level of strength as a composite with limestone.

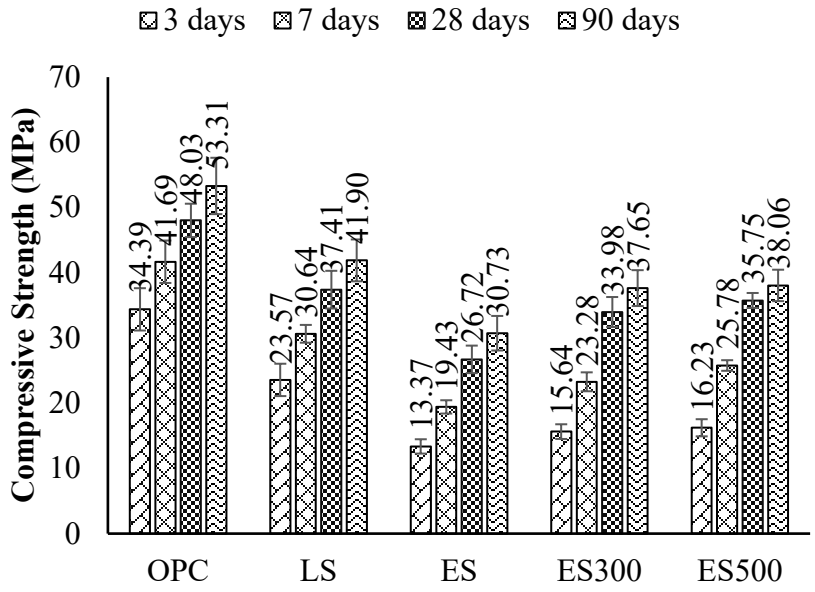

Figure 32 Compressive strength of mortar mixes with 35% limestone, eggshell powder, and treated eggshell powder.

5.1.2 Drying and autogenous shrinkage

The drying shrinkage of the mixtures is plotted in Figure 33. From the data, the major variable influencing the shrinkage value is the clinker factor. After 15ES, OPC had the highest drying shrinkage, while mixtures with 15% and 35% calcite filles experienced less shrinkage. Comparing mixtures containing eggshell and limestone, 15ES experienced slightly higher drying shrinkage compared to 15LS. Likewise, 35LS had the lowest drying shrinkage of all mixtures, while the two 35ES mixtures had higher drying shrinkage. The increased drying shrinkage was because of membrane in eggshell. Unlike calcite which has an affinity to water, eggshell membrane is comprised of fibrous proteins such as type 1 collagen (Wong et al., 1984). This membrane is insoluble in water and shrinks in size when subjected to dehydration (Bond & Huffman, 2023; Eke et al., 2013). The shrinkage of type 1 collagen is elucidated in (Haverkamp et al., 2022). As mortar was subjected to drying, eggshell membranes shrunk in size too, causing greater drying shrinkage of the sample. Another notable difference was the drying shrinkage values between 35ES I and 35ES II. Drying shrinkage of mortar was significantly affected by the w/cm ratio of the mixture, and it was apparent in the comparison of those two mixtures. At a higher w/cm ratio, the drying shrinkage of 35ES I was much higher, suppressing that of 15LS which had a higher clinker factor. In this regard, the usage of more superplasticizer to produce

35ES II was effective in controlling the shrinkage to a more acceptable level. Regardless, the reduction of portland cement content always resulted in lower shrinkage in this case. The drying shrinkage of cementitious composites is an indirect indication of the possibility of cracking, as the reduction in volume can generate tensile stresses within the material. Eggshell powder incurred a minor increase in the drying shrinkage, but the cracking potential of the composite should not be majorly affected, as the additional shrinkage is associated with the eggshell powder and not the composite. Regardless, a more advanced experimental procedure such as restrained ring test will be needed to further investigate the implication of the phenomenon.

Figure 34 provides additional insight into the autogenous shrinkage behavior of the mixtures. Different from drying shrinkage, the autogenous shrinkage of eggshell mixes was lower than the limestone mixtures. Autogenous shrinkage of mortar bars was ascribed to the self-desiccation of cement paste as it hydrates. Limestone powder may be more effective at aiding hydration and providing nucleation sites to hydration products compared to eggshell powder which contained inert membranes. Accordingly, the autogenous shrinkage of limestone mixtures was greater than eggshell mixtures. In addition, the effect of varying water content is clear from the difference between 35ES I and 35ES II. For 35ES I prepared with a higher w/cm ratio, the autogenous shrinkage was lower compared with 35LS and 35ES II that has lower w/cm ratio. The contradicting trend between different shrinkage mechanisms illustrated the influence of eggshell membrane.

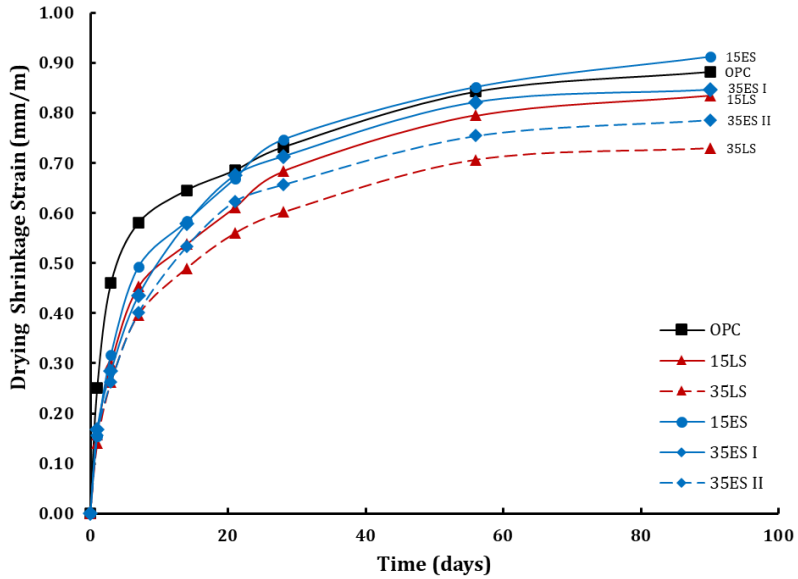

Figure 33 Drying shrinkage of mortar bars.

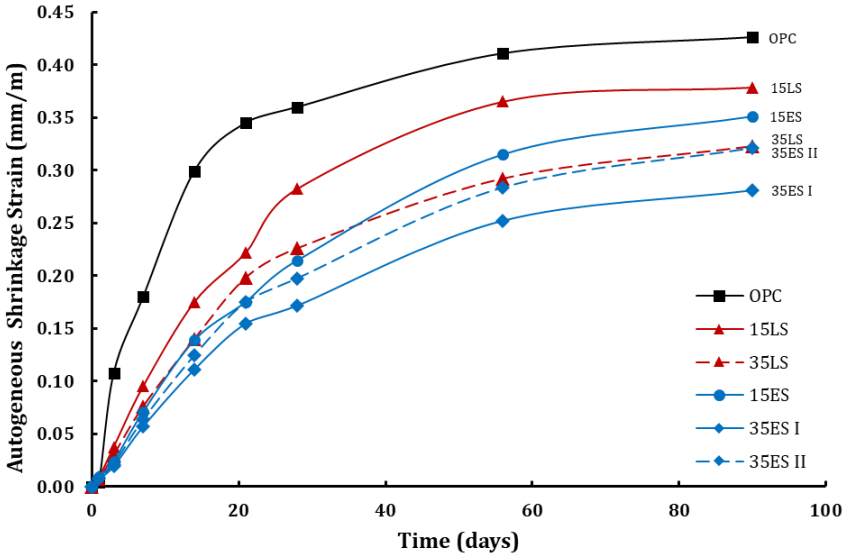

Figure 34 Autogenous shrinkage of mortar bars.

5.2 Mortar test of SCBA cement

5.2.1 Mortar flow

Table 18 demonstrates the flow variability of the mixtures without containing any superplasticizer usage at a constant w/cm of 0.485.

Table 18 Flow variation among the mixtures without superplasticizer

Mixture	SCM Dosage (%)	Flow (%)
Reference	0	89.75
Oven Dried, Sieved SCBA	5	80.75
	10	74.50
	20	71.75
Oven Dried, Raw SCBA	5	78.25
	10	72.50
	20	70.00

The mortar mixtures containing SCBA generally had low flow values, resulting from the replacement of OPC by SCBA in the mixtures, which necessitated the introduction of the chemical admixture to adjust the flow of the mortars to remain within 110± 5% range. Figure 35 demonstrates the flow table test conducted with the mortar mixtures. MasterGlenium 3030, a polycarboxylate based high-range water reducer, was used to improve the mortar workability.

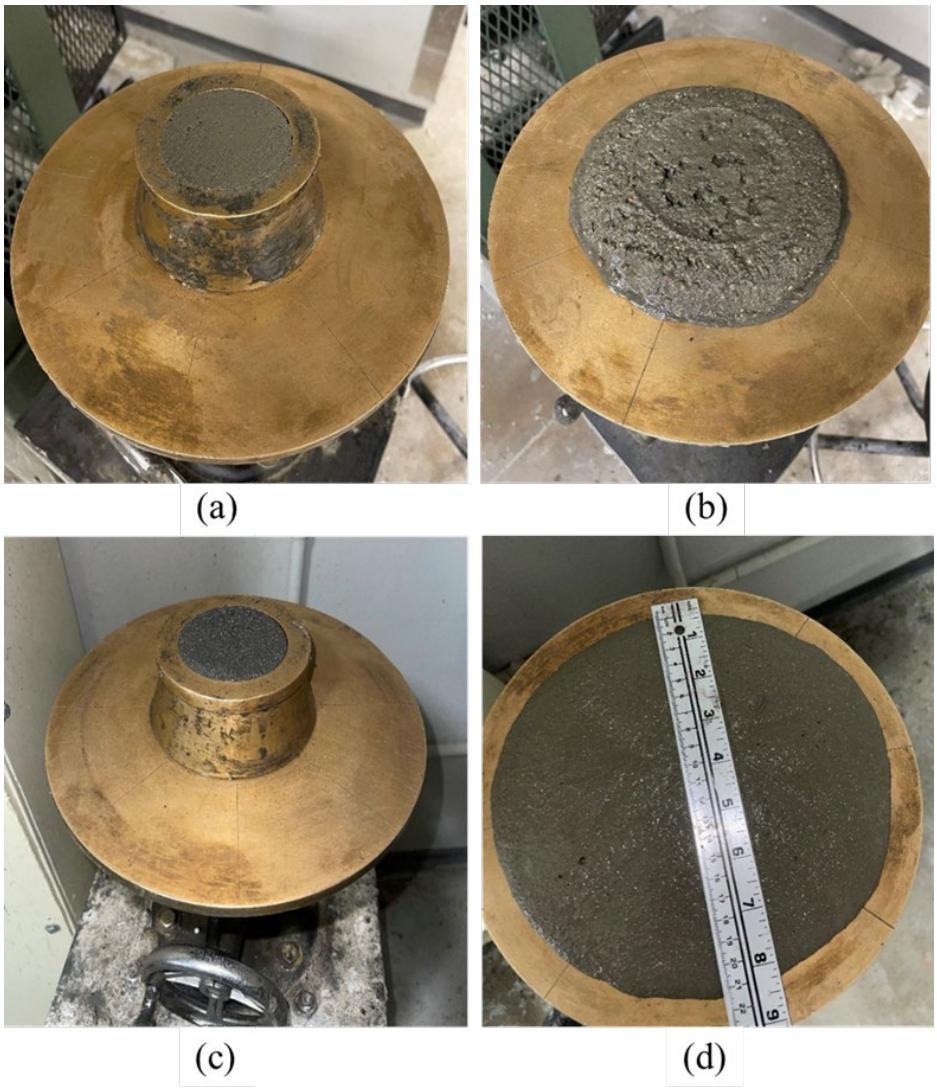

Figure 35 Flow Table test of mortar mixtures at w/cm of 0.485 without (a, b) and with superplasticizer dosage (c, d)

Table 19 demonstrates the flowability of the mixtures at a constant w/cm of 0.485 with the addition of superplasticizer.

Table 19 Flow adjustment of mortar mixtures with superplasticizer

Mixture	**SCM Dosage (%)**	**Flow (%)**
Reference	0	108.75
Oven Dried, Sieved SCBA	5	112.75
	10	108.00
	20	112.25
Oven Dried, Raw SCBA	5	111.50
	10	109.50
	20	110.25

5.2.2 Superplasticizer requirement

From Table 9, it can be observed that when the mixes were prepared with the water-to-cement ratio of 0.485, and without using any types of superplasticizers, the decreasing trend of flow was observed in both the sieved and raw ash blended mortar mixtures when compared to reference mix. Increasing the replacement rates of SCBAs showed a declined trend of flow, which necessitated the introduction of chemical admixtures to adjust the flow as per ASTM requirements. A similar pattern of flow was observed by MC Chi in previous study that targeted on the influence of SCBA replacement on the concrete properties (Chi, 2012).

Figure 36 demonstrates the relationship between the addition of sugarcane bagasse ash both sieved (S-SCBA) and raw (R-SCBA), to cement mixes and the resulting increase in superplasticizer dosage needed. The reference mix, without any addition of SCBA, required the least amount of superplasticizer, which set a baseline for comparison. As SCBA were introduced, the deviation from this baseline demonstrates the impact of SCBA on the mix's properties. The superplasticizer requirement of reference mix was 0.425% of cementitious materials weight, while 5% Sieved SCBA, 10% Sieved SCBA and 20% Sieved SCBAs were 0.60%, 0.87% and 1.49% respectively. Those of 5% Raw SCBA, 10% Raw SCBA and 20% Raw SCBA mixtures required 0.65%, 0.95% and 1.60% superplasticizer of the binder’s weight to achieve the target flow. This trend suggests several underlying factors influencing mixed behavior.

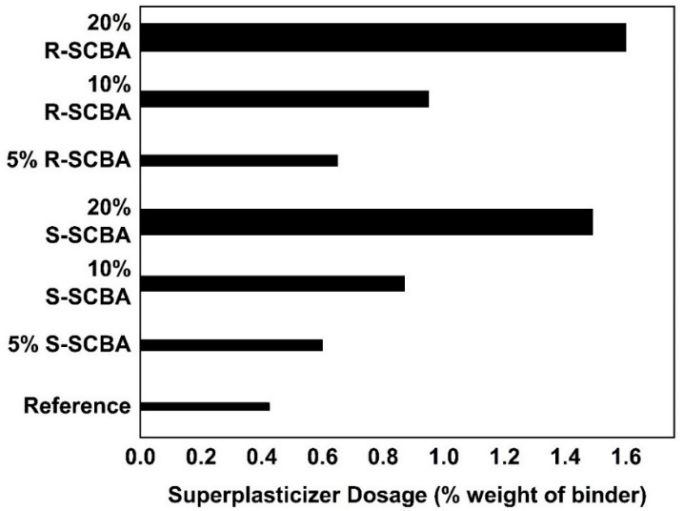

Figure 36 Superplasticizer dosage requirement (% weight of binder material)

Because of their irregular shapes, SCBA particles could not pack well within the cement mixture. To obtain the appropriate workability and fluidity, this irregularity increases the number

of voids and the surface area that needs to be coated with superplasticizer. The ability of SCBA particles to absorb water could be increased by their porous texture or porosity. To counteract this absorption and keep the mix sufficiently wet for appropriate hydration and workability, extra superplasticizer is needed. The mixture could also be impacted by the unburnt carbon in SCBA. Superplasticizers can be absorbed by unburnt carbon, which decreases their capacity to interact with cement particles. This means that a larger dosage of superplasticizer is required to make up for the carbon content's absorption (Akram et al., 2009; Arif et al., 2016; Rukzon and Chindaprasirt, 2014).

SCBA, particularly in its unprocessed form (R-SCBA), contains various chemical impurities that can interfere with the hydration process of cement. These impurities likely necessitate higher superplasticizer dosages to maintain the workability of the cement mix. Sieved SCBA, although processed to remove larger and coarser particles and impurities, might still retain enough fine particles that alter the surface area and chemical behavior of the mix, thereby requiring more superplasticizer compared to reference mixture. Sieved SCBA is finer than raw SCBA due to the removal of coarser particles, which increases the total surface area that must be coated by the superplasticizer. The coarser materials of raw SCBAs typically absorb more admixture to maintain flow. As the percentage of SCBA increases in the cement mixes (from 5% to 20%), there is a clear trend of increased superplasticizer dosage across both R-SCBA and S-SCBA. Chindaprasirt et al. also observed a similar upward trend of superplasticizer dosage with the increased replacement rate of SCBA in cement concrete (Chindaprasirt et al., 2020). This suggests a dosage-proportional relationship where higher quantities of SCBA exacerbate its impact on the mix, likely due to cumulative effects of increased particle interaction and chemical complexity.

5.2.3 Strength activity index

The Strength Activity Index (SAI) results provided in Figure 37 for both sieved SCBA (S-SCBA) and raw SCBA (R-SCBA) made mortars show that these materials are appropriate for many concrete applications. When used as supplementary cementitious materials, both marginally exceed the ASTM C618 standard requirement of 75% of the compressive strength of mortars made with OPC at both 7 and 28 days. The reference sample made with OPC serves as the benchmark, with its relative strength set at 100%. At 7 days, the mortar with 20% S-SCBA achieves 78% of the OPC's strength, and the mortar with 20% R-SCBA achieves 79%. Both

SCBA replacements exceed the ASTM standard requirement of at least 75% of the reference's strength at 7 days, indicating that both materials are reactive and contribute effectively to early-age strength development. By 28 days, the relative strength of the 20% S-SCBA mortar is 77% of the OPC's strength, while the 20% R-SCBA mortar shows a relative strength of 76%. Although there is a slight decrease in the percentage relative to the 7-day strengths, both SCBA variants maintain performance above the 75% threshold required by ASTM standards, confirming their continued reactivity and suitability for use as SCMs over a longer curing period. This performance indicates a satisfactory fulfillment of the criteria set for qualifying as reactive SCMs.

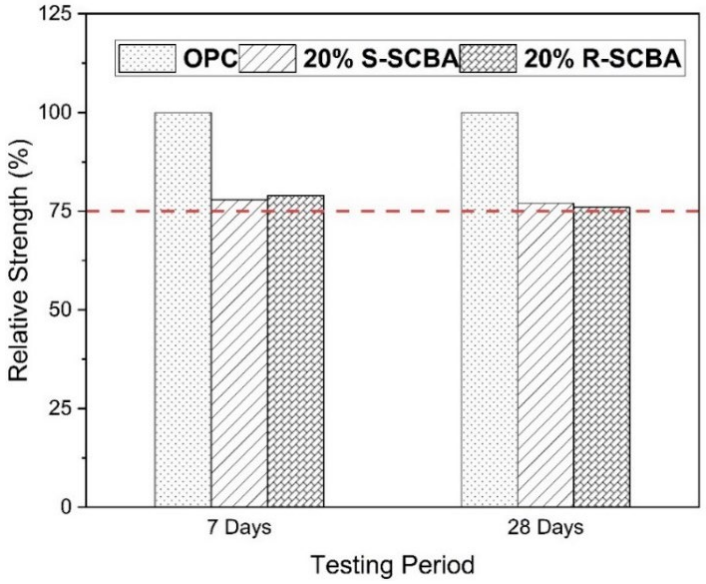

Figure 37 Strength activity index of OPC and 20% replaced specimen

The marginal performance of SCBAs can be attributed to several factors inherent to their composition and processing. SCBAs are derived from agricultural waste; thus, their chemical and physical properties may vary significantly depending on the source material and the combustion process. This variability can affect their consistency and reactivity as pozzolanic materials.

5.2.4 Compressive strength

Comparing the concrete mixes containing sieved sugarcane bagasse ash (S-SCBA) and raw sugarcane bagasse ash (R-SCBA) with the reference mix (pure cement without SCBA) across different curing times (3, 7, and 28 days) provides insight into how SCBA impacts the

mechanical properties of concrete. The compressive strength test results for all mixtures are provided in Table 20.

Table 20 Compressive strength test results for mixtures up to 28 days

Mix	Replacement Rate (%)	Compressive Strength (MPa) at different ages		
		3 days	7 days	28 days
Reference	0	29.30	37.97	43.35
Oven Dried, Sieved SCBA	5	23.84	34.27	42.98
	10	21.57	30.66	41.31
	20	19.93	29.42	38.69
Oven Dried, Raw SCBA	5	22.57	29.28	42.22
	10	20.96	28.22	38.48
	20	17.15	26.47	37.89

Also, the compressive strength for all mixes at w/cm ratio of 0.485 are graphically represented below in Figure 38.

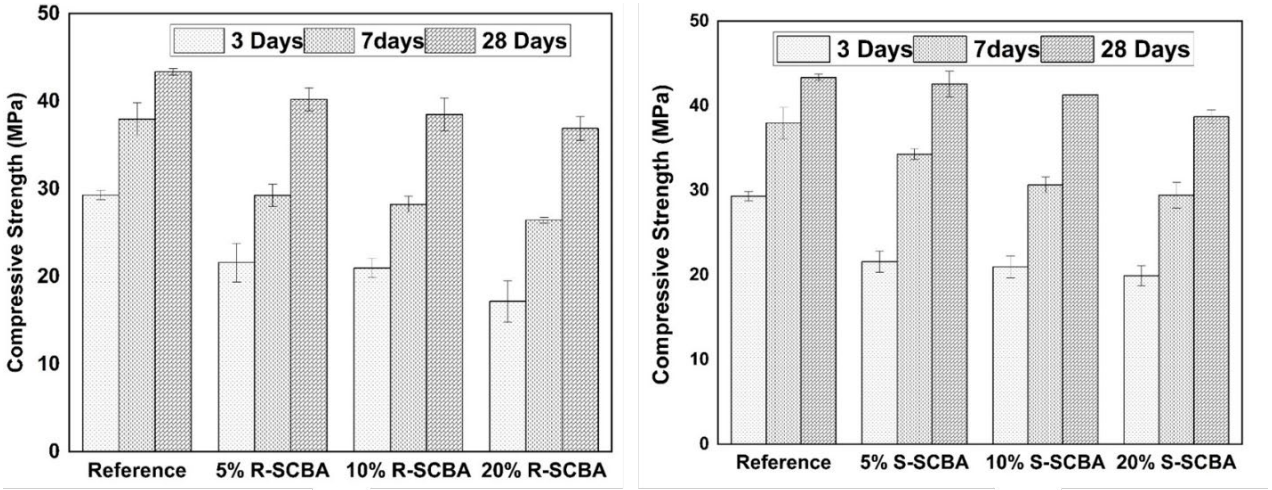

Figure 38 Compressive strength of mortar mixtures at different ages

The reference mix demonstrates higher early strength compared to all SCBA mixes at 3 days. This indicates that the immediate reaction and strength development are more efficient in the reference mix; this is because it contains no replacement materials that could dilute the cement's effectiveness. When a small dosage (5%) is used to replace portland cement, the SCBA mixes, both sieved and raw, demonstrated a small decrease in strength compared to the reference mix. This strength reduction becomes more noticeable when a higher dosage of SCBA (20%) is used, especially in the early stages. By 7 days, the compressive strength of all mixes increases as

more cement hydration reactions occur over time. However, the reference mix still maintains a strength advantage over the SCBA mixes. This period highlights the slower rate of strength gain in the SCBA mixes, possibly due to the gradual initiation of pozzolanic reactions between the silica in SCBA and calcium hydroxide in the cement paste. The primary factor is the dilution of cement's hydrating components when replaced by SCBA, which does not hydrate or contribute to the initial matrix formation as effectively as portland cement. This dilution results in lower strength, particularly evident at early ages and higher replacement levels. The result conforms with prevalent studies by other researchers (Akkarapongtrakul et al., 2017; N. Amin, 2011; Cordeiro et al., 2019). Additionally, higher levels of SCBA could disrupt the packing density and cohesion within the cement matrix. This increases the pores due to larger particle size, which further weakens the structures mechanical strength properties (Chi, 2012). The finer particles of S-SCBA likely fill voids more effectively and might even accelerate early hydration reactions due to increased surface area, leading to slightly better strength outcomes at lower replacement levels compared to R-SCBA. This conforms with the statements made by Isaia et al., (Isaia et al., 2003).

At later ages, specifically at 28 days, the reference mix reaches its highest strength, showcasing the effectiveness of uninterrupted cement hydration. In contrast, the SCBA mixes generally exhibit lower strength compared to the reference, which can be attributed to the dilution and pozzolanic nature of reaction. However, there is a notable recovery in strength in some SCBA mixes (particularly those with 5% and 10% replacement), suggesting that pozzolanic reactions have progressed to partially compensate for the initial reduction in strength. The 20% replacement mixes still show significant strength reductions, 10.8% for S-SCBAs and 12.6% for R-SCBAs when compared to reference mixes). This underscores the limitations of high replacement rate of SCBAs without impacting long-term strength negatively. Over time, the pozzolanic properties of SCBA can help develop additional strength. The reaction between the silica in SCBA and the calcium hydroxide from cement forms additional C-S-H, enhancing the matrix's strength. This effect is more observable in long-term strength (28 days) but doesn't fully compensate for the initial strength loss at higher replacement levels.

Since 5% mixtures included greater portland cement and lower SCBA contents than those of higher replacement mixtures, the mortars containing 5% SCBA had a better strength than other mixtures with high dosage. A similar decreasing trend of compressive strength with the

increasing replacement rates of SCBAs was also observed by P. Jagadesh et al. when the ashes were used without any kind of processing. Further processing the ashes significantly altered the characteristics (Jagadesh et al., 2018). The high loss on ignition (15.2%) in bagasse ashes also could interfere with the process of hydration in cement. This could result in lowering workability, increasing the requirement for water, and significantly affecting the compressive strength of the concrete (Chindaprasirt et al., 2020). The differences between S-SCBA and R-SCBA mixes suggest that the treatment and quality of SCBA significantly affect its efficiency as a portland cement replacement. The sieved SCBA, being finer, likely offers better initial dispersion and reactivity compared to the coarser raw SCBA. Other studies have shown that adding even modest percentages of unprocessed or slightly processed sugarcane bagasse ash to cementitious materials might have a negative impact on the materials' compressive strength (Bahurudeen and Santhanam, 2015; Cordeiro, Barroso, et al., 2018; Cordeiro et al., 2016; Ríos-Parada et al., 2017).

5.2.5 Dynamic modulus of elasticity

Figure 39 illustrates the dynamic modulus of elasticity (MOE) for mortar samples containing different proportions of S-SCBA and R-SCBA, tested at 14 and 28 days. This analysis focuses on the influence that SCBA has on the stiffness of concrete over time. The dynamic MOE, a measure of the material's ability to resist deformation under applied dynamic loads, is crucial for structural applications where resilience to varying loads is required. Each set of samples is tested at two curing ages, 14 and 28 days, to observe the change in elasticity over time.

It can be concluded that reference specimens demonstrated the highest MOE among all samples, starting at approximately 31.47 GPa at 14 days and slightly increasing to around 33 GPa by 28 days. This indicates a good, early and continued development of concrete strength and stiffness, which is typical for standard concrete mixes. The addition of 5% S-SCBA results in a modest increase in MOE compared to the other cement-replaced mortar cylinders. The dynamic modulus of elasticity values for 5% S-SCBA mixes are 31 GPa at 14 days and 32.93 GPa at 28 days, slightly lower than those of the reference. This slight decrease suggests that incorporating a small percentage of SCBA, like 5%, does not significantly affect the elasticity properties of the concrete. The modulus increases slightly from 14 to 28 days, indicating ongoing hydration and pozzolanic reactions that might be contributing to strength gain. 10% replacement by S-SCBA

demonstrated nearly similar performance to 5% S-SCBA mixtures. At a 10% replacement level, the dynamic modulus values at 14 and 28 days are 30.6 GPa and 32.47 GPa respectively. However, increasing the S-SCBA contents from 10% to 20% significantly reduces the MOE at both testing intervals.

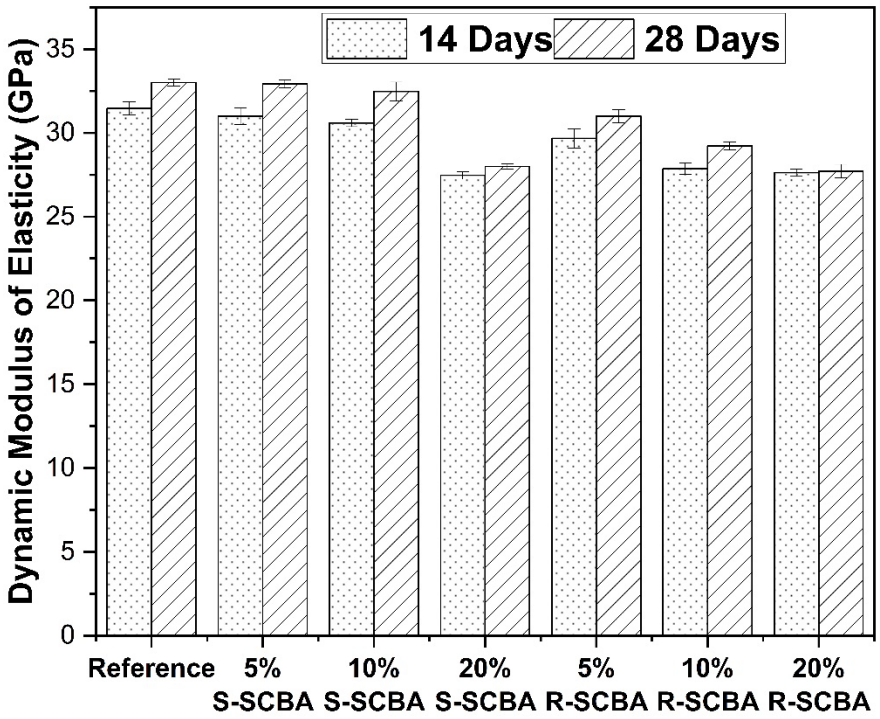

Figure 39 Dynamic modulus of elasticity of the mortar cylinders at different ages

The greater the SCBA content, the more pronounced the reduction in modulus of elasticity, which could be due to the dilution of supplementary cementitious material and the different physical properties of the SCBA compared to cement (Kazmi et al., 2017b). However, all S-SCBA mixes show some increase in MOE from 14 to 28 days, which is a positive sign of continuing maturation and pozzolanic action, albeit at a slower rate than the reference. R-SCBA samples generally show a similar trend to S-SCBA, with the 5% R-SCBA mix having a slightly lower MOE than its sieved counterpart. This might reflect variations in particle size distribution and the resultant packing density and bonding characteristics within the concrete matrix. At higher percentages (10% and 20%), R-SCBA samples also exhibit lower MOE values than the reference and corresponding S-SCBA samples. This decrement is more significant, because it possibly indicates raw ash's less uniform and possibly coarser nature which could be affecting the concrete structure more profoundly. As with R-SCBA, there is an increase in MOE from 14

to 28 days, although the overall values remain lower compared to the reference and S-SCBA samples. The higher amount of addition of both S-SCBA and R-SCBA generally decreases the dynamic MOE of concrete, indicating a reduction in stiffness with increasing SCBA content. This could impact the structural application where higher stiffness is required.

The continued increase in MOE from 14 to 28 days across all samples suggests that while the initial reactions may be slowed or altered due to the presence of SCBA, the long-term pozzolanic reactions are beneficial and potentially offset some early losses in stiffness. The differences between S-SCBA and R-SCBA impacts on MOE underscore the importance of ash processing and its physical properties on concrete behavior. This was also found by Jagadesh et al. when processed SCBA were compared to raw SCBA. Researchers reasoned that the cause was increased formation of hydration products and microstructural improvement by reduction in pore structure through particle packing (Jagadesh et al., 2018) . More uniform and finer SCBA (as in S-SCBA) tends to perform better in terms of preserving the dynamic MOE.

5.2.6 Drying shrinkage

When moisture escapes into the atmosphere, concrete shrinks. This impact is mostly caused by the evaporation of water, which is influenced by both ambient temperature and humidity. Drying shrinkage is a critical factor in concrete performance, affecting its durability and structural integrity due to potential cracking.

In analyzing the effects of SCBA as an SCM on concrete drying shrinkage, a comparative approach reveals insightful patterns. From Figure 40, it can be observed that the reference mix, devoid of SCBA, demonstrated a typical progression in drying shrinkage, where the shrinkage measurements increased steadily from -236 microstrain on the first day to -711 microstrain by the fourteenth day, serving as a baseline for assessing the impact of SCBA incorporation. This continuous increase is expected in conventional concrete due to the evaporation of water as the concrete sets and hardens. In contrast, the inclusion of SCBA in the concrete mixes yielded varying results. The 5% S-SCBA and 10% S-SCBA mixes showed less drying shrinkage by the end of the 14-day period compared to the reference mix. Specifically, the 5% S-SCBA mix started with a shrinkage of -240 microstrain on day 1 and concluded at -569 microstrain on day 14, while the 10% S-SCBA mix started at -249 microstrain and ended at -596 microstrain. For Sieved SCBA, all replacement levels (5%, 10%, 20%) started with a slightly higher initial

shrinkage than the reference, suggesting an initial adjustment in the concrete mix due to the SCBA's particle

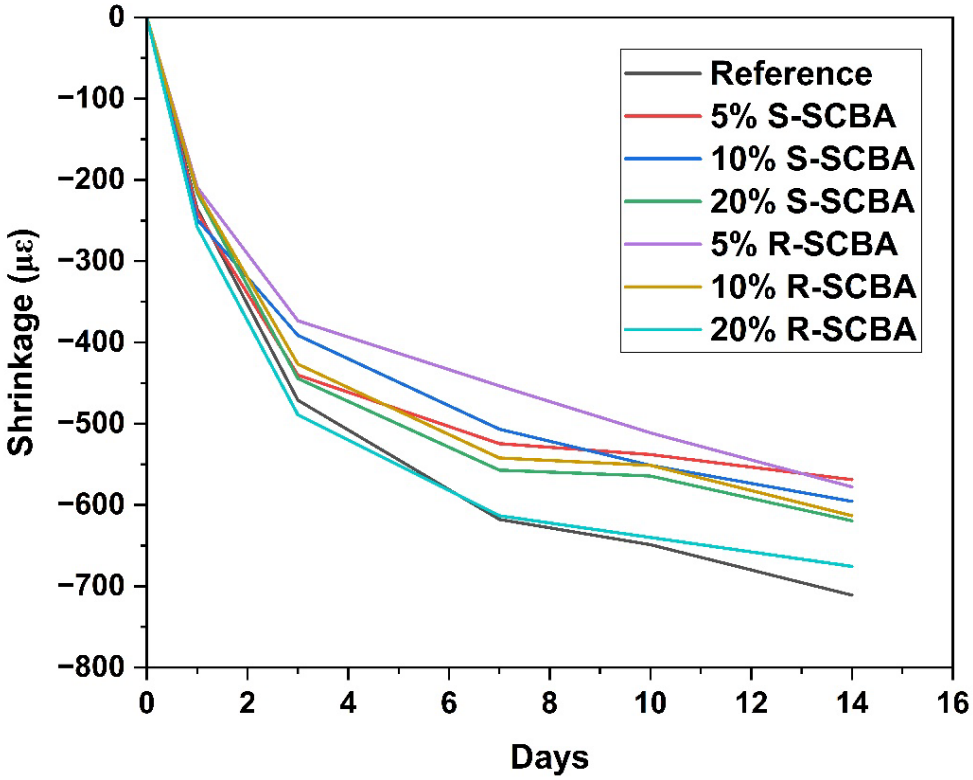

Figure 40 Drying shrinkage by length change of mortar bars

characteristics and possible changes in water retention. Despite this initial increase in shrinkage measurement, the long-term shrinkage (by day 14) for these samples was lower than the reference. This indicates that the pozzolanic reaction facilitated by the SCBA, particularly with the sieved variant, might enhance the microstructure of the concrete by refining pore structure and increasing the density of C-S-H formations, thus reducing shrinkage over time. However, the 20% S-SCBA mix, despite starting with shrinkage similar to the lower percentages, ended at -619 microstrain after 14 days, indicating a lesser degree of effectiveness at higher concentrations.

The concrete mixes with R-SCBA showed a broader range of shrinkage behaviors. The 5% R-SCBA mix exhibited the lowest shrinkage among all mixes at -578 microstrain on day 14, starting from -216 microstrain on day 1. This significant reduction suggests effective shrinkage, likely due to the filling of voids by finer particles of SCBA and the subsequent hydration reactions. Conversely, the 10% R-SCBA mix displayed a moderate reduction, ending at -613 microstrain, whereas the 20% R-SCBA mix approached the reference level of shrinkage at -676 microstrain. This suggests that while raw SCBA can reduce shrinkage at lower levels, higher

concentrations may be less beneficial or even detrimental, possibly due to inconsistent properties of the raw material affecting the hydration process. This indicates a threshold beyond which the benefits of raw SCBA diminish, likely due to negative impacts on the concrete's hydration process and overall matrix integrity from excessive SCBA content. A similar increasing pattern of drying shrinkage was observed in previous studies when the replacement ratios increased (Praveenkumar et al., 2020).

An important way to understand how sieved and raw sugarcane bagasse ash impacts drying properties is to look at the mass loss data from the concrete samples that were changed with SCBA at different percentages. This information allows us to better understand the drying behavior of concrete using SCBA as a partial replacement for OPC. Predominantly, water evaporation from the mix causes mass loss in concrete, especially in the early stages of curing. While the concrete cures and the rate of internal moisture migration and evaporation slows down, the high rates of mass loss at first signify rapid surface drying, which subsequently stabilizes. Because it indirectly represents the porosity and integrity of the concrete matrix, which both affect strength, durability, and overall performance, mass loss is an important measure.

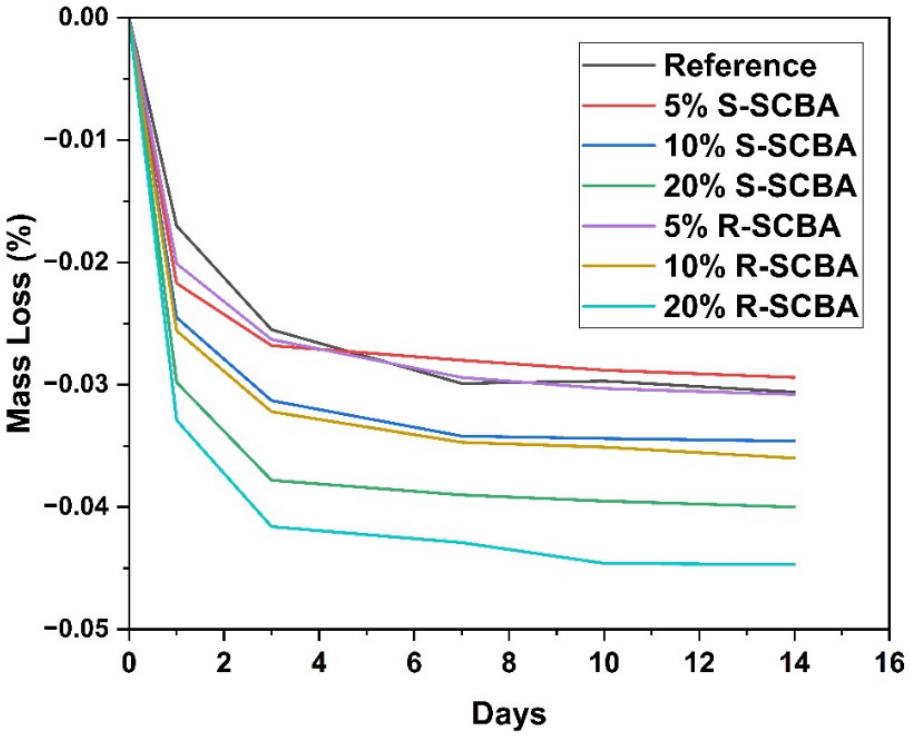

Figure 41 Drying shrinkage through mass loss of mortar bars

From Figure 41, it can be observed that early on, the mass of every sample, including the reference—shows a noticeable drop within the first day. This is to be expected as the initial mass loss is primarily due to the evaporation of free surface water. Both the sieved and raw samples containing 20% SCBA show the greatest mass loss, suggesting that a larger SCBA content may be causing increased porosity or less efficient in water retention due to irregular shapes and higher surface area of SCBA particles. The rate of mass loss usually slows down during the mid-period as the concrete cures, although it still happens at a significant rate until about day seven. This is an important stage since pores become refined, the cement matrix densifies, therefore the permeability becomes lower, and mass loss slows down as most of the free water has already evaporated.

In comparison to samples with greater percentages of SCBA, the 5% SCBA samples—especially the sieved version—show a mass loss that is closer to the reference sample, indicating good performance in terms of reducing drying rate. Afterwards, by day 14, the mass loss tends to level off, meaning the majority of the free water has evaporated. At this point, the variations in mass loss between samples become more noticeable and consistent. Reiterating its effectiveness as a replacement material with negligible negative impacts on the qualities of the concrete, the 5% S-SCBA sample exhibits the least divergence from the reference.

5.2.7 Alkali-silica reaction (Accelerated mortar bar test)

ASR is the result of a reaction between specific types of silica present in aggregates and alkalis in cement. Over time, internal stress and concrete cracking are caused by this reaction, which creates an expanding gel that swells after absorbing water. Assuming reactive silica is present in the aggregates, the likelihood of this reaction happening increases with the concentration of alkalis (Na_2O and K_2O).

The accelerated mortar test expansion data for all the mixes are given in Table 21. The test results for all the mixtures containing SCBA up to 20% replacement as well as the reference mixture are demonstrated on Figure 42.

Table 21 ASR of reference and SCBA blended mixtures up to 28 days

Mix	**Replacement Rate (%)**	**Expansion (%) different ages in**					
		3 days	**5 days**	**7 days**	**14 days**	**21 days**	**28 days**
Reference	0	0.14	0.26	0.37	0.48	0.54	0.57

Oven Dried, Sieved SCBA	5	0.09	0.14	0.18	0.26	0.29	0.31
	10	0.11	0.17	0.23	0.31	0.36	0.40
	20	0.16	0.22	0.29	0.37	0.42	0.47
Oven Dried, Raw SCBA	5	0.09	0.14	0.19	0.26	0.29	0.32
	10	0.10	0.16	0.25	0.36	0.41	0.47
	20	0.15	0.22	0.32	0.41	0.48	0.54

All mixtures up to 20% replacement of OPC by SCBA including the reference mix expanded beyond 0.10% in 14 days and according to ASTM C1567; this is reasonable because reactive sand was used to purposely induce ASR. The reference had the highest expansion nearly at all ages followed by the mixture containing 20% of SCBAs (both raw and sieved ashes). Even though at the lower replacement level lower expansion is observed compared to reference mix, none of them produced an acceptable expansion of less or equal to 0.10% in 14 days, which is due to the reactive sand. The reference mix demonstrated an expansion of 0.14% in 3 days, which further expanded to 0.57% over the 28-day period.

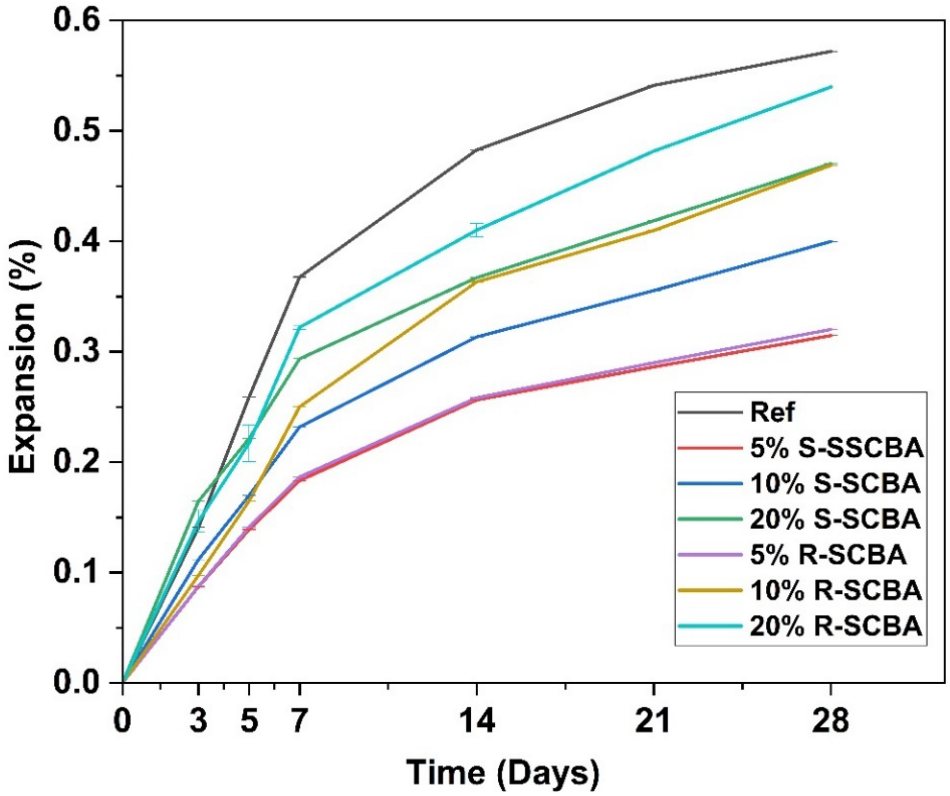

Figure 42 ASR of mortar bars at different mixtures up to 28 days

The above results show that a 5% replacement of the ashes by the weight of OPC reduces the ASR compared to the reference mixtures. This can be attributed to the positive effect of the

pozzolanic reaction (pore refinement) that surpasses the negative impact. Here, the increase in the alkali content in the mixture. The significant increase in expansion of mortars containing natural rice husk ash is also observed with the increase of replacement rates (Zerbino et al., 2012). Certain pozzolanic materials, like SCBA, can reduce the alkalis available in the solution even when their alkali content is higher than that of OPC (M. Thomas, 2011). This reduction occurs because the pozzolanic reactions consume portlandite, thereby lowering the hydroxyl ion concentration necessary for ASR. Additionally, these reactions increase the formation of C-S-H, which absorbs some of the alkalis, further mitigating ASR risks (Maas et al., 2007; M. Thomas, 2011).

The oxide composition analysis of the collected SCBA ashes in Table 8 demonstrated the higher percentages of sodium oxide (0.77%) and potassium oxide (8.09%) present in the ashes, which are already known as alkalis. Their presence in cement and concrete can contribute to the significant risk of ASR expansion. The effectiveness of SCBA in reducing ASR decreases noticeably when the replacement rate is increased, which was also found in preceding study (Andrade Neto et al., 2021). This decrease is explained by the production of SCBA agglomerates and a rise in the mixture's alkali concentration. These agglomerates might exacerbate ASR by acting as reactive aggregates, like the ones noticed in concrete containing silica fume (H. T. Le and Ludwig, 2020). From the alkali silica reaction data, it can be concluded that the inclusion of sugarcane bagasse ash considerably reduces expansion, and this can be attributed to the pore refinement, reduced alkalinity, and higher C-S-H formation.

6. CONCLUDING REMARKS

6.1 Summary of eggshell powder in cementitious composites

Waste eggshell collected from an egg breaking plant of Pennsylvania contained about 20% moisture including egg liquid residue that lingered on the shells after the industrial process. The organic content of the eggshell was determined to be about 6% based on the results of combustion test and TGA. SEM imaging of ground waste eggshell showed that it has irregular morphology and similar sphericity as limestone powder. However, further examination at a higher magnification found dendritic features due to organic content adhering to calcium-rich eggshell particles. Combustion of eggshell at 300ºC and 500ºC removed the dendritic feature on eggshell particles, indicating that the temperatures are effective at denaturing the organic content

of eggshell powder. XRD analysis confirmed that no calcination of eggshell occurred after 500ºC heat treatment for 2 hours.

Powder wettability tests of limestone, untreated eggshell and eggshell were performed to evaluate the interaction between each powder with water. Limestone was found to be hydrophilic, while untreated eggshell was highly hydrophobic. The hydrophobicity of eggshell could be reverted through heat treatment, and eggshell powder treated at 500ºC displayed hydrophilic properties similar to limestone. The hydration mechanism of cement paste with limestone and eggshell was investigated, and it was found that the hydration reaction of cement with 15% limestone and eggshell powder were similar. However, at 35% portland cement replacement, limestone powder accelerated the hydration of cement, while eggshell powder delayed cement hydration due to the dominant influence of organic content. The paste minerology of cement mixtures with limestone and eggshell were found to be similar. A relative degree of hydration test based on bound water measurement showed that mixtures with eggshell powder achieved lower degree of hydration at 35% replacement, but that was improved when treated eggshell powder was used.

On the other hand, chemical shrinkage tests of eggshell cement mixtures are higher than mixtures with limestone powder. The organic content present within the eggshell powder caused additional chemical shrinkage due to the volume change of the eggshell membrane. Likewise, eggshell mortars experienced greater drying shrinkage compared to limestone mortars at the same level of replacement. This is because the protein fiber of the eggshell membrane experiences shrinkage when it loses moisture to the environment. The chemical shrinkage test was deemed to be unreliable when it was used to access cementitious materials with organic impurities. The contradiction was further studied by examining rinsed eggshell powder to extract eggshell powder with a higher and lower organic content and eggshell powder after heat treatment. Untreated eggshell powder with higher organic content caused additional chemical shrinkage that is not correlated with its degree of hydration. On the other hand, eggshell powder after heat treatment had a slightly higher chemical shrinkage reflecting its ability to improve cement hydration similar to limestone powder.

Flowability test of mortar mixtures concluded that limestone powder increased the flow of mortar, while eggshell powder compromised the flow of mortar. This agrees with the findings from the wettability test. With heat treatment, the detrimental effect of eggshell powder to the

flow was mitigated. The mortar mixture prepared with eggshell powder after combustion at 500ºC for 2 hours displayed the same flow as the control mortar. This indicates that the negative impact of eggshell powder to flow can be fully overcome with the treatment.

At 15% replacement, both limestone powder and untreated eggshell powder mortar have comparable strength. Hence, heat treatment of eggshell powder is not necessarily at a lower percentage of inclusion, as the organic content within the matrix is lower and does not impact the hardened performance of the mortar. However, at 35% replacement, the compressive strength of mortar with untreated eggshell powder is significantly lower than that with limestone powder. The strength loss can be recovery by using heat-treated eggshell powder. After 500ºC heat treatment, eggshell mortar has comparable performance with limestone mortar even at higher replacement proportions.

To conclude, eggshell can become a direct alternative to limestone at 15% inclusion and achieve comparable strength. However, the influence of organic content becomes dominant at 35%, which delays hydration, reduces flowability, and increases shrinkage of cementitious composite. Heat treatment at 500˚C denatures all organic content within the eggshell and 35% eggshell mortar performs comparatively to limestone mortar. Hence, waste eggshell is a feasible material that can be recovered from the landfill to be utilized as a material for portland cement production.

6.2 Summary of SCBAs Performance as SCM

Raw SCBA samples collected from the sugarcane mill are black in color and contain a high amount of moisture. The loss on ignition is found to be approximately 15.39%, which does not meet the requirements as per ASTM C618 for supplementary cementitious materials. Thus, the material requires further processing to be included in the concrete system. Also, high amounts of burnt/unburnt coarse and fine fibers in the raw samples can contribute to high LOI values, thus, it cannot be clearly stated that the mass loss at high temperatures is only due to the presence of high carbon contents in the ashes. Thermogravimetric analysis can be used for a better understanding of the mass loss mechanism of the collected ash sample.

Visual inspection and SEM analysis revealed that the raw sugarcane bagasse ashes consist of heterogeneous, irregularly shaped particles. This variability in particle size and its distribution negatively affected the workability of fresh mortar mixtures containing the ashes, leading to an increased water demand at higher replacement levels. However, despite the

negative effects, the mortar mixtures still reached the target flow value when a polycarboxylate-based admixture was added in this study. It has been noted that as the rate of OPC replacement increases, the required amount of admixture also rises. Furthermore, mixtures containing unsieved ashes demand a greater quantity of superplasticizers compared to those with either the reference mix or sieved ashes.

From the XRF analysis, it is evident that heating SCBA up to 600°C slightly alters its chemical composition in a way that could enhance its effectiveness as a pozzolanic material for concrete. However, the benefits are modest and do not offset the higher energy costs and limited production capacity. As a result, sieving without heating was performed on the collected ashes to optimize their properties.

The XRD pattern comparison further demonstrates how processing impacts SCBA. SCBA exhibited larger peaks, indicating a potential for increased reactivity when finely processed, which could lead to better pozzolanic activity beneficial for portland cement applications. Meanwhile, the sharp, clear peaks seen in cement confirm its crystalline and reactive nature. The XRD results also revealed that the predominant oxide in the ash is SiO_2, constituting over 65%, based on the presence of an amorphous hump between 15° to 30° 2θ in the XRD diffractogram. This information supports the potential for SCBA's application in cementitious systems.

The analysis of cement paste mixtures containing sugarcane bagasse ash reveals two main effects on the cement hydration process, as shown by heat flow data. First, there is a noticeable delay in the time to peak heat flow, and second, there is a reduction in the magnitude of peak heat flow. These effects are more pronounced with SCBA content ranging from 5% to 30%. Unlike pure portland cement hydration, which features prompt and higher peaks, the delayed peaks and reduced heat production with SCBA suggest its pozzolanic activity. This activity includes a dilution effect, reducing the total reactive material available for hydration and contributing to the observed trends. These findings have significant practical implications, particularly in controlling heat generation in mass concrete constructions, where excessive heat can lead to thermal cracking. However, the slower hydration rate could delay early strength development, which is a critical factor in time-sensitive construction projects. Moreover, finer particles and a higher specific surface area of SCBA can accelerate hydration reactions. This leads to increased chemical shrinkage and consumption of portlandite, enhancing the pozzolanic

activity. Consequently, the fine, supplementary cementitious material exhibits a denser microstructure, improved mechanical properties, and increased durability. Thus, optimizing SCBA's particle size through mechanical processing can be crucial to maximizing its reactivity and effectiveness as a sustainable additional cementitious material.

When compared to a reference mix without SCBA, mortar mixes containing both raw sugarcane bagasse ash (R-SCBA) and sieved sugarcane bagasse ash (S-SCBA) initially exhibit lower compressive strength. However, strength increased notably by day 28, particularly in mixes with SCBA replacements ranging from 5 to 10%. This increase in strength is attributed to the pozzolanic reactions between SCBA and the calcium hydroxide produced during cement hydration, forming additional calcium silicate hydrate that enhances strength. The finer particle size of sieved SCBA contributes to higher early strength compared to the coarser raw SCBA. Despite some recovery at later stages, all SCBA mixes maintain lower strength compared to the reference mix, highlighting the trade-offs of using SCBA as a cement substitute in sustainable concrete production. Careful management of SCBA incorporation is necessary to balance environmental benefits with the need for adequate mechanical properties in concrete. The results indicate that a 5 to 10% SCBA replacement strikes an effective balance, reducing cement usage while minimally impacting concrete’s compressive strength. This level allows for the environmental advantages of utilizing waste material while preserving the structural integrity necessary for practical construction applications. However, higher replacement levels, especially 20%, significantly compromise concrete performance in the early curing stages, suggesting that more moderate SCBA levels are preferable for practical use.

The dynamic modulus of elasticity is impacted by the proportion of SCBA added to concrete mixtures: greater replacement levels result in lower stiffness. Mixtures with 20% SCBA experience the most significant reductions, pointing to the influence of SCBA's particle size and chemical properties on the hydration process and concrete microstructure development. In contrast, mixtures with 5% and 10% SCBA exhibit more moderate decreases, suggesting that this range may offer an optimal balance between maintaining structural integrity and achieving environmental benefits. This balance supports reduced environmental impact and the reuse of agricultural by-products.

Quantitative analysis of drying shrinkage length change data enhances our understanding of the drying behavior of SCBA cement mortars. It confirms that SCBA, particularly when

sieved and used in moderate concentrations, can effectively slow shrinkage potential, thus enhancing durability. However, careful attention must be given to the type and amount of SCBA used to avoid adverse effects at higher concentrations. Results indicate that sieved SCBA at lower replacement levels, around 5 to 10%, show promising outcomes. At these levels, it is feasible to optimize SCBA usage to foster sustainable concrete practices without compromising structural integrity. Conversely, higher SCBA levels, particularly 20% of raw SCBA, tend to be less effective and may even worsen shrinkage issues, likely due to variations in ash quality and impurities. Based on the data, the optimal SCBA replacement level appears to be between 5% and 10%. Evidence suggests that this range strikes a balance between reducing shrinkage, maintaining practical concrete performance and SCM availability.

From the alkali silica reaction data, it can be concluded that the sugarcane bagasse ash considerably as SCM reduces expansion, however, to include higher amounts of sugarcane bagasse ashes in a concrete system, it requires further processing to particularly leach off the alkali substances present in the sugarcane bagasse ashes through washing and acid cleaning. Based on the shrinkage data, the optimal SCBA replacement rate is 5%.

Based on the outcome of this research, it can be stated that for real-world applications, 5 to 10% of the sieved SCBA is suggested as the ideal replacement rate, considering mechanical and durability test outcomes.

DATA AVAILABILITY STATEMENT

All metadata that support the findings of this study are in the Zenodo DataShare repository with the identifier https://doi.org/10.5281/zenodo.16968886 and https://doi.org/10.5281/zenodo.13831278. https://zenodo.org/records/16995777

REFERENCES

AASHTO M 240 Standard Specification for Blended Cement. (2023). In. AASHTO, Washington D.C, United States: American Association of State Highway and Transportation Officials.

Afkhami, B., Akbarian, B., Beheshti, N., Kakaee, A., & Shabani, B. (2015). Energy consumption assessment in a cement production plant. *Sustainable Energy Technologies and Assessments*, *10*, 84-89. https://doi.org/10.1016/j.seta.2015.03.003

Ahmed, T. A. E., Wu, L., Younes, M., & Hincke, M. (2021). Biotechnological Applications of Eggshell: Recent Advances [Review]. *Frontiers in Bioengineering and Biotechnology*, *9*. https://doi.org/10.3389/fbioe.2021.675364

Andrew, R. M. (2019). Global CO2 emissions from cement production, 1928–2018. *Earth Syst. Sci. Data*, *11*(4), 1675-1710. https://doi.org/10.5194/essd-11-1675-2019

ASTM C114-24 Standard Test Methods for Chemical Analysis of Hydraulic Cement. (2024). In. ASTM International, West Conshohocken, PA: ASTM International.
ASTM C157/C157M-24 Standard Test Method for Length Change of Hardened Hydraulic-Cement Mortar and Concrete. (2024). In. ASTM International, West Conshohocken, PA: ASTM International.
ASTM C230-20 Standard Specification for Flow Table for Use in Tests of Hydraulic Cement. (2020). In. ASTM International, West Conshohocken, PA: ASTM International.
ASTM C230/C230M-23 Standard Specification for Flow Table for Use in Tests of Hydraulic Cement. (2023). In. ASTM International, West Conshohocken, PA: ASTM International.
ASTM C270-19 Standard Specification for Mortar for Unit Masonry. (2019). In. ASTM International, West Conshohocken, PA: ASTM International.
ASTM C511-21 Standard Specification for Mixing Rooms, Moist Cabinets, Moist Rooms, and Water Storage Tanks Used in the Testing of Hydraulic Cements and Concretes. (2021). In. ASTM International, West Conshohocken, PA: ASTM International.
ASTM C595/C595M-24 Standard Specification for Blended Hydraulic Cements. (2024). In. ASTM International, West Conshohocken, PA: ASTM International.
ASTM C618-22 Standard Specification for Coal Fly Ash and Raw or Calcined Natural Pozzolan for Use in Concrete. (2022). In. ASTM International, West Conshohocken, PA: ASTM International.
ASTM C1567-23 Standard Test Method for Determining the Potential Alkali-Silica Reactivity of Combinations of Cementitious Materials and Aggregate (Accelerated Mortar-Bar Method). (2023). In. ASTM International, West Conshohocken, PA: ASTM International.
ASTM C1608-17 Standard Test Method for Chemical Shrinkage of Hydraulic Cement Paste. (2017). In. ASTM International, West Conshohocken, PA: ASTM International.
ASTM C1608-23 Standard Test Method for Chemical Shrinkage of Hydraulic Cement Paste. (2023). In. ASTM International, West Conshohocken, PA: ASTM International.
ASTM C1876-19 Standard Test Method for Bulk Electrical Resistivity or Bulk Conductivity of Concrete. (2019). In. ASTM International, West Conshohocken, PA: ASTM International.
Bond, A. T., & Huffman, D. G. (2023). Nematode eggshells: A new anatomical and terminological framework, with a critical review of relevant literature and suggested guidelines for the interpretation and reporting of eggshell imagery. *Parasite*, *30*, 6. https://doi.org/10.1051/parasite/2023007 (La coque des œufs des nématodes : un nouveau cadre anatomique et terminologique, avec une revue critique de la littérature pertinente et des lignes directrices suggérées pour l'interprétation et la communication de l'imagerie des coques des œufs.)
Cheng, D., Reiner, D. M., Yang, F., Cui, C., Meng, J., Shan, Y., Liu, Y., Tao, S., & Guan, D. (2023). Projecting future carbon emissions from cement production in developing countries. *Nature Communications*, *14*(1), 8213. https://doi.org/10.1038/s41467-023-43660-x
Chong, B. W., Othman, R., Jaya, R. P., Li, X., Hasan, M. R. M., & Abdullah, M. M. A. B. (2023). Meta-analysis of studies on eggshell concrete using mixed regression and response surface methodology. *Journal of King Saud University - Engineering Sciences*, *35*(4), 279-287. https://doi.org/https://doi.org/10.1016/j.jksues.2021.03.011
Chong, B. W., Othman, R., Ramadhansyah, P. J., Doh, S. I., & Li, X. (2020). Properties of concrete with eggshell powder: A review. *Physics and Chemistry of the Earth, Parts A/B/C*, *120*, 102951. https://doi.org/https://doi.org/10.1016/j.pce.2020.102951

Clare, K., & Sherwood, P. (2007). The effect of organic matter on the setting of soil - cement mixtures. *Journal of Applied Chemistry*, *4*, 625-630. https://doi.org/10.1002/jctb.5010041107

Conrad, Z., Johnson, L. K., Roemmich, J. N., Juan, W., & Jahns, L. (2017). Time Trends and Patterns of Reported Egg Consumption in the U.S. by Sociodemographic Characteristics. *Nutrients*, *9*(4). https://doi.org/10.3390/nu9040333

Cree, D., & Rutter, A. (2015). Sustainable Bio-Inspired Limestone Eggshell Powder for Potential Industrialized Applications. *ACS Sustainable Chemistry & Engineering*, *3*(5), 941-949. https://doi.org/10.1021/acssuschemeng.5b00035

CSA A3000-18 Cementitious materials compendium. (2018). In. CSA Group, Toronto, Canada: Canadian Standards Association.

Eke, M. O., Olaitan, N. I., & Ochefu, J. H. (2013). Effect of Storage Conditions on the Quality Attributes of Shell (Table) Eggs. *Nigerian Food Journal*, *31*(2), 18-24. https://doi.org/https://doi.org/10.1016/S0189-7241(15)30072-2

EN 197-1:2011 Cement - Part 1: Composition, specifications and conformity criteria for common cements. In. British Standard Institute, London.

Friedemann, K., Stallmach, F., & Kärger, J. (2006). NMR diffusion and relaxation studies during cement hydration—A non-destructive approach for clarification of the mechanism of internal post curing of cementitious materials. *Cement and Concrete Research*, *36*(5), 817-826. https://doi.org/https://doi.org/10.1016/j.cemconres.2005.12.007

Grzeszczyk, S., Kupka, T., Kałamarz, A., Sudoł, A., Jurowski, K., Makieieva, N., Oleksowicz, K., & Wrzalik, R. (2022). Characterization of eggshell as limestone replacement and its influence on properties of modified cement. *Construction and Building Materials*, *319*, 126006. https://doi.org/https://doi.org/10.1016/j.conbuildmat.2021.126006

Han, C., Chen, Y., Shi, L., Chen, H., Li, L., Ning, Z., Zeng, D., & Wang, D. (2023). Advances in eggshell membrane separation and solubilization technologies. *Front Vet Sci*, *10*, 1116126. https://doi.org/10.3389/fvets.2023.1116126

Haverkamp, R. G., Sizeland, K. H., Wells, H. C., & Kamma-Lorger, C. (2022). Collagen dehydration. *International Journal of Biological Macromolecules*, *216*, 140-147. https://doi.org/https://doi.org/10.1016/j.ijbiomac.2022.06.180

He, Y., Che, D., Ouyang, X., & Niu, Y. (2022). Surface Properties of Eggshell Powder and Its Influence on Cement Hydration. *Materials (Basel)*, *15*(21). https://doi.org/10.3390/ma15217633

Henley, R., & Ruiz, F. J. (2021). *Roadmap to Carbon Neutrality*.

Honorio, T., Bary, B., Benboudjema, F., & Poyet, S. (2016). Modeling hydration kinetics based on boundary nucleation and space-filling growth in a fixed confined zone. *Cement and Concrete Research*, *83*, 31-44. https://doi.org/https://doi.org/10.1016/j.cemconres.2016.01.012

Hu, J., Ge, Z., & Wang, K. (2014). Influence of cement fineness and water-to-cement ratio on mortar early-age heat of hydration and set times. *Construction and Building Materials*, *50*, 657-663. https://doi.org/https://doi.org/10.1016/j.conbuildmat.2013.10.011

Keegan, M. (2020). *The world's growing concrete coasts*. BBC. Retrieved 3 October from https://www.bbc.com/future/article/20200811-the-eco-friendly-alternatives-to-ocean-concrete

Khan, K., Ahmad, W., Amin, M., & Deifalla, A. (2023). Investigating the feasibility of using waste eggshells in cement-based materials for sustainable construction. *Journal of Materials Research and Technology*, *23*. https://doi.org/10.1016/j.jmrt.2023.02.057

Kittipongvises, S. (2017). Assessment of Environmental Impacts of Limestone Quarrying Operations in Thailand. *Scientific Journal of Riga Technical University. Environmental and Climate Technologies*, *20*, 67-83. https://doi.org/10.1515/rtuect-2017-0011

Lothenbach, B., Le Saout, G., Gallucci, E., & Scrivener, K. (2008). Influence of limestone on the hydration of Portland cements. *Cement and Concrete Research*, *38*(6), 848-860. https://doi.org/https://doi.org/10.1016/j.cemconres.2008.01.002

Lura, P., Winnefeld, F., & Fang, X. (2017). A simple method for determining the total amount of physically and chemically bound water of different cements. *Journal of Thermal Analysis and Calorimetry*, *130*, 653-660. https://doi.org/10.1007/s10973-017-6513-z

Mantellato, S., Palacios, M., & Flatt, R. J. (2019). Relating early hydration, specific surface and flow loss of cement pastes. *Materials and Structures*, *52*(1), 5. https://doi.org/10.1617/s11527-018-1304-y

Mench, J. A., Sumner, D. A., & Rosen-Molina, J. T. (2011). Sustainability of egg production in the United States—The policy and market context1. *Poultry Science*, *90*(1), 229-240. https://doi.org/https://doi.org/10.3382/ps.2010-00844

Mignardi, S., Archilletti, L., Medeghini, L., & De Vito, C. (2020). Valorization of Eggshell Biowaste for Sustainable Environmental Remediation. *Scientific Reports*, *10*(1), 2436. https://doi.org/10.1038/s41598-020-59324-5

Narmluk, M., & Nawa, T. (2011). Effect of fly ash on the kinetics of Portland cement hydration at different curing temperatures. *Cement and Concrete Research*, *41*(6), 579-589. https://doi.org/https://doi.org/10.1016/j.cemconres.2011.02.005

Nowak, E., Combes, G., Stitt, E. H., & Pacek, A. W. (2013). A comparison of contact angle measurement techniques applied to highly porous catalyst supports. *Powder Technology*, *233*, 52-64. https://doi.org/https://doi.org/10.1016/j.powtec.2012.08.032

Owuamanam, S., & Cree, D. (2020). Progress of Bio-Calcium Carbonate Waste Eggshell and Seashell Fillers in Polymer Composites: A Review. *Journal of Composites Science*, *4*(2), 70. https://www.mdpi.com/2504-477X/4/2/70

Pang, X. (2015, 16 October 2015). *The effect of water-to-cement ratio on the hydration kinetics of Portland cement at different temperatures* The 14th international congress on cement chemistry, Beijing, China.

Parthiban, P., Sakthi Ganapathy, R., Karthick, S., Navin Ganesh, V., & Sudharsan, N. (2023). A review on environmental impact assessment of limestone mining operations. AIP Conference Proceedings,

Pisciotta, M., Pilorgé, H., Davids, J., & Psarras, P. (2023). Opportunities for cement decarbonization. *Cleaner Engineering and Technology*, *15*, 100667. https://doi.org/https://doi.org/10.1016/j.clet.2023.100667

Quina, M. J., Soares, M. A. R., & Quinta-Ferreira, R. (2017). Applications of industrial eggshell as a valuable anthropogenic resource. *Resources, Conservation and Recycling*, *123*, 176-186. https://doi.org/https://doi.org/10.1016/j.resconrec.2016.09.027

Shiferaw, N., Habte, L., Thenepalli, T., & Ahn, J. W. (2019). Effect of Eggshell Powder on the Hydration of Cement Paste. *Materials*, *12*(15). https://mdpi-res.com/d_attachment/materials/materials-12-02483/article_deploy/materials-12-02483.pdf?version=1564999072

Snellings, R., Chwast, J., Cizer, Ö., De Belie, N., Dhandapani, Y., Durdzinski, P., Elsen, J., Haufe, J., Hooton, D., Patapy, C., Santhanam, M., Scrivener, K., Snoeck, D., Steger, L., Tongbo, S., Vollpracht, A., Winnefeld, F., & Lothenbach, B. (2018). RILEM TC-238 SCM recommendation on hydration stoppage by solvent exchange for the study of hydrate assemblages. *Materials and Structures*, *51*(6), 172. https://doi.org/10.1617/s11527-018-1298-5

Tutus, A., Killi, U., & Cicekler, M. (2022). Evaluation of eggshell wastes in office paper production. *Biomass Conversion and Biorefinery*, *12*(4), 1115-1124. https://doi.org/10.1007/s13399-020-00768-0

Ummartyotin, S., & Manuspiya, H. (2018). A critical review of eggshell waste: An effective source of hydroxyapatite as photocatalyst. *Journal of Metals, Materials and Minerals*, *28*, 124-135. https://doi.org/10.14456/jmmm.2018.17

Vuong, T. T., Rønning, S. B., Ahmed, T. A., Brathagen, K., Høst, V., Hincke, M. T., Suso, H.-P., & Pedersen, M. E. (2018). Processed eggshell membrane powder regulates cellular functions and increase MMP-activity important in early wound healing processes. *PLoS One*, *13*(8), e0201975. https://journals.plos.org/plosone/article/file?id=10.1371/journal.pone.0201975&type=printable

Waheed, M., Yousaf, M., Shehzad, A., Inam-Ur-Raheem, M., Khan, M. K. I., Khan, M. R., Ahmad, N., Abdullah, & Aadil, R. M. (2020). Channelling eggshell waste to valuable and utilizable products: A comprehensive review. *Trends in Food Science & Technology*, *106*, 78-90. https://doi.org/https://doi.org/10.1016/j.tifs.2020.10.009

Wang, D., Shi, C., Farzadnia, N., Shi, Z., & Jia, H. (2018). A review on effects of limestone powder on the properties of concrete. *Construction and Building Materials*, *192*, 153-166. https://doi.org/https://doi.org/10.1016/j.conbuildmat.2018.10.119

Wijaya, V., & Teo, S. S. (2019). Evaluation of Eggshell as Organic Fertilizer on Sweet Basil.

Wong, M., Hendrix, M. J. C., von der Mark, K., Little, C., & Stern, R. (1984). Collagen in the egg shell membranes of the hen. *Developmental Biology*, *104*(1), 28-36. https://doi.org/https://doi.org/10.1016/0012-1606(84)90033-2

Yang, B., Wei, C., Yang, Y., Wang, Q., & Li, S. (2018). Evaluation about wettability, water absorption or swelling of excipients through various methods and the correlation between these parameters and tablet disintegration. *Drug Dev Ind Pharm*, *44*(9), 1417-1425. https://doi.org/10.1080/03639045.2018.1453519

Yang, D., Zhao, J., Ahmad, W., Nasir Amin, M., Aslam, F., Khan, K., & Ahmad, A. (2022). Potential use of waste eggshells in cement-based materials: A bibliographic analysis and review of the material properties. *Construction and Building Materials*, *344*, 128143. https://doi.org/https://doi.org/10.1016/j.conbuildmat.2022.128143